NOTE TO USERS

Genetic and Biochemical Analysis of the *Drosophila melanogaster* Homolog of the Human *SCA2* Gene

Terrence Forrest Satterfield

A dissertation submitted in partial fulfillment of the requirements for the degree of

Doctor of Philosophy

University of Washington

2005

Program authorized to offer degree:
Department of Genome Sciences

University of Washington
Graduate School

This is to certify that I have examined this copy of a doctoral dissertation by

Terrence Forrest Satterfield

and have found that it is complete and satisfactory in all respects,
and that any and all revisions required by the final
examining committee have been made.

Chair of Supervisory Committee:

Leo Pallanck

Reading Committee:

Leo Pallanck

Albert LaSpada

Celeste Berg

Date: 4/22/15

In presenting this dissertation in partial fulfillment of the requirements for the doctoral degree at the University of Washington, I agree that the Library shall make its copies freely available for inspection. I further agree that extensive copying of the dissertation is allowable only for scholarly purposes, consistent with "fair use" as prescribed in the U.S. Copyright Law. Requests for copying or reproduction of this dissertation may be referred to Proquest Information Learning, 300 North Zeeb Road, Ann Arobor, MI 48106-1346, to whom the author has granted "the right to reproduce and sell (a) copies of the manuscript in microform and/or (b) printed copies of the manuscript made from microform."

Signature _____

Date 4/22/05

University of Washington

Abstract

Genetic and Biochemical Analysis of the *Drosophila melanogaster* Homolog of the Human *SCA2* Gene

Terrence Forrest Satterfield

Chair of Supervisory Committee:

Assistant Professor Leo Pallanck

Department of Genome Sciences

The polyglutamine repeat diseases are a group of dominantly inherited neurodegenerative disorders characterized by progressive degeneration of specific neuronal populations and a shared mutational mechanism involving expansion of a glutamine-encoding repeat in the corresponding genes. Work on several polyglutamine diseases has led to the finding that nuclear localization of long polyglutamine tracts can trigger neurodegeneration via mechanisms involving transcriptional interference. While transcriptional interference may account for pathology in some of the polyglutamine disorders, increasing evidence indicates that unique nuclear and non-nuclear pathways are involved in the different polyglutamine disorders.

An alternative model to explain pathology in the polyglutamine repeat disorders is that pathogenesis results from an alteration of the normal cellular function of the polyglutamine disease gene as a consequence of polyglutamine expansion. Although data support this hypothesis for several polyglutamine repeat disorders, this model has not been broadly tested, in part because the normal cellular functions of most polyglutamine disease genes remain unknown.

This dissertation focuses on studies involving *SCA2*, the human gene underlying the polyglutamine disease spinocerebellar ataxia type 2 (SCA2). To understand the mechanism of SCA2 pathogenesis, I have used the fruit fly *Drosophila melanogaster* as a model system to investigate the normal cellular function of a *SCA2* homolog (*Datx2*). I have shown that, like its human counterpart, *Datx2* encodes a cytoplasmic

protein present throughout development in a variety of tissue types, including the nervous system. Loss of *Datx2* function in the retina, sensory bristles, and female germline results in cellular and tissue morphological changes indicative of actin filament formation defects. Moreover, loss-of-function or overexpression of *Datx2* in these same tissues results in alterations in the structural characteristics of actin filaments. Biochemical analysis of Datx2 and ataxin-2 (encoded by *SCA2*) reveal that both proteins physically assemble with polyribosomes, thus indicating that these proteins function in cytoplasmic RNA metabolism. These results suggest that *SCA2*/*Datx2* function to regulate RNAs encoding components of actin filament formation pathways. Further, these results raise the possibility that polyglutamine induced alteration of *SCA2* function causes dysregulation of the actin cytoskeleton, resulting in the neural pathology observed in SCA2.

TABLE OF CONTENTS

LIST OF FIGURES

LIST OF TABLES

ACKNOWLEDGEMENTS

I thank Leo Pallanck who supported me in many ways during my graduate school career. Leo's thorough love of discovery and his commitment to my training provided the basis for much of my success as a graduate student. I also thank Leo for demonstrating steady patience and understanding through all the ups and downs of graduate school. I owe Leo very much for molding me into a true scientist. I thank my committee for being very supportive and providing steady guidance to me. I thank my grade school science teacher Patricia Schmitz for steadily fostering my interest in science over several years. I thank the Pallanck Laboratory for providing a stimulating and friendly working environment. I thank my lab mate Michael Babcock for being a friend and for providing significant scientific advice. I thank Chuck Connoly and the laboratory of David Morris for providing valuable assistance with my biochemical experiments. I thank Celeste Berg for teaching me the value of the Drosophila ovary. I thank Stan Gartler for extensive use of his tissue culture facilities. I thank Steve Jackson for teaching me immunofluorescence procedures. I thank the Berkeley Drosophila Genome Project and the Bllomington Drosophila stock center for sequence data and fly stocks used in this work. I thank the staff at the Electron Microscopy Shared Resource laboratory for assistance with scanning electron microscopy analysis. Finally, I thank my mom and dad and brother for making many sacrifices for me and always supporting me in all my endeavors and misadventures. I additionally want to thank my dad for being the most knowledgeable person I know and for always supporting my inquisitive nature as a child.

CHAPTER 1:
INTRODUCTION

TRIPLET REPEAT DISEASES

In 1991, investigators identified the genes and mutations that underlie the diseases fragile X mental retardation and spinal and bulbar muscular atrophy (SBMA; VERKERK *et al.* 1991; LA SPADA *et al.* 1991). In doing so, they also identified a new mutational mechanism for disease. They discovered that repetitive DNA sequences known as trinucleotide or triplet repeats could expand and cause disease. At present, we know that triplet repeat expansions cause 24 diseases (Table 1.1; BROWN and BROWN 2003; CUMMINGS and ZOGHBI 2000; KOIDE *et al.* 1999). Disease causing triplet repeats can be located in non-coding or coding regions of genes. As with most repetitive DNA sequences, triplet repeats tend to be unstable, expanding and contracting in somatic and germline tissue. Because longer repeats have a tendency to expand (LAHUE and SLATER 2003), germline instability tends to cause earlier onsets in successive generations of affected families, a phenomenon called genetic anticipation (Figure 1.1; reviewed in CUMMINGS and ZOGHBI 2000).

There are six known diseases caused by non-coding triplet repeat expansions (Table 1.1). Non-coding triplet repeats can disturb cellular processes in several ways. Friedreich ataxia is an autosomal recessive disease caused by expansion of a GAA repeat in the first intron of the *FRDA* gene. The GAA repeat expansion promotes the formation of an unusually stable DNA structure that interferes with transcription of *FRDA* (CUMMINGS and ZOGHBI 2000). Fragile X syndrome is an X-linked recessive disease caused by expansion of a CGG repeat expansion in the 5'-UTR of the *FMR1* gene. The CGG repeat expansion promotes hypermethylation and reduced expression of *FMR1*

(CUMMINGS and ZOGHBI 2000). Myotonic dystrophy is an autosomal dominant disease caused when a CTG repeat expands within the 3'-UTR of the *DMPK* gene. mRNAs transcribed from mutant *DMPK* alleles sequester CUG-binding proteins and interfere with the splicing of several RNAs (RANUM and DAY 2004).

Eighteen diseases are caused by triplet repeat expansions that are translated. Nine of these are caused by expansions encoding polyalanine repeats (Table 1.1; BROWN and BROWN 2004). Most polyalanine diseases are marked by severe developmental defects. Eight of nine polyalanine disease genes encode transcription factors. In most cases, the polyalanine expansions in these transcription factors cause defects that are similar to those caused by loss-of-function mutations in these genes, suggesting that polyalanine expansions reduce the activity of their host proteins. CAG/polyglutamine repeats account for the remaining nine diseases caused by translated triplet repeats. These are: spinal and bulbar muscular atrophy (SBMA), Huntington disease (HD), dentatorubral pallidoluysian atrophy (DRPLA), and six spinocerebellar ataxias (SCA1, 2, 3, 6, 7, and 17; table 1.1).

Besides a shared mutational mechanism, polyglutamine diseases share a number of features. All nine are progressive disorders with typical late-onsets and durations of 10-20 years (reviewed in CUMMINGS and ZOGHBI 2000). The number of CAG repeats on the expanded allele strongly influences disease severity. With the exception of SBMA, all polyglutamine diseases are dominantly inherited. SBMA has sex-limited expression and is inherited in an X-linked recessive pattern. Though most of the genes are widely expressed in the brain and elsewhere, the only cells obviously affected are neurons. Notably, although neurons are affected in all polyglutamine diseases, the pattern of neural tissues typically affected is unique to each disease. Intracellular

proteinaceous aggregates called inclusion bodies are a prominent feature of these diseases. Inclusion bodies accumulate in neuronal and non-neuronal tissues of patients. Though especially prominent in the nucleus, inclusions can be found in the cytoplasm also. Although the composition of these inclusion bodies is largely unknown, they are known to contain molecular chaperones, proteasome components, and components of the transcription machinery. Despite the numerous similarities among these diseases, apart from each harboring a polyglutamine tract, the disease proteins bear no resemblance to one another.

The intrinsic toxicity model of polyglutamine disease:

The lack of shared homology among the polyglutamine disease proteins led many to speculate that long polyglutamine repeats are intrinsically toxic. In part, this idea was attractive because it is consistent with the dominant mode of inheritance observed in nearly all polyglutamine diseases. In the first test of this hypothesis, investigators inserted a 146-unit CAG repeat into the coding sequence of the housekeeping gene *hypoxanthine phosphoribosyl transferase* (*Hprt*; ORDWAY *et al.* 1997). This construct was then expressed in mice. Like humans with polyglutamine disease, mice expressing this modified *Hprt* construct developed neuronal inclusion bodies and a late-onset neurological phenotype that progressed to premature death (ORDWAY *et al.* 1997). This result indicated that long polyglutamine tracts could be toxic even when removed from the context of specific disease proteins. The next question was whether long polyglutamine tracts could be toxic in the absence of any flanking protein sequence. To test this, investigators generated several constructs encoding pure polyglutamine without

any flanking sequences. In cultured cells, expression of (CAG)80, (CAG)130, and (CAG)180, but not (CAG)27 or (CAG)40, caused cell-shrinkage, rounding and surface blebbing (BOK *et al.* 1999). Similar experiments in Drosophila revealed that expressing (CAG)108 causes tissue degeneration and lethality, whereas expressing (CAG)22 does not (MARSH *et al.* 2000). These experiments demonstrated convincingly that long polyglutamine tracts are intrinsically toxic.

Polyglutamine is toxic in the nucleus:

Once studies established that long polyglutamine tracts are toxic, investigators turned to addressing the potential mechanisms underlying this toxicity. The presence of nuclear inclusion bodies in most polyglutamine diseases suggested that mutant polyglutamine proteins might disturb the cell by interfering with processes in the nucleus. This model predicts that preventing mutant polyglutamine proteins from entering the nucleus would impede their toxicity. Investigators tested this model by performing experiments in which they forcibly prevented pathogenic polyglutamine proteins from entering the nucleus.

Ataxin-1 is encoded by the *SCA1* gene. This protein possesses a nuclear localization signal (NLS), and thus under normal and disease conditions, a fraction of ataxin-1 can be found in the nucleus. By mutating the NLS, one group addressed whether nuclear localization of ataxin-1 is required for polyglutamine-induced pathogenesis in SCA1 (KLEMENT *et al.* 1998). Using mice, investigators expressed a mutant *SCA1* construct bearing a pathogenic (CAG)82 repeat and a mutated NLS. These mice were compared to mice expressing a similar control construct that possessed an

intact NLS. Whereas mice expressing the control construct developed ataxia and Purkinje cell pathology, these defects were not seen in mice expressing *SCA1* with the mutated NLS (KLEMENT *et al.* 1998). As expected, in mice with the NLS, expanded ataxin-1 was present in the nucleus, whereas in mice lacking the NLS, the expanded ataxin-1 remained in the cytoplasm.

Studies of spinal and bulbar muscular atrophy (SMBA) also indicate that the nucleus is the primary site of toxicity in this disease. SBMA is caused by polyglutamine expansions in the androgen receptor, encoded by the *AR* gene. Whereas males with expanded *AR* alleles develop SBMA, female carriers are generally asymptomatic. How could this be explained? Upon binding its ligand, the androgen receptor translocates to the nucleus. In females, however, nuclear translocation of androgen receptor is limited due to their low levels of androgen hormones. Together, these observations suggested that, to be toxic, mutant androgen receptor must translocate to the nucleus.

Experiments in mice and flies have supported this model of SBMA pathogenesis. Trangenic male mice carrying a full-length human *AR* gene with an expanded polyglutamine tract manifest late-onset neuromuscular phenotypes that resemble SBMA. These phenotypes are suppressed when testosterone levels are reduced by castration. Similarly, reducing testosterone by administering a luteinizing hormone releasing hormone agonist also suppresses the phenotypes in these mice (KATSUNO *et al.* 2004). In a Drosophila model of SBMA, expression of human *AR* with an expanded polyglutamine tract does not cause an overt phenotype. Upon ingestion of androgen, however, the mutant androgen receptor translocates to the nucleus and causes

neurodegeneration (TAKEYAMA *et al.* 2002). Taken together these results strongly indicate that mutant androgen receptor must localize to the nucleus to cause dysfunction.

Experiments in cell culture suggest that, although they can be toxic in the cytoplasm, the nucleus appears to be the primary site of polyglutamine toxicity. Using a 293T cell culture model, one group observed that a polyglutamine expanded huntingtin fragment was equally toxic whether it was targeted to the cytoplasm or to the nucleus (HACKAM *et al.* 1999). In contrast, using cultured striatal neurons, another group demonstrated that whereas an expanded huntingtin fragment caused neurodegeneration when in the nucleus, when forcibly exported to the cytoplasm, a similar fragment did not cause neurodegeneration (SAUDOU *et al.* 1998). A third group used neuro-2a cells to show that attaching a nuclear localization signal to an expanded huntingtin fragment increased cell death by 111% compared to an unmodified control fragment (PETERS *et al.* 1999). By contrast, attaching a nuclear export signal reduced cell death by 56%.

The role of protein aggregation in polyglutamine pathogenesis:

The observation that inclusion bodies accumulate in all polyglutamine diseases, suggested that abnormal protein aggregation might play a critical role in disease pathogenesis. To determine whether inclusion bodies contribute to the pathogenesis of polyglutamine diseases, one group investigated the role of protein aggregation in a mouse model of SCA1. The ataxin-1 protein possesses a self-association domain, a domain essential for aggregate formation in a mouse model of SCA1. When expressing an expanded *SCA1* transgene carrying an intact self-association domain, mice developed

neuropathology and inclusion bodies. Mice expressing a similar transgene containing a deletion of the self-association domain also manifest pathology. The pathology in these mice, however, developed without any visible inclusion bodies (KLEMENT *et al.* 1998). In cultured striatal cells expressing an expanded huntingtin fragment there is no correlation between inclusion formation and cell death (SAUDOU *et al.* 1998). Similarly, though inclusion bodies accumulate in cultured motor neurons expressing expanded androgen receptor, there is no correlation between inclusion formation and cell death (SIMEONI *et al.* 2000). Taken together, these data suggest that inclusion bodies are neither necessary nor sufficient for polyglutamine-induced toxicity.

Studies of molecular chaperones support the idea that inclusion bodies are not the toxic entities in polyglutamine diseases. Molecular chaperone are prominent constituents of inclusion bodies, an observation that suggested these proteins might have a role in polyglutamine pathogenesis (CUMMINGS *et al.* 1998; PAULSON 1999; CHAI *et al.* 1999). Molecular chaperones assist in normal protein folding and in the refolding of misfolded proteins. Thus the presence molecular chaperones in inclusion bodies raised the possibility that protein misfolding might contribute to pathogenesis in polyglutamine diseases. One idea was that molecular chaperones recognize misfolded polyglutamine proteins and prevent their aggregation. In this model, inclusion bodies form because there are not enough molecular chaperones available to prevent the aggregation of misfolded polyglutamine proteins. This model predicts that increasing chaperone activity ought to prevent the misfolding, aggregation, and subsequent deposition of polyglutamine proteins into inclusion bodies.

To test this model, several groups investigated the effects of chaperone expression on inclusion body formation of polyglutamine proteins. In cell culture, expression of the chaperone HDJ-2 significantly suppresses the accumulation of inclusion bodies caused by mutant ataxin-1 or mutant androgen receptor (CUMMINGS *et al.* 1998; STENOIEN *et al.* 1999). In PC12 neurons, in addition to suppressing inclusion body formation, the chaperone HDJ-1 suppresses the cell death caused by a GFP-polyglutamine (80Q) fusion protein (CHAI *et al.* 1999). These results demonstrated that molecular chaperones are capable of suppressing inclusion body formation, and in some cases this suppression correlates with reduced polyglutamine toxicity. Although this correlation seemed to suggest that inclusion bodies might underlie polyglutamine pathology, this interpretation was difficult to reconcile with previous studies that indicated inclusions were not required for pathogenesis (KLEMENT *et al.* 1998; SAUDOU *et al.* 1998).

Subsequent studies of molecular chaperones again challenged the idea that inclusions cause toxicity. In Drosophila, overexpression of either Hsp70 or dHDJ-1 significantly suppresses polyglutamine-induced neurodegeneration (WARRICK *et al.* 1999; KAZEMI-ESFARJANI and BENZER 2000). Unlike the effects in PC12 neurons, however, in Drosophila chaperones suppressed polyglutamine toxicity without visibly affecting aggregate formation. Similar results have been seen in mice. In a mouse model of SCA1, overexpression of Hsp70 suppresses polyglutamine-induced pathology and the associated behavioral phenotypes (CUMMINGS *et al.* 2001). As seen in Drosophila, Hsp70 expression has no clear influence on aggregate formation when analyzed by light microscopy.

If molecular chaperones can suppress polyglutamine-induced toxicity without necessarily influencing inclusion body formation, then how do these proteins mitigate toxicity? *In vitro* studies demonstrated that molecular chaperones can change the physical properties of expanded polyglutamine proteins. These studies found that molecular chaperones can change the solubility of inclusion bodies and the proteins contained within, a change that was not discernible by light microscopy (MUCHOWSKI *et al.* 2000). Findings in Drosophila are consistent with these *in vitro* findings. In Drosophila, chaperones suppress the toxicity of a truncated ataxin-3 fragment bearing an expanded polyglutamine tract (78Q). Though the chaperones did not visibly alter inclusion body formation, biochemical analyses revealed that chaperone expression increased the solubility of the expanded ataxin-3 protein (CHAN *et al.* 2000). Collectively, these observations suggested that insoluble polyglutamine oligomers might be the toxic agents in polyglutamine disease and that molecular chaperones might suppress toxicity by making these oligomers more soluble. This idea is strongly supported by studies demonstrating that using Congo red to inhibit formation of polyglutamine oligomers significantly decreases the toxicity of an expanded huntingtin fragment (SANCHEZ *et al.* 2003).

Although the observations from cell culture and Drosophila indicated that molecular chaperones could substantially influence polyglutamine toxicity, results in mice have been mixed. In transgenic mice expressing an *SCA1* allele with a polyglutamine expansion (82Q), overexpression of Hsp70 suppresses neuropathology and behavioral phenotypes without visibly affecting inclusion body formation (CUMMINGS *et al.* 2001). In mice expressing androgen receptor carrying a polyglutamine expansion

(97Q), overexpression of Hsp70 also suppresses neuropathology and behavioral phenotypes (ADACHI *et al.* 2003). Along with suppressing polyglutamine toxicity, Hsp70 also reduces the overall abundance of both insoluble and soluble species of mutant androgen receptor, suggesting that Hsp70 may promote degradation of the mutant androgen receptor. Contrasting with these findings, however, Hsp70 did not significantly influence the pathology of mice expressing a truncated huntingtin fragment bearing a polyglutamine expansion (150Q; HANSSON *et al.* 2003). Likewise, neither Hsp70 nor HDJ-2 suppressed the inclusion formation and retinal degeneration observed in a mouse model of SCA7 (HELMLINGER *et al.* 2004). The results from mice, though mixed, suggest that, at least in some cases, molecular chaperones can mitigate the toxicity of expanded polyglutamine. Though it is not clear why chaperones do not influence polyglutamine toxicity in all mouse models, these apparent inconsistencies might reflect differences in expression levels of polyglutamine and chaperone proteins between the different model systems. Another possibility is that these inconsistencies reflect fundamental differences in the pathogenic mechanisms underlying the various polyglutamine diseases.

Some observations suggest that molecular chaperones may provide protection independent of their effects on aggregate formation or protein solubility. Molecular chaperones have well documented anti-apoptotic effects (reviewed in CREAGH *et al.* 2000). Given this, one possibility is that molecular chaperones suppress polyglutamine-induced toxicity by preventing apoptosis. One group addressed this possibility by analyzing the anti-apoptotic effects of molecular chaperones in cells expressing a truncated huntingtin fragment with a polyglutamine expansion (120Q). This study

showed that in HEK293 cells, expression of the chaperones Hsp40, Hsp70, or N-ethylmaleimide-sensitive factor suppressed polyglutamine-induced cell death (ZHOU *et al.* 2001). Even though all three chaperones suppressed cell death, only Hsp40 had any effect on inclusion body formation or protein solubility. Significantly, however, all three chaperones prevented mutant huntingtin from activating caspase-3 and caspase-9, suggesting that chaperones can indeed mitigate the pro-apoptotic effects of expanded polyglutamine proteins.

The role of aberrant transcription in polyglutamine pathogenesis:

Several observations suggest that transcriptional dysregulation might contribute to polyglutamine disease pathology. First, as mentioned above, several studies suggest that the nucleus is the primary site of polyglutamine toxicity. Second, nuclear inclusion bodies contain numerous proteins that regulate gene transcription. These proteins include the general transcription factor TATA-binding protein and the transcriptional coactivators TAFII130 and CREB-binding protein. Finally, several polyglutamine disease proteins normally regulate transcription.

CREB-binding protein is a transcriptional coactivator that functions by regulating the activity of the cAMP-response-element-binding protein (CREB). CREB-binding protein is present in the inclusion bodies of several polyglutamine diseases and several disease models. In cultured cells, CREB-binding protein localizes to aggregates of expanded forms of androgen receptor (mutated in SBMA), and ataxin-3 (mutated in SCA3; MCCAMPBELLL *et al.* 2000). CREB-binding protein also localizes to aggregates in the brains of HD transgenic mice and brain tissue from SBMA, HD, and

DRPLA patients (MCCAMPBELL *et al.* 2000; STEFFAN *et al.* 2000; NUCIFORA *et al.* 2001). In HD patients, the redistribution of CREB-binding protein into aggregates reduces the levels of soluble CREB-binding protein in cells.

Taken together, these observations suggested that reduced levels of CREB-binding protein might contribute to polyglutamine-induced pathology. Proper levels of CREB-binding protein are essential, as demonstrated by Rubinstein-Taybi syndrome, a serious developmental disorder caused by haploinsufficiency of the CREB-binding protein gene (PETRIJ *et al.* 1995). To address whether reduced CREB-binding protein activity might contribute to polyglutamine disease pathology, several groups investigated whether modulating CREB-binding protein activity influences polyglutamine-induced toxicity. One cell culture study revealed that overexpression of CREB-binding protein suppresses cell death caused by truncated androgen receptor fragments carrying polyglutamine expansions (MCCAMPBELL *et al.* 2000). In other studies, similar results were observed using truncated fragments of huntingtin carrying polyglutamine expansions (STEFFAN *et al.* 2000; NUCIFORA *et al.* 2001). These results supported the idea that mutant polyglutamine proteins exert toxicity, in part, through sequestering CREB-binding protein.

CREB-binding protein is a histone acetyl transferase. It is recruited to specific sites of transcription by the cAMP response-element binding protein (CREB) where, by acetylating histones, it alters chromatin structure to favor transcription (Figure 1.2; reviewed in MARMORSTEIN 2001). Thus, the function of CREB-binding protein suggested that it suppresses polyglutamine toxicity by directly promoting transcription of CREB-responsive genes. This model suggested that increasing transcription by alternate

means would also relieve polyglutamine toxicity. To address this, investigators turned to manipulating the activities of histone deacetylases.

By repressing transcription histone deacetylases (HDACs) directly oppose the activities of histone acetyltransferases like CREB-binding protein. Inhibiting the activities of HDACs thus promotes transcription. To clarify whether CREB-binding protein suppresses polyglutamine toxicity through its positive effects on transcription, investigators determined whether inhibition of HDACs could also suppress this polyglutamine. In these experiments, investigators tested the effects of several chemical inhibitors of HDAC activity. In yeast, a GFP-polyglutamine (75Q) fusion protein represses the transcription of a reporter gene. In the presence of the HDAC inhibitor Trichostatin A, however, this effect is mitigated (HUGHES *et al.* 2001). Consistent with this result, in Drosophila, polyglutamine-induced neurodegeneration is suppressed by the HDAC inhibitor suberoylanilide hydroxamic acid (STEFFAN *et al.* 2001). Suberoylanilide hydroxamic acid is also effective in mice. In a mouse model of Huntington disease, this HDAC inhibitor ameliorated neuropathology and motor deficits caused by expression of a mutant huntingtin fragment (HOCKLY *et al.* 2003). In a mouse model of SBMA, the HDAC inhibitor sodium butyrate suppresses neuromuscular pathology and motor deficits caused by expansions in the androgen receptor (MINAMIYAMA *et al.* 2004). The finding that polyglutamine toxicity can be suppressed by HDAC inhibition and CREB-binding protein overexpression, strongly suggests that transcriptional repression contributes substantially to polyglutamine toxicity.

Further support for the role of aberrant transcription in these diseases has come from analyzing the normal functions of polyglutamine disease genes. Initially, investigators did not emphasize the potential relationship between disease pathogenesis and the normal functions of these genes. The lack of interest in normal gene function was fueled by the observed intrinsic toxicity of polyglutamine tracts and by the striking lack of homology among the disease proteins. These observations supported a paradigm in which the disease proteins were viewed as irrelevant carriers of the toxic polyglutamine entity. The accumulated data on the normal functions of these genes now challenges this simplified view.

The first polyglutamine disease gene identified, *AR*, encodes the androgen receptor, a ligand-activated transcription factor (LA SPADA *et al.* 1991; reviewed in MCEWAN 2004). Upon activation, the androgen receptor binds DNA and activates target gene expression through physical interactions with transcriptional coactivators and components of the general transcription machinery. Polyglutamine expansions in the androgen receptor appear to cause pathology by interfering with some of these interactions. Aberrant interaction of the mutant androgen receptor with CREB-binding protein causes abnormal transcriptional repression of vascular endothelial growth factor (VEGF; SOPHER *et al.* 2004). The resulting reduction in VEGF levels contributes substantially to motor neuron degeneration in these mice.

Ataxin-7 (SCA7) is a component multi-subunit TFTC and STAGA transcriptional complexes. Though incompletely characterized, these complexes are related to the yeast SAGA complex, a transcriptional coactivator complex that acts on a subset of RNA polymerase II-dependent genes (GRANT *et al.* 1998). Like the yeast SAGA complex,

TFTC/STAGA complexes also contain histone acetyltransferase activity. In the retina, a tissue affected in SCA7, ataxin-7 interacts with Crx, an essential photoreceptor-specific transcriptional activator required for the expression of several photoreceptor genes (LA SPADA *et al.* 2001; LIVESEY *et al.* 2000). Polyglutamine expansions in ataxin-7 cause it to strongly repress Crx mediated transcriptional activation, causing cellular dysfunction and degeneration.

TBP (SCA17) associates with TBP-associated factors (TAFs) to form the multi-subunit complex TAFIID (reviewed in CHEN and HAMPSEY 2002). The TAFIID complex is essential for the expression of most, if not all, protein encoding genes. TBP is the DNA-binding subunit of TAFIID, and it can stimulate transcription alone *in vitro*.

Atrophin-1 (DRPLA) normally binds to and colocalizes with the transcriptional corepressor ETO/MTG8. In cell culture, mammalian atrophin-1 can repress transcription (WOOD *et al.* 2000). Drosophila atrophin-1 functions as a transcriptional repressor in multiple developmental processes (ZHANG *et al.* 2002). Drosophila atrophin-1 protein binds to the transcriptional repressor Even-skipped, and is required *in vivo* for the activity of this protein. Human and Drosophila atrophin-1 proteins can function *in vivo* to repress the transcription of a reporter construct (ZHANG *et al.* 2002).

Ataxin-3 (SCA3) is a transcriptional corepressor. Overexpression of ataxin-3 inhibits transcription of a reporter gene under control of the cAMP-response element, the target of the transcriptional activator CREB (LI *et al.* 2002). Ataxin-3 inhibits CREB-mediated transcription by physically binding to histones and blocking their acetylation by transcriptional coactivators such as CREB-binding protein.

Though several studies indicate that the *HD* gene participates in vesicle trafficking (WANKER *et al.* 1997; KALCHMAN *et al.* 1997; VELIER *et al.* 1998; METZLER *et al.* 2001), other studies indicate that *HD* might also have roles in regulating transcription. One study found that full-length huntingtin physically interacts with the transcriptional corepressor C-terminal binding protein and represses transcription when targeted to DNA (KEGEL *et al.* 2002). Another study found that full-length huntingtin promotes transcription of specific genes by inhibiting the activity of the neuron restrictive silencing factor protein (ZUCCATO *et al.* 2003). Huntingtin also interacts with the nuclear receptor co-repressor, a protein that represses the activity of sequence-specific ligand activated receptors (BOUTELL *et al.* 1999).

The above observations strongly suggest that polyglutamine expansions are toxic because they interfere with transcriptional processes, processes that polyglutamine disease proteins normally regulate. Thus, for some polyglutamine diseases, the data suggest that the normal function of the disease gene is directly related to the pathogenic mechanism. Not all polyglutamine disease genes appear to function in transcription, however. This observation raises the possibility that disruptions in processes other than transcription might underlie some polyglutamine diseases. Given that polyglutamine expansions can disrupt processes regulated by proteins carrying these expansions, understanding the normal functions of all polyglutamine disease genes might advance our understanding of the mechanisms underlying these diseases.

This dissertation focuses on the polyglutamine disease spinocerebellar ataxia type 2 (SCA2). In contrast to other polyglutamine diseases, the *SCA2* gene does not appear to regulate transcription, and SCA2 does not appear to stem from transcriptional

dysregulation. The normal function of the *SCA2* gene and the mechanism of SCA2 pathogenesis are unclear. To better understand pathogenic mechanisms underlying polyglutamine diseases, I have used *Drosophila melanogaster* as a model system to elucidate the normal function of the *SCA2* gene. Below I summarize the known features of this disease and of the *SCA2* gene.

SPINOCEREBELLAR ATAXIA TYPE 2

The "W" family of Rhode Island, first reported in 1969, was a five-generation kindred of Anglo-Saxon origin, segregating an autosomal dominant adult-onset ataxia. Clinical findings suggested these patients had dysfunction of several brain regions, including the olivary nuclei, pons, and cerebellum (BOLLER and SEGARRA *et al.* 1969; POGACAR *et al.* 1978). Based on this observation, this disease was classified as an "olivopontocerebellar ataxia." Although the disease segregating in the "W" family appeared similar to spinocerebellar ataxia type 1 (SCA1), it was not linked to the same genetic region and thus appeared to represent a novel SCA locus. This disease was designated "spinocerebellar ataxia type 2" (SCA2; LAZZARINI *et al.* 1992; RANUM *et al.* 1992).

Population Studies of SCA2:

Several studies have looked at the prevalence of SCA2 in various populations. SCA2 is classified as an autosomal dominant cerebellar ataxia. Autosomal dominant cerebellar ataxias have a worldwide prevalence of between 0.3-2.0 per 100,000 (VAN

DE WARRENBURG *et al.* 2002). Worldwide, studies estimate that SCA2 accounts for 5.9 to 29% of autosomal dominant cerebellar ataxias, with most estimates in the range of 10-14% (RIESS *et al.* 1997: GESCHWIND *et al.* 1997; SCHOLS *et al.* 1997; WATANABE *et al.* 1998; PAREYSON *et al.* 1999; SALEEM *et al.* 2000; STOREY *et al.* 2000). SCA2 appears to have particularly high prevalence in Cuba, India, and among ethnic Malay families in Singapore (OROZCO *et al.* 1989; SALEEM *et al.* 2000; ZHAO *et al.* 2002). The prevalence in the Holguin province of Cuba is 41 per 100,000 among persons of Spanish ancestry (OROZCO *et al.* 1989).

Neuropathological and clinical features of SCA2:

Several brain regions can be affected in SCA2. The core abnormality in SCA2 is degeneration of the inferior olivary nuclei, pons, and cerebellum, though degeneration can be observed in several brain tissues. As with other polyglutamine diseases,s widespread atrophy can occur in SCA2, especially in severe cases, with larger repeat expansions and earlier age of onset (GIUFFRIDA *et al.* 1999). In some cases, investigators have observed degeneration of the substantia nigra, striatum, pallidum, cerebral cortex, and retina (ESTRADA *et al.* 1999). SCA2 patients can also manifest symptoms outside the central nervous system. Peripheral sensory and sensorimotor neuropathy is a relatively common finding in SCA2. Electrophysiological studies and nerve biopsies have revealed evidence of aberrant nerve conduction and chronic axonopathy in the peripheral nervous system (BALE *et al.* 1998; SPADARO *et al.* 1998; MALANDRINI *et al.* 1998; KUBIS *et al.* 1999; VAN DE WARRENBURG *et al.* 2004).

Several clinical features are associated with SCA2. As with other SCAs, the primary finding is loss of coordination (ataxia). This feature derives from loss of the cerebellar Purkinje cells. Cerebellar Purkinje cells are a central site for integrating sensory inputs and controlling motor outputs. Other common features of SCA2 include abnormally slow eye movements (slow saccades), slow reflexes, and slurred speech (dysarthria). These symptoms derive from dysfunction of the midbrain, inferior olivary nuclei, and cerebellum, respectively. Consistent with reports of cerebral atrophy, several studies have reported dementia in SCA2, with one reporting it in 25% of patients studied (POGACAR *et al.* 1978; SASAKI *et al.* 1998; BURKE *et al.* 1999). Other, less common SCA2 features, include muscle twitching (fasciculations), unusually limp or stiff muscle tone (dystonia), spasmodic movements (chorea), difficulty swallowing (dysphagia), and sudden muscle jerks (myoclonus). SCA2 with infant onset (60 and >200 repeats) can be associated with delays in language acquisition and motor skill development. Additionally, these young patients can show drooling, incontinence, arm tremor, retinal degeneration (retinitis pigmentosa), and reduced muscle tone (hypotonia) (BABOVICH-VUKSANOVIC *et al.* 1998; MORETTI *et al.* 2004).

Recent studies have shown that repeat expansions in the *SCA2* gene can cause symptoms that resemble Parkinson disease. Several studies have linked *SCA2* mutations with parkinsonism in people of diverse ethnic backgrounds (SHAN *et al.* 2001; FURTADO *et al.* 2002; LU *et al.* 2004; RAGOTHAMAN *et al.* 2004). These patients often have features typical of Parkinson disease, including tremor, rigidity, and slowness of movement (bradykinesia). Most patients respond well to L-dopa therapy (GWINN-HARDY *et al.* 2000). The clinical findings of parkinsonism are consistent with the

observed degeneration of the substantia nigra in some patients carrying expanded *SCA2* alleles (INFANTE *et al.* 2004; OROZCO *et al.* 1989; ESTRADA *et al.* 1999).

Identification of the *SCA2* gene:

In the early 1990s several groups began mapping the SCA2 locus. By 1992 at least two families had been reported to segregate an autosomal dominant SCA that was clinically distinct from Machado-Joseph disease (later named SCA3) and not linked to the SCA1 locus. Based on linkage studies of families in Holguin, Cuba, this new locus, "SCA2", was assigned to the chromosomal region 12q23-24. Haplotype studies identified a common disease haplotype in these patients, indicating the presence of a founder effect and thus explaining the high prevalence of SCA2 in this population. Subsequently, other groups reported pedigrees with autosomal dominant cerebellar ataxia linked to 12q (PULST *et al.* 1993, BELAL *et al.* 1994, IHARA *et al.* 1994). In one study, investigators observed genetic anticipation in fourteen of fifteen parent-child pairs. Because anticipation was also observed in families with SCA1, a triplet repeat expansion disease, the authors of this study suggested that triplet repeat expansion also underlies SCA2 (PULST *et al.* 1993). In 1996, using various methods for identifying triplet repeat expansions, three groups identified the SCA2 locus (PULST *et al.* 1996, SANPEI *et al.* 1996, IMBERT *et al.* 1996). As predicted, the investigators found that the SCA2 mutation is a CAG triplet repeat expansion. The newly identified gene was designated "*SCA2*". The CAG repeat lies in the coding region of the *SCA2* gene and thus encodes a polyglutamine tract. Normal alleles were reported to range from 15-29 repeats, whereas disease-causing alleles ranged from 35-59 repeats. The groups also observed a strong

inverse correlation between age of onset and CAG repeat number (SANPEI *et la.* 1996; IMBERT *et al.* 1996).

Features of the *SCA2* gene product:

The *SCA2* gene encodes the 1312 residue ataxin-2 protein. Ataxin-2 is a widely expressed cytoplasmic protein that is conserved in organisms including *S. cerevisae*, *C. elegans*, *D. melanogaster*, and *M. musculus*. The polyglutamine repeat of ataxin-2 is located in the amino terminus of the protein. Just downstream of the repeat are Sm1 and Sm2 motifs, motifs known to function in RNA splicing, turnover, and translation (NEUWALD and KOONIN *et al.* 1998). The carboxyl terminus of ataxin-2 contains a PAM2 motif, a motif known to interact with poly(A)-binding protein (PABP), a key regulator of mRNA translation (KOZLOV *et al.* 2001; reviewed in KAHVEJIAN *et al.* 2001). The evolutionary conservation of ataxin-2 proteins is limited to the regions containing Sm1/Sm2 and PAM2 motifs, the only regions predicted to have any structure. The remainder of the protein is predicted to be non-globular (ALBRECHT *et al.* 2004).

The presence of the N-terminal Sm motifs in ataxin-2 suggests that ataxin-2 may interact directly with RNA molecules. Sm motifs and like-Sm (Lsm) motifs are evolutionarily ancient motifs that function in several aspects of RNA metabolism. Sm proteins assemble into hexameric and heptameric ring structures that appear essential for their functions. In bacteria, Sm proteins can function in turnover and translation of RNA (STORZ *et al.* 2004). Whereas in eukaryotes, Sm proteins are most well known as the proteins providing the core structure of spliceosomal RNP complexes in the nucleus,

though they also function in mRNA turnover (reviewed in PANNONE and WOLIN 2000).

The PAM2 motif resides in the carboxyl terminus of ataxin-2. Several proteins utilize PAM2 motifs to interact with the global translational regulator poly(A)-binding protein (PABP; ROY *et al.* 2002; KOZLOV *et al.* 2004), and thus the presence of this motif in ataxin-2 suggests that this protein may interact with PABP and thereby translation. PABP appears to promote translation, in part, by promoting interactions between the 5' and 3' ends of mRNAs (Figure 1.3). Proteins containing PAM2 motifs can either promote or inhibit this activity of PABP, and thus these proteins can be positive or negative regulators of translation (CRAIG *et al.* 1998; KHALEGHPOUR *et al.* 2001). The influence of PAM2 proteins is significant as interfering with their functions can have severe phenotypic consequences (ROY *et al.* 2004).

The molecular pathology of SCA2:

Ubiquitinated nuclear inclusion bodies are a prominent feature of most polyglutamine diseases. In contrast to this pattern, however, nuclear inclusion bodies are rarely observed in SCA2 patients (HUYNH *et al.* 1999; PANG *et al.* 2002). Instead, ataxin-2 protein accumulates in cytoplasmic inclusion bodies. Thus, in normal and disease states, ataxin-2 maintains a cytoplasmic distribution. The finding that ataxin-2 localizes to the cytoplasm in both normal and disease states distinguishes SCA2 from most polyglutamine diseases and raises the possibility that SCA2 arises from pathogenic mechanisms distinct from other polyglutamine diseases.

To elucidate the pathogenic mechanisms underlying SCA2, investigators developed a mouse model of the disease. They found that transgenic mice expressing an *SCA2* construct with 58 CAG repeats (58Q) show functional and anatomic changes similar to the changes observed in SCA2 patients (HUYNH *et al.* 2000). Though the ataxin-2(58Q) protein clearly causes neural dysfunction in these mice, it remains in the cytoplasm. This contrasts sharply from results in SCA1 mice, where mutant ataxin-1 must localize to the nucleus to cause pathology (KLEMENT *et al.* 1998). These results indicate that SCA2 arises from disturbances originating in the cytoplasm.

Studies of *SCA2* and its homologs:

Studies of ataxin-2 suggest that this protein functions in several processes (Figure 1.4). One study revealed that ataxin-2 interacts with ataxin-2-binding protein, a putative RNA binding protein (SHIBATA *et al.* 2000). Both proteins localize and fractionate with markers of the Golgi apparatus. Another study showed that ataxin-2 is required for neuroblastoma cells to respond to apoptotic stimuli (WIEDEMEYER *et al.* 2003). Ataxin-2-related protein, a human homolog of ataxin-2, binds to the cytoplasmic domain of the thrombopoeitin receptor (MEUNIER *et al.* 2002). Upon receptor activation it is released and phosphorylated.

Studies of *SCA2* orthologs from distantly related organisms suggest that this family of genes functions in RNA metabolism. Nearly all ataxin-2 orthologs contain the PABP-interacting PAM2 motif (SATTERFIELD *et al.* 2002). Consistent with this, experiments have demonstrated that both *C. elegans* and *S. cerevisiae* ataxin-2 orthologs (ATX2 and Pbp1p, respectively) physically interact with PABP (Figure 1.4; CIOSK *et al.*

2004; MANGUS *et al.* 1998). Interestingly, this interaction takes place in yeast even though Pbp1p does not have a discernible PAM2 motif.

A link between ataxin-2 proteins and RNA metabolism is also supported by genetic studies. Mutations in the yeast *SCA2* ortholog (*PBP1*) alter polyadenylation of mRNAs and cause a petite-negative phenotype, the inability to live without mitochondrial DNA (MANGUS *et al.* 1998; DUNN and JENSEN 2003). Null mutations in *PBP1* can also suppress the lethality caused by mutations in the yeast PABP gene (*PAB1*), indicating that *PBP1* and *PAB1* have opposing activities (Figure 1.4; MANGUS *et al.* 1998). Because PABP promotes mRNA translation, this genetic interaction indicates that *PBP1* might act to inhibit this process. In *C. elegans*, reduced activity of *ATX2* causes ectopic translation of germline mRNAs that are normally repressed (Figure 1.4; CIOSK *et al.* 2004). This alteration causes the hermaphrodite germline to become abnormally masculinized.

Given the substantial evidence that SCA2 derives from a cytoplasmic disturbance, a distinct possibility is that this disease arises through mechanisms distinct from other polyglutamine diseases. Studies on the normal functions of several polyglutamine disease genes strongly suggest that, in these diseases, pathogenic mechanism is linked to normal gene function. This might also be true for SCA2. Unfortunately, the specific functions of ataxin-2 are not well understood, and studies of ataxin-2 function have been difficult to interpret. The data on ataxin-2 orthologs strongly suggest that these proteins function in various aspects of RNA metabolism, but the specific roles of these proteins in RNA metabolism remains unclear. This lack of information on ataxin-2 function has

made it difficult to develop models of how polyglutamine expansions in ataxin-2 cause SCA2 pathogenesis.

To further our understanding of SCA2 pathogenesis, I have chosen to investigate the potential relationship between normal ataxin-2 function and disease pathology. To do this, I have utilized genetic and biochemical approaches to study the *Drosophila melanogaster* ortholog of the *SCA2* gene.

Figure 1.1

Longer CAG repeats cause earlier age of onset in polyglutamine diseases. SCA2, spinocerebellar ataxia type 2; SCA1, spinocerebellar ataxia type 1; HD, huntington disease; DRPLA, dentatorubral pallidoluysian atrophy; SCA3, spinocerebellar ataxia type 3. (figure derived from Zoghbi and Orr 2000)

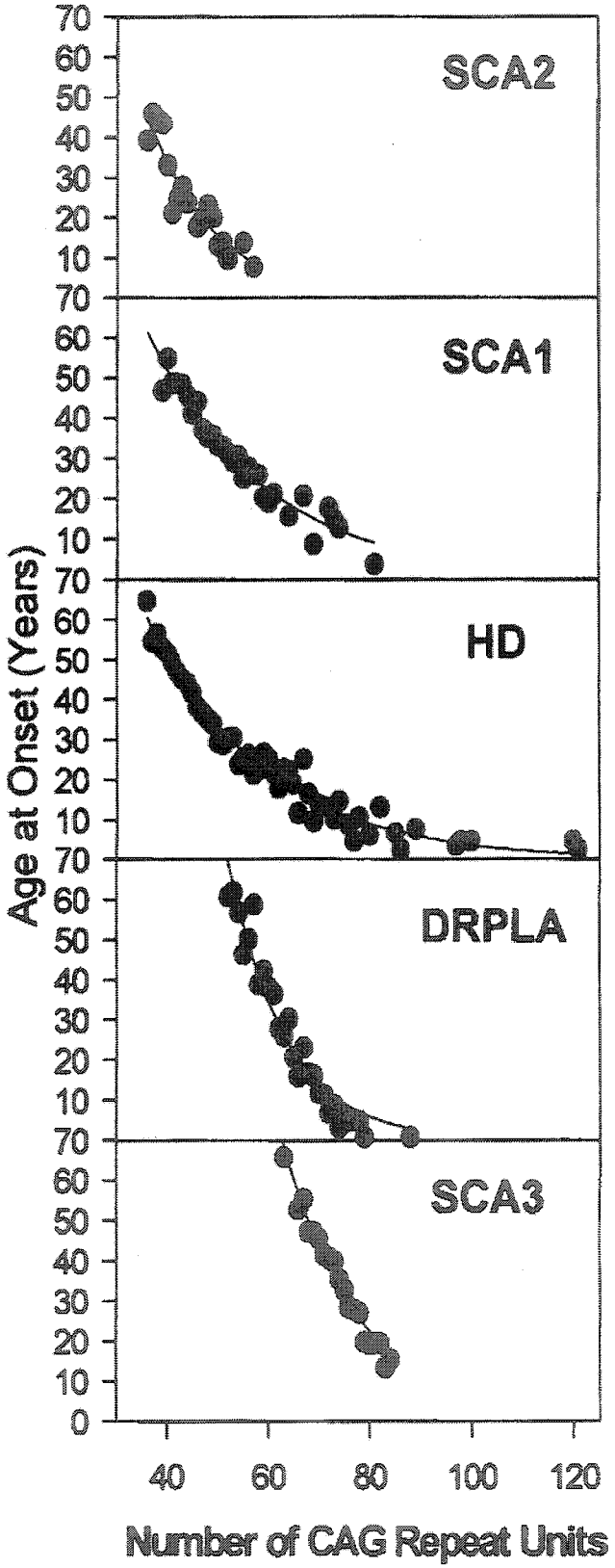
SCA2
SCA1
HD
DRPLA
SCA3
Age at Onset (Years)
Number of CAG Repeat Units
70
60
50
40
30
20
10
0
40
60
80
100
120

Figure 1.2

Polyglutamine proteins inhibit transcription. Expanded polyglutamine represses transcription by interfering with the activity of transcriptional coactivator proteins. Histone deacetylase inhibitors promote transcription, counteracting the repressive effects of expanded polyglutamine.

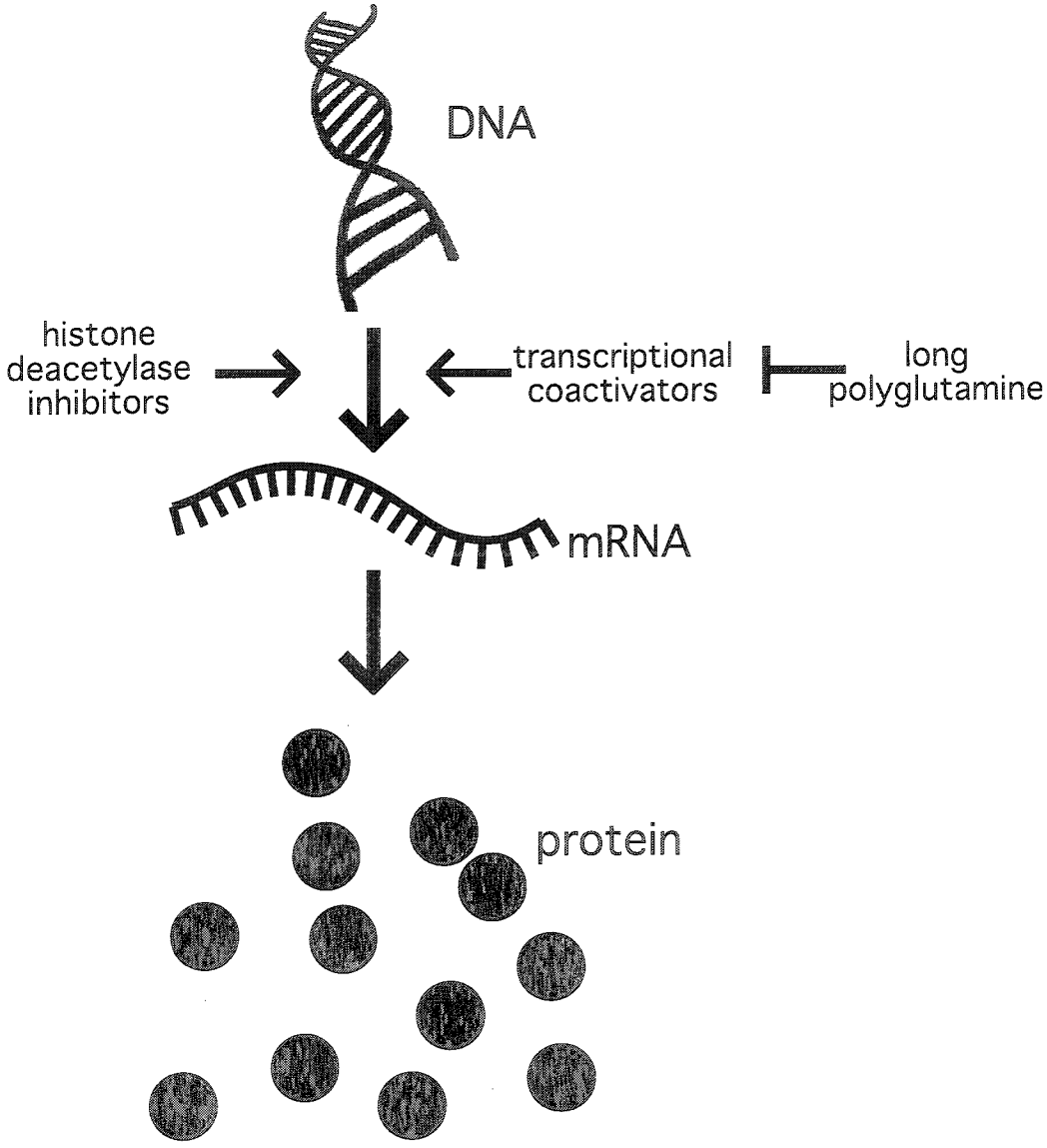
DNA
histone
deacetylase
inhibitors
transcriptional
coactivators
long
polyglutamine
mRNA
protein

Figure 1.3

Proposed activities for ataxin-2 proteins. Ataxin-2 sensitizes cells to apoptotic stimuli. Ataxin-2 localizes to the Golgi apparatus. An ataxin-2 ortholog, ataxin-2 related protein (A2RP) binds to the erythropoeitin receptor and is released and phosphorylated upon receptor activation.

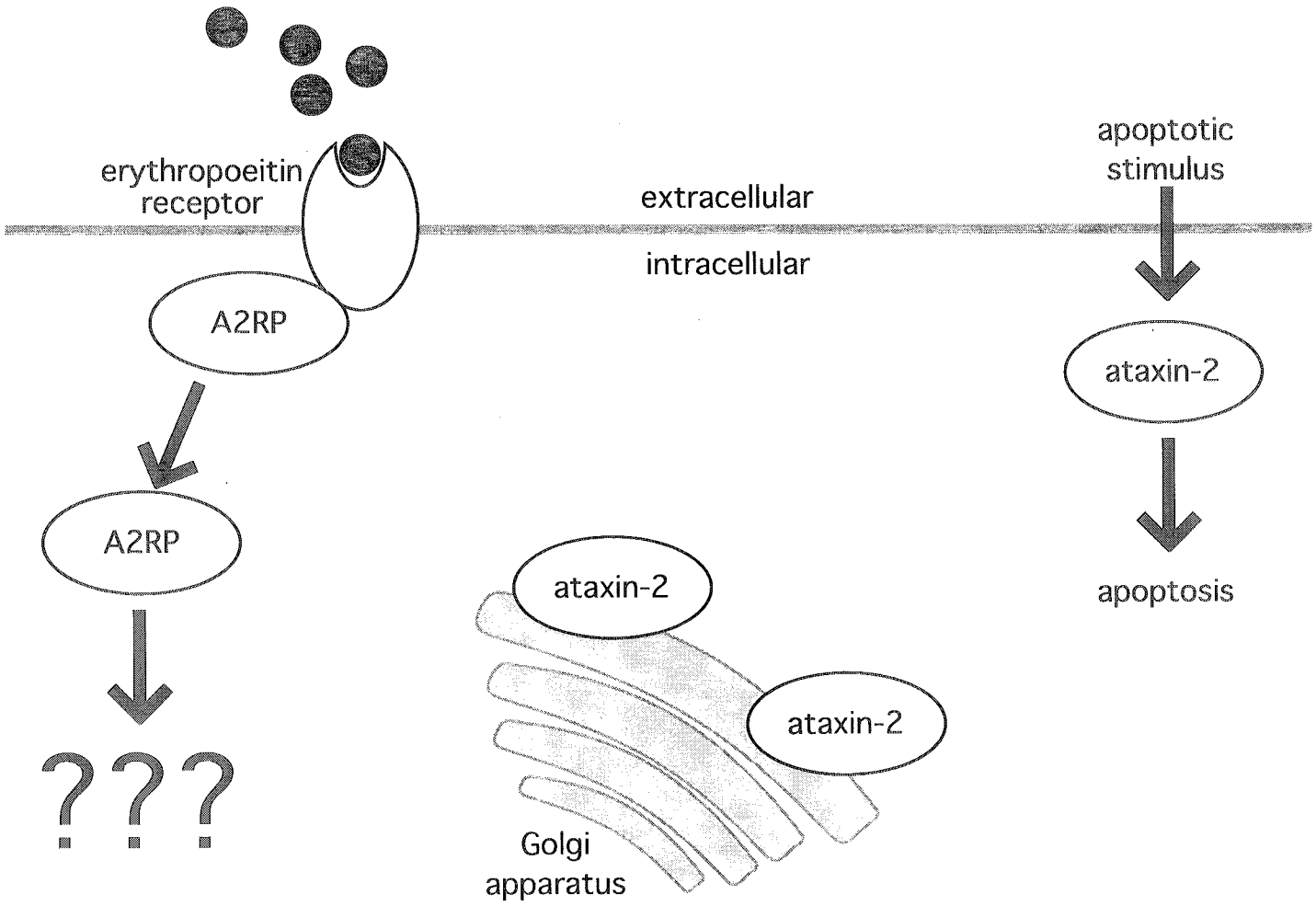
erythropoeitin
receptor
extracellular
intracellular
apoptotic
stimulus
A2RP
ataxin-2
A2RP
apoptosis
ataxin-2
ataxin-2
Golgi
apparatus
???

Table 1.1: Summary of Trinucleotide Repeat Diseases

Disease	Inheritance Pattern	Gene	Cellular Function	Protein	Repeat	Amino Acid	Repeat Size Normal	Repeat Size Disease	Repeat Location
Fragile X syndrome	X-linked	*FMR1*	mRNA translation	FMR-1 protein (FMRP)	CGG	none	6-53	>230	5'-UTR
Fragile XE syndrome	X-linked	*FMR2*	transcription	FMR-2 protein	GCC	none	6-53	>200	5'-UTR
Friedreich ataxia	autosomal recessive	*X25*	iron homeostasis	Frataxin	GAA	none	7-34	>200	Intron-1
Myotonic dystrophy	autosomal dominant	*DMPK*	kinase activity	Myotonic dystrophy protein kinase (DMPK)	CTG	none	5-37	50->1000	3'-UTR
Spinocerebellar ataxia type 8	autosomal dominant	*KLHL1*	???	none	CTG	none	16-37	110 to <250?	3'-Terminal exon (antisense?)
Spinocerebellar ataxia type 12	autosomal dominant	*SCA12*	phosphatase activity	PP2A-PR55β(PPP2R2B)	CAG	none	7-28	66-78	5'-UTR
Synpolydactyly	autosomal dominant	*HOXD13*	transcription	HOXD13	GCX	Ala	15	22-29	Coding
Cleidocranial dysplasia	autosomal dominant	*RUNX2*	transcription	Runx2	GCG GCA GCT	Ala Ala Ala	17	27	Coding
Oculopharyngeal muscular dystrophy	autosomal dominant	*PABPN1*	transcription	PABPN1	GCG GCA	Ala Ala	10	11-17	Coding
Holoprosenchephaly (HPE)	autosomal dominant	*ZIC2*	transcription	ZIC2	GCG GCA GCT	Ala Ala Ala	15	25	Coding
Hand-foot-genital syndrome	autosomal dominant	*HOXA13*	transcription	HOXA13	GCX	Ala	18	24-26	Coding
Blepharophimosis, ptosis and epicanthus inversus	autosomal dominant	*FOXL2*	transcription	FOXL2	GCX	Ala	14	22-24	Coding
Mental retardation; X-linked, with isolated growth hormone deficiency	X-linked	*SOX3*	transcription	SOX3	GCX	Ala	15	26	Coding
Infantile spasm syndrome, X-linked; Partington syndrome; lissencephaly with ambiguous genitalia, X-linked; mental retardation X-linked 36 and 54	X-linked	*ARX*	transcription	ARX	GCG GCA GCC	Ala Ala Ala	12-16	18-23	Coding
Congenital central hypoventilation syndrome/Ondine curse	autosomal dominant	*PMX2B*	transcription	PMX2B	GCG GCA GCC	Ala Ala Ala	20	25-29	Coding
Spinobulbar muscular atrophy	X-linked	*AR*	transcription	Androgen receptor (AR)	CAG	Gln	9-36	38-62	Coding
Huntington disease	autosomal dominant	*HD*	transcription	Huntingtin	CAG	Gln	6-35	36-121	Coding
Dentatorubral-pallidoluysian atrophy	autosomal dominant	*DRPLA*	transcription	Atrophin-1	CAG	Gln	6-35	49-88	Coding
Spinocerebellar ataxia type 1	autosomal dominant	*SCA1*	RNA transport	Ataxin-1	CAG	Gln	6-44	39-82	Coding
Spinocerebellar ataxia type 2	autosomal dominant	*SCA2*	???	Ataxin-2	CAG	Gln	15-31	36-63	Coding
Spinocerebellar ataxia type 3	autosomal dominant	*SCA3 (MJD1)*	transcription	Ataxin-3	CAG	Gln	12-40	55-84	Coding
Spinocerebellar ataxia type 6	autosomal dominant	*SCA6*	calcium homeostasis	α_{1A}-Voltage-dependent calcium channel subunit	CAG	Gln	4-18	21-33	Coding
Spinocerebellar ataxia type 7	autosomal dominant	*SCA7*	transcription	Ataxin-7	CAG	Gln	4-35	37-306	Coding
Spinocerebellar ataxia type 17	autosomal dominant	*TBP*	transcription	TATA-binding protein	CAG	Gln	25-44	50-63	Coding

adapted from Zoghbi and Orr 2000 and Brown and Brown 2004

CHAPTER 2:

A Drosophila Homolog of the Polyglutamine Disease Gene SCA2 Is a Dosage-Sensitive Regulator of Actin Filament Formation

SUMMARY

In this study we have used genetic and molecular approaches to investigate the normal function of a Drosophila homolog of the *SCA2* gene (*Datx2*). Like human ataxin-2, Datx2 is found throughout development in a variety of tissue types and localizes to the cytoplasm. Mutations that reduce *Datx2* activity or transgenic overexpression of *Datx2* result in female sterility, aberrant sensory bristles morphology, loss or degeneration of tissues, and lethality. These phenotypes appear to result from actin filament formation defects occurring downstream of actin synthesis. Further studies demonstrate that Datx2 does not assemble with actin filaments, suggesting that the role of Datx2 in actin filament formation is indirect. These results indicate that *Datx2* is a dosage-sensitive regulator of actin filament formation. Given that loss of cytoskeleton-dependent dendritic structure defines an early event in SCA2 pathogenesis, our findings suggest the possibility that dysregulation of actin cytoskeletal structure resulting from altered ataxin-2 activity is responsible for neurodegeneration in SCA2.

INTRODUCTION

To understand the mechanism of SCA2 pathogenesis, we are using Drosophila as a model system to investigate the normal cellular function of a *SCA2* homolog (*Datx2*). In this study, we show that the *Datx2* gene encodes a protein that is highly conserved with ataxin-2 in two domains, including a putative PABP interaction domain. Like its human counterpart, *Datx2* encodes a cytoplasmic protein present throughout development in a variety of tissue types, including the nervous system. Mutations that reduce *Datx2* activity, or transgenic overexpression of *Datx2* results in severe phenotypic consequences, including dysfunction, loss, or degeneration of mesoderm, nerve and other tissue types. Loss of *Datx2* function in the retina, sensory bristles, and female germline results in cellular and tissue morphological changes indicative of actin filament formation defects. Moreover, loss of function or overexpression of *Datx2* in these same tissues results in alterations in the structural characteristics of actin filaments. These phenotypes do not arise from alterations in the cellular abundance of actin, and Datx2 does not appear to assemble with actin filaments. Our results, coupled with other work linking several ataxin-2 family members to RNA metabolism (SHIBATA *et al.* 2000; MANGUS *et al.* 1998; KOZLOV *et al.* 2001), indicate that *Datx2* is a dosage-sensitive regulator of actin filament formation, possibly acting to control translation, stability, or localization of transcripts encoding mediators of actin polymerization. These findings may be relevant to the mechanism of neurodegeneration in SCA2, since loss of the actin-dependent dendritic arbor of cerebellar Purkinje cells is an early event in SCA2 pathogenesis (HUYNH *et al.* 2000). Our results provide a foundation for a direct test of this hypothesis.

MATERIALS AND METHODS

Molecular genetics and fly strains:

Genomic and cDNA sequences encoding the Drosophila ataxin-2 homolog were identified by searching the BDGP database (ADAMS et al. 2000; RUBIN et al. 2000) using a human ataxin-2 polypeptide query sequence (AAB19200). One of the Datx2 cDNA clones (GH2324) was fully sequenced and this sequence was compared to genomic DNA sequence to identify splice junctions in the Datx2 gene. The validity of the splicing arrangements predicted by the GH2324 cDNA clone was then verified by analyzing a larger collection of Datx2 cDNA clones (GH27029, SD08349, GH13857, LD47794) by restriction mapping, sequencing, and PCR. The Datx2 polypeptide sequence encoded by the GH27029 cDNA was aligned to human ataxin-2 (AAB19200), human ataxin-2 related protein (NP_009176), C. elegans ATX-2 (D2045.1), S. cerevisiae Pbp1p (NP_011694), and A. thaliana polypeptide sequences (F15I1.27 and MDC16.14) using the ClustalW algorithm. The developmental expression profile of *Datx2* was determined using the Rapid-Scan semiquantitative PCR system (Origene Technologies) following conditions suggested by the manufacturer. The PCR primers used for amplification of Datx2 were as follows: 5'GGCGTCTACAACAAC3' and 5'CCGAGAATGTGCGGAAT3'. These primers amplify sequences encoding the evolutionarily conserved ATX2N domain of Datx2. rp49 control primers were supplied with the cDNA panel. The insertion locations of the l(3)06490, EP(3)3022 and

EP(3)3145 P elements were confirmed by recovery and sequencing of DNA flanking the P elements. The GH27029 cDNA clone was subcloned into the pUAST vector (BRAND and PERRIMON 1993) as a Bgl II-Xho I fragment and used to generate germline transformant flies using standard procedures (ASHBURNER 1989). The Df(3R)Po4 stock, which removes the *Datx2* locus, was used in complementation and lethal phase analysis with the *Datx2* mutants. A minimum of 100 progeny were scored for each of these experiments. Females with germline clones of the *Datx2* mutations were generated using the FLP-DFS technique (CHOU and PERRIMON 1993). $Datx2^{X1}$ cuticle clones were generated by using a heatshock inducible FLP recombinase to drive mitotic recombination. With the exception of the Datx2 transgenic lines and the imprecise excision alleles of Datx2, all fly stocks described in this work were obtained from the Bloomington Stock Center or Berkeley Drosophila Genome Project.

Immunological methods:

The Datx2 antiserum was commercially prepared by immunizing rabbits with a synthetic peptide corresponding to residues 151-165 in Datx2 (SDKCNGARPDEKELE) conjugated to keyhole limpet hemocyanin (Research Genetics Corporation). Actin and tubulin antibodies were obtained from Chemicon and Sigma, respectively. Western blot analyses were performed essentially as described (TOLAR and PALLANCK 1998). Wild-type embryos were collected, fixed, and stained according to standard procedures. Ovaries were dissected, fixed and stained as described (JACKSON and BERG 1999). Ventral ganglion tissues, eye discs, and thoraces were dissected, fixed, and stained in the same manner as ovaries. Fluorescence microscopy of stained ovaries was carried out

using a Nikon MICROPHOT-FXA fluorescent microscope. Images were captured on 35mm Kodak Ektachrome slide film and digitally scanned using a Polaroid Sprint Scan 35 digital slide scanner. Optical sections of stained tissues were obtained on a Bio-Rad MRC600 confocal microscope and projected into a single plane in NIH Image.

Scanning electron microscopy:

Adult flies were dehydrated by 15 min incubations in a graded ethanol series. The dehydrated flies were treated with hexamethyldisilazane, mounted on SEM stubs, sputter coated with goldpalladium and examined with SEM.

TUNEL assays:

Eye discs from wandering third instar larvae were dissected in PBS and fixed at room temperature in 2% formaldehyde in PBS for 10 min. Discs were rinsed with PBTE (PBS plus 1mM EDTA and 0.2% Tween20), digested with proteinase K (10μg/ml) in PBS for 5 min at room temperature, rinsed with PBTE, refixed in 2% formaldehyde/PBS, and rinsed five times with PBS. TUNEL assays were performed with the Apo-BrdU TUNEL kit (Molecular Probes) according to manufacturer's instructions. Labeled discs were mounted in PBS/50% glycerol plus Vectashield, and analyzed by confocal microscopy as described above. As a control for apoptotic background using the EGUF/hid system, identically-staged eye discs bearing FRT82B Nmyc clones were examined. No significant apoptosis above background was detected.

Actin filament binding studies:

Ovaries were dissected in PBS, rinsed once in modified G-PEM buffer plus 0.05% Tween-20 (80mM PIPES, 1mM MgCl2, 1mM EGTA, 0.2mM GTP, 1mM DTT, 1mM PMSF, 1mM paclitexel, 1:100 dilution of phosphatase inhibitor and protease inhibitor cocktails (Sigma)), and homogenized in 20µl/ovary of the same buffer. Biotinylated phalloidin (Molecular Probes) was added to a final concentration of 0.15 units/ovary and incubated at room temperature with rotation for 30 min. Streptavidin-coated magnetic beads (Dynal) were prepared by blocking 30 min in PBS/5% BSA, rinsed and resuspended in modified G-PEM buffer. Phalloidin-bound complexes were precipitated by adding blocked beads (0.08µg/ovary) to the extracts and rotating at room temp for 30 min. Beads were collected magnetically, washed five times with PBS plus 0.05% Tween-20 and resuspended in 1/10 original volume of PBS. Complexes were then analyzed by immunoblotting according to standard protocols (TOLAR and PALLANCK, 1998).

RESULTS

Identification and characterization of a Drosophila SCA2 homolog:

To identify Drosophila homologs of the *SCA2* gene, the human ataxin-2 protein sequence was used to query the BDGP database (ADAMS *et al.* 2000; RUBIN *et al.* 2000). A single homolog of *SCA2* (designated *Datx2* was identified from this search. The *Datx2* gene maps to polytene region 88F-89A of the third chromosome and encodes a polypeptide of 1084 amino acids exhibiting 23% amino acid identity and 36% amino

acid similarity overall with human ataxin-2. Most of the sequence conservation is confined to two domains (here designated ATX2N and ATX2C) that correspond to the most highly conserved sequences in the ataxin-2 family (Figure 2.1). Sequences outside these two domains are poorly conserved among ataxin-2 family members and share no homology to other known or predicted proteins. The ATX2N domain of the ataxin-2 family contains Sm motifs, which are found in proteins involved in pre-mRNA splicing, snRNP biogenesis, and mRNA decapping (MAYES *et al.* 1999; HE and PARKER 2000; THARUN *et al.* 2000). The ATX2N and ATX2C sequences also align well to proteins known to bind to PABP (MANGUS *et al.* 1998; KOZLOV *et al.* 2001). Although the polyglutamine-containing amino terminal sequence of human ataxin-2 are not present in Datx2, the Drosophila polypeptide does contain three polyglutamine tracts ranging from 11 to 18 residues elsewhere in the sequence. Reverse transcriptase (RT)-PCR analysis was used to detect *Datx2* transcript abundance at different developmental stages. Results of this analysis indicate that *Datx2* transcripts are more abundant in early embryos, late larvae, pupae, and adult heads (Figure 2.2A). Northern blot analysis using poly(A)+ RNA from embryos, larvae, and adults confirmed the results of RT-PCR analysis and revealed a 5.7-kb transcript at all developmental stages analyzed (data not shown).

To elucidate the spatial and subcellular distribution of the Datx2 protein, a rabbit antiserum was generated against a peptide corresponding to residues 151-165 of Datx2. Western blot analysis of an adult head extract using the Datx2 antiserum revealed a 140-kDa band not detected by preimmune serum (Figure 2.2B). The intensity of this band is dramatically increased in lanes containing a protein extract from flies overexpressing *Datx2*, and experiments with *Datx2* mutants further demonstrate the specificity of this

antiserum (Figures 2.5 and 2.10A). The size discrepancy between the 140-kDa band recognized by this antiserum and the 118-kDa expected from theoretical translation of the *Datx2* suggests that Datx2 migrates aberrantly on an SDS gel or that this protein is subject to post-translational modifications. Use of this antiserum to determine the *Datx2* expression pattern in embryos revealed Datx2 protein in most tissues, with particularly high levels in the central nervous system (Figure 2.2C). Consistent with the subcellular localization of human ataxin-2, Datx2 localizes to the cytoplasm in all tissues examined, including neurons of the central nervous system and developing egg chambers (Figures 2.2, E and F, and 5.5A). Subcellular fractionation experiments using an adult head lysate confirmed the cytoplasmic localization observed in *in situ* analyses (data not shown).

Identification of *Datx2* mutants:

Datx2 genomic sequence was used to search a Drosophila database composed of sequences flanking known *P* element insertions in the 5'-untranslated region (5'-UTR) of *Datx2* (Figure 2.3). The *l(3)06490* and *EP(3)3022* insertions are inviable as homozygotes and fail to complement one another and the *Df(3R)Po4* chromosome. By contrast, the *EP(3)3145* insertion is inviable as a homozygote, but fully complements the *l(3)06490* and *EP(3)3022* insertions and the *Df(3R)Po4* deletion chromosome. Subsequent experiments revealed that the recessive lethality associated with the *EP(3)3145* line results from a mutation unrelated to the *EP(3)3145* insertion. This mutation was removed by recombination and the resulting homozygous viable line was designated *EP(3)3145V*. Unlike the *l(3)06490* and *EP(3)3022* insertions, the *EP(3)3145* insertion contains a promoter designed to drive expression of flanking sequences and is

oriented properly to drive expression of *Datx2* (RORTH *et al.* 1998). Weak expression from the exogenous *EP(3)3145* promoter may therefore drive sufficient levels of *Datx2* expression to circumvent lethality.

To determine whether the recessive lethal phenotypes conferred by the *l(3)06490* and *EP(3)3022* insertions result from disruption of *Datx2* function, transgenic lines consisting of a full-length *Datx2* cDNA under GAL4 transcriptional regulation (BRAND and PERRIMON 1993) were generated and introduced into *Datx2* mutant backgrounds. Surprisingly, the *Datx2* transgenes were able to complement the *l(3)06490* and *EP(3)3022* recessive lethal phenotypes in the absence of GAL4 induction, presumably owing to leaky transgenic expression of *Datx2* (Table 2.1; data not shown). These results demonstrate that the recessive lethal phenotypes of the *l(3)06490* and *EP(3)3022* insertions result from loss of *Datx2* activity. Additional experiments using antiserum to Datx2 revealed a dramatic reduction of Datx2 protein levels in *l(3)06490* and *EP(3)3022* homozygous tissues relative to wild-type controls (Figure 2.10A), further verifying that these *P*-element insertions specifically affect *Datx2* function. For the remainder of this report the *l(3)06490* and *EP(3)3022* insertion strains are designated $Datx2^{l(3)06490}$ and $Datx2^{EP(3)3022}$, respectively, to denote that these insertions are alleles of the *Datx2* gene.

To generate more severe alleles of *Datx2*, the viable *EP(3)3145V* insertion was excised and imprecise excision alleles of the *P*-element were identified by failure to complement the $Datx2^{l(3)06490}$ allele. Two imprecise excision lines, designated $Datx2^{X1}$ and $Datx2^{X2}$, were characterized further. The $Datx2^{X1}$ allele is a 1.4-kb deletion that removes the first 22 codons of the *Datx2* coding sequence and extends into the first intron (Figure 2.3). The $Datx2^{X2}$ allele is a 1.3-kb deletion, but this deletion does not extend

into the *Datx2* coding sequence. Both imprecise excision alleles confer second instar larval lethality *in trans* to a *Datx2* deletion chromosome and this lethality can be rescued by transgenic expression of *Datx2*.

To compare the severity of the imprecise excision alleles to the *Datx2 P*-element alleles, the *Eyeless-GAL4 UAS-FLP/hid* (*EGUF/hid*) system (STOWERS and SCHWARZ 1999) was used to generate mosaic flies homozygous for the *Datx2* mutations in the retina. Flies bearing retinal clones of the $Datx2^{l(3)06490}$ or $Datx2^{EP(3)3022}$ alleles exhibit a mildly disorganized ommatidial pattern and a slight reduction in eye size (Figure 2.4B; data not shown). by contrast, flies bearing retinal clones of the $Datx2^{X1}$ or *Datx2X2* alleles exhibit a severe loss of eye tissue (Figure 2.4C; data not shown). These phenotypes could result from defective cell division, defective cell growth, cell death, or a combination of these factors. To begin to distinguish between these possibilities, eye discs from third instar larvae bearing *Datx2* retinal clones were dissected and assayed for programmed cell death by TUNEL (Figure 2.4, D-F). Loss of *Datx2* function increased the number of cells undergoing apoptosis, with more cells appearing positive for TUNEL in $Datx2^{X1}$ retinal clones than in $Datx2^{l(3)06490}$ retinal clones. In addition, eye discs from the $Datx2^{X1}$ allele were smaller and manifest a disorganized ommatidial structure. The increased apoptosis in *Datx2* retinal clones indicates that the loss of eye tissue observed in adults results at least in part from apoptosis, although defects in cell division or growth might also play contributing roles. Given the severe molecular nature of the $Datx2^{X1}$ allele and similar phenotypic characteristics of the $Datx2^{X1}$ and $Datx2^{X2}$ mutations, these mutations likely represent null alleles of the *Datx2* gene. By contrast, the relatively

milder phenotypes conferred by the *Datx2*$^{l(3)06490}$ and *Datx2*$^{EP(3)3022}$ alleles indicate that these mutations are hypomorphic alleles of *Datx2*.

Datx2 is required for actin filament formation, oocyte specification, and oocyte positioning in the female germline:

The finding that *Datx2* mutants bearing alleles of varying severities all exhibit second larval lethality, coupled with the large abundance of *Datx2* transcripts at the earliest stages of embryonic development, suggested that early development requirements for *Datx2* are supplied maternally. To investigate this possibility, *Datx2* expression was analyzed in the female germline. In Drosophila, oogenesis proceeds through a series of incomplete mitotic divisions of the germline lineage to yield an egg chamber consisting of 16 interconnected germ cells surrounded by a layer of somatically derived follicle cells. One of the 16 cells from the germline lineage proceeds through meiosis and becomes the future oocyte while the 15 remaining cells differentiate into supporting polyploid nurse cell (SPRADLING 1993). Results of immunocytochemical analysis indicate that Datx2 is present in nurse cells and the oocyte (Figure 2.5). Consistent with observations in other tissues (Figure 2.2E), immunoreactivity appeared to be nearly exclusively cytoplasmic. Notably, increased Datx2 staining was observed in the oocyte and was enriched at the posterior cortex, confirming that a large maternal contribution of Datx2 is present during early embryogenesis.

To investigate the functional consequences of eliminating the maternal supply of *Datx2*, female flies bearing germline clones of the *Datx2* mutations were examined. Germline clones of the *Datx2*$^{l(3)06490}$, *Datx2*^{X1}, and *Datx2*^{X2} alleles were completely sterile

and failed to lay eggs, whereas females bearing *Datx2*$^{EP(3)3022}$ germline clones were also sterile, but occasionally laid small deformed eggs that failed to hatch. By contrast, female flies bearing germline clones of a precise excision derivative of the *Datx2*$^{l(3)06490}$ chromosome produced normal-looking eggs and were fertile. Furthermore, homozygous *Datx2* mutants bearing a *Datx2* rescuing transgene laid normal-looking eggs, at least some of which were capable of hatching, verifying that the egg-laying defect in *Datx2* mutants derives from loss of *Datx2* function.

To analyze the nature of the germline defect in *Datx2* mutants, ovaries were dissected from females bearing *Datx2* germline clones and stained with fluorescent phalloidin to highlight filamentous actin and 4',6-diamidino-2-phenylindole (DAPI) to highlight cell nuclei. Most egg chambers from females with homozygous clones of hypomorphic *Datx2*$^{l(3)06490}$ and *Datx2*$^{EP(3)3022}$ alleles are able to progress normally through the early and middle stages of oogenesis (Table 2.2; data not shown). However, most of these egg chambers arrest development at a stage in oogenesis when nurse cells rapidly transport their cytoplasmic contents into the oocyte through intercytoplasmic bridges termed ring canals that connect these cells to one another. The arrested egg chambers manifest enlarged nurse cells and a small poorly developed oocyte (Figure 2.6, C and D). Normally, nurse cell nuclei are tethered by an actin filament cage that forms immediately prior to the cytoplasmic transport stage. Most of these anchoring filaments fail to form in *Datx2* mutants (Figure 2.6, E and F). In addition, the nurse cell nuclei are inappropriately positioned in close proximity to the ring canals and are sometimes observed stretching partially through the ring canals, indicating that the cytoplasmic transport failure in the *Datx2* mutants results from occlusion of the ring canals by nurse

cell nuclei (Figure 2.6, G and H). Mutations in genes regulating actin polymerization and bundling also disrupt the formation of this cage and result in cytoplasmic transport defects identical to those seen in *Datx2* mutant egg chambers (PEIFER *et al.* 1993; reviewed by ROBINSON and COOLEY 1997). These results suggest that actin filament polymerization or bundling defects are responsible for the cytoplasmic transport failure in the $Datx2^{l(3)06490}$ and $Datx2^{EP(3)3022}$ mutants.

Although most $Datx2^{X2}$ germline stem cells appear to undergo normal cell division to yield the 16-cell cystoblast (Table 2.2), all of these egg chambers arrested development prior to the cytoplasmic transport stage. Normally the oocyte resides at the posterior end of the egg chamber, adjacent to the posterior somatic follicle cells. However, in egg chambers homozygous for the $Datx2^{X1}$ allele, the oocyte was often found in the middle of the egg chamber or the oocyte failed to be specified at all (Table 2.2; Figure 2.6, I-L). Oocyte contact with the posterior follicle cells is required to prevent these cells from pursuing their default anterior state (GODT and TEPASS 1998). As a consequence, oocyte mispositioning in the $Datx2^{X1}$ egg chambers often results in egg chambers with two anterior ends (Figure 2.6L). Despite these defects, however, several aspects of egg chamber development appear to proceed normally. For example, the oocyte induces surrounding somatic follicle cells to become columnar in share, and this process appears to be intact in $Datx2^{X1}$ egg chambers (Figure 2.6, K and L). Furthermore, the border cells, which normally delaminate from the follicular epithelium and migrate toward the oocyte under direction of a signal emanating from the oocyte, migrate toward the mispositioned oocyte in $Datx2^{X1}$ egg chambers, demonstrating that this process is also intact. Because proper cell adhesion between the oocyte and the

posterior somatic follicle cells is required for the oocyte to maintain its posterior position in the egg chamber (GODT and TEPASS 1998), the oocyte-mispositioning defect suggests a possible requirement for *Datx2* in mediating cell adhesion. Females bearing germline clones of hypomorphic *Datx2* alleles produced egg chambers with some of these same defects, but much less frequently (Table 2.2).

Reduced *Datx2* activity results in bristle defects:

In the absence of GAL4-induced expression, several *UAS-Datx2* transgenes are capable of rescuing the *Datx2* larval lethality (Table 2.1). Rescued adult flies display several defects, however, *Datx2* mutants rescued by the *UAS-Datx2.1B* transgene are uncoordinated, display a rough eye phenotype like that of flies bearing retinal clones of the $Datx2^{l(3)06490}$ allele, and exhibit bent and forked thoracic sensory bristles. These phenotypes are fully penetrant in flies rescued by this transgene, although typically only a small number of bristles exhibited gross structural alterations, with the scutellar, humeral, and sternopleural bristles being primarily affected. *Datx2* mutants rescued by the *UAS-Datx2.3* and *UAS-Datx2.4* transgenes exhibit normal motor behavior and eye structure, but continue to manifest bent and forked sensory bristles (Figure 2.7, A and B), although the penetrance of the sensory bristle phenotypes was reduced in these flies. These phenotypes appear to arise as a consequence of reduced *Datx2* function rather than overexpression or misexpression of *Datx2* because these same transgenes do not produce detectable phenotypes in a wild-type background. Moreover, the phenotypes in partially rescued *Datx2* mutants do not result from other recessive mutations on the chromosome

bearing the *Datx2* mutations, as these phenotypes are observed in flies bearing independently generated *Datx2* mutations.

Sensory bristle development depends initially on the assembly of parallel bundles of actin filaments arranged in repeated units (TILNEY *et al.* 1996). These bundles serve as a temporary support scaffold for the subsequent deposition of cuticle. Following cuticle deposition, the actin filament scaffold is disassembled. The parallel ridge pattern of the adult bristle is thus a reflection of the parallel actin bundle organization in the developing bristle. Many of the bristles in partially rescued *Datx2* mutants exhibit highly disorganized cuticular ridges, indicating that the actin filament scaffold in the developing bristle was improperly assembled (Figure 2.7, C and D). To examine the structure of the actin scaffold in the developing bristle, thoraces from 48-hr-old pupae were dissected, and actin filaments in the developing bristles were examined by staining with fluorescent phalloidin conjugates. In wild-type bristles, the individual units of bundled fibers and the stereotypical arrangement of the transverse breaks in these bundles were apparent (Figure 2.7E). However, in partially rescued *Datx2* mutants and flies bearing clones of the $Datx2^{XI}$ allele, the actin filament bundle repeat unit is significantly shorter and heterogeneous in length, leading to discontinuities in the transverse breaks of actin bundles (Figure 2.7, F-H). Although the lengths of these bundles are shorter than those from wild-type flies, most of the bundles are assembled parallel to the long axis of the growing bristle. Thin bundles of actin filaments were also observed. These results indicate that the defective bristle morphology observed in partially rescued *Datx2* mutant adults arises from defective actin filament structure during bristle development.

Datx2 function is dosage sensitive:

To determine tissue-specific requirements for *Datx2*, attempted to rescue the *Datx2* bristle, eye, and behavioral phenotypes resulting from reduced *Datx2* activity by using the *GAL4/UAS* system (BRAND and PERRIMON 1993) to induce elevated *Datx2* expression in specific tissues. In each of these experiments, however, the increased *Datx2* expression conferred by GAL4 resulted in overexpression phenotypes, precluding a detailed analysis of *Datx2* tissue-specific requirements (Table 2.3). For example, ectopic expression of *Datx2* in the retina using *GMR-GAL4* (ELLIS *et al.* 1993) produces a range of eye phenotypes, with the *UAS-Datx2.1B* transgene producing progressive loss of pigmentation, and the *UAS-Datx2.3* and *UAS-Datx2.4* transgenes producing more severe disruptions of retinal structure (Figure 2.8). Ectopic expression of *Datx2* in the nervous system using the *elav-GAL4* (ROBINOW and WHITE 1988) or *eyeless-GAL4* drivers (CALLAERTS *et al.* 2001) or in mesoderm using the *24B-GAL4* driver (BRAND and PERRIMON 1993) results in significant developmental delays and lethality (Table 2.3). Weak ubiquitous expression of *Datx2* using a heat-shock promoter-driven GAL4 line in the absence of heat shock results primarily in lethality with rare survivors exhibiting thin and somewhat flattened bristles (Figure 2.7, I and J). The severity of the phenotypes resulting from overexpression of *Datx2* correlates with the levels of *Datx2* expression conferred by the *UAS-Datx2* transgenes (data not shown). These results indicate that *Datx2* function is dosage sensitive.

Altered *Datx2* dosage in the retina results in aberrant actin structures:

Since altered *Datx2* dosage is associated with actin filament formation defects in ovaries and bristles, we investigated whether altered *Datx2* function also elicits cytoskeletal defects in the nervous system. This analysis was performed by comparing eye imaginal discs from wild-type flies, *Datx2* mutants, and flies overexpressing *Datx2*. Third instar larval eye discs from wild-type Drosophila exhibit ommatidial cell clusters posterior to the morphogenetic furrow (rosettes) consisting, in part, of photoreceptor precursor cells with filamentous actin distributed near the subcortical regions of the individual cells within the clusters (Figure 2.9A). By comparison, the arrangement of filamentous actin in rosettes appears disorganized in similarly staged eye discs from mosaic larvae lacking *Datx2* in the retina, and punctate accumulations of actin are seen throughout these clusters (Figure 2.9B). Overexpression of *Datx2* in the retina using a *UAS-Datx2* transgene in conjunction with *GMR-GAL4* results in similar punctate actin aggregates and disorganized actin clusters (Figure 2.9C). Together, these results demonstrate that proper *Datx2* expression levels are critical for regulating morphology of actin structures in prephotoreceptor cells.

***Datx2* does not regulate actin abundance or physically associate with filamentous actin:**

To determine whether the actin filament formation defects associated with altered *Datx2* dosage result from changes in actin abundance, protein extracts were prepared from germline clones of *Datx2* mutant ovaries and steady-state actin levels were analyzed by Western blot analysis. Although Datx2 abundance was markedly reduced in extracts

from mutant ovaries, actin abundance remained essentially unchanged (Figure 2.10A). Actin abundance in flies overexpressing *Datx2* was similarly unaffected (data not shown). These results indicate that the *Datx2* phenotypes do not result from defective actin synthesis and suggest instead that *Datx2* function is required for mobilization of actin monomers into filaments or bundles.

To investigate the possibility that Datx2 coordinates actin filament formation by assembling with actin filaments, a biochemical approach was used to test for physical interactions between Datx2 and actin filaments. Filamentous actin was precipitated from ovarian extracts using biotinylated phalloidin. Although much of the actin in these extracts was precipitated by phalloidin, all of the Datx2 was found in the soluble fraction (Figure 2.10B). Further subcellular fractionation experiments and *in vitro* actin filament-binding studies confirmed these results (data not shown). These experiments demonstrate that Datx2 is not a structural component of actin filaments and suggest that *Datx2* regulates actin filament pathways through an indirect mechanism.

DISCUSSION

In this work we describe the identification and mutational analysis of *Datx2*, a Drosophila homolog of the human *SCA2* gene. The Datx2 protein shares two domains homology with human ataxin-2, and these domains are evolutionarily conserved from yeast to humans. Like human *SCA2*, *Datx2* is widely expressed and its gene product is distributed throughout the cytoplasm. *Datx2* is essential for viability, and *Datx2* function is required for proper formation of actin filaments and bundles in retinal cells, sensory

bristles, the female germline, and perhaps other tissues. Overexpression of *Datx2* is toxic in several tissues and results in actin filament formation defects in all tissues analyzed. These findings indicate that a principal function of *Datx2* is to regulate the formation or bundling of actin filaments in multiple cell types.

The most conclusive evidence for a role of *Datx2* in actin filament metabolism derives from studies of germline clones of *Datx2* hypomorphic alleles and from analyses of bristle structure in *Datx2* mutants. Females with germlines homozygous for hypomorphic *Datx2* alleles are sterile owing to a reduction in nurse cell cytoplasmic actin filaments and an ensuing nurse cell cytoplasmic dumping defect. This phenotype is nearly identical to the germline phenotypes in the Drosophila mutants *chickadee*, *quail*, and *singed* (reviewed by ROBINSON and COOLEY 1997). *chickadee* encodes a Drosophila homolog of profilin, which recruits actin monomers into polymerized microfilaments (VERHEYEN and COOLEY 1994), and *quail* and *singed* encode the microfilament-bundling proteins villin and fascin, respectively (CANT *et al.* 1994; MAHAJAN-MIKLOS and COOLEY 1994). The similar phenotypes produced by these mutants suggest that *Datx2* may regulate or function in parallel with these gene products in the ovary. Notably, the *chickadee* and *singed* mutations also result in bristle phenotypes similar to those of the partially rescued *Datx2* mutants (CANT *et al.* 1994; MAHAJAN-MIKLOS and COOLEY 1994). These bristle phenotypes also derive from defective actin filament formation and bundling in the developing bristle. Furthermore, mutations in a number of other genes involved in actin filament formation and bundling pathways produce similar sensory bristle anomalies (HOPMANN *et al.* 1996; CHEN *et al.* 2001; GRIESHABER *et al.* 2001). Like these mutants, the aberrant actin bundles in

Datx2 mutants likely compromise the strength or stiffness of the scaffold, resulting in insufficient support during cuticle deposition. Subsequent buckling of the underlying actin scaffold may thus be responsible for the disorganized ridges and bent and forked bristles observed in *Datx2* mutants. The actin filament formation defects observed in *Datx2* mutants do not appear to result from reduced actin synthesis since actin levels are not significantly affected by altered *Datx2* dosage. Rather, phenotypic similarities between *Datx2*, *chickadee*, *quail*, and *singed* suggest that, like these factors, *Datx2* mediates actin filament formation or bundling.

The oocyte-mispositioning defect observed in the $Datx2^{X1}$ egg chambers might also result from actin filament formation defects. For example, germline clone analysis of particular *chickadee* alleles produces oocyte-mispositioning phenotypes similar to those seen in $Datx2^{X1}$ germline clones (PEIFER *et al.* 1993). Furthermore, the Drosophila b-catenin homolog (*armadillo*) has been shown to function by anchoring the cell adhesion molecule DE-cadherin to the subcortical actin cytoskeleton (BARTH *et al.* 1997). Like the $Datx2^{X1}$ allele, null alleles of *armadillo* also result in egg chambers with mispositioned oocytes (PEIFER *et al.* 1993). Defects in the subcortical actin cytoskeleton of *Datx2* egg chambers might therefore phenocopy *armadillo* mutants by interfering with DE-cadherin attachment to the subcortical cytoskeleton. While the oocyte mispositioning defect can be related to actin filament defects, a precise interpretation of the oocyte specification defect observed in $Datx2^{X1}$ egg chambers is complicated by the somewhat limited understanding of oocyte specification mechanisms, and further experimentation will be required to elucidate the role of *Datx2* in early egg chamber development.

Consistent with our observations in bristles and the female germline, altered *Datx2* dosage in the nervous system also affected actin filament structure. Prephotoreceptor neurons homozygous for the *Datx2* mutations or overexpressing *Datx2* from a transgene exhibited punctate, disorganized aggregates of actin. An increase in the frequency of apoptosis accompanied these actin filament formation defects. Both phenotypes were observed early in development of the photoreceptor neurons and occur before any other visible signs of gross cellular dysfunction, indicating that the eye phenotypes resulting from altered *Datx2* dosage derive from perturbations in actin filament formation and/or apoptosis. The coincident occurrence of actin filament formation defects and apoptosis in prephotoreceptor neurons raises the possibility that the anomalies in filamentous actin-containing structures are secondary consequences of previous apoptotic events. However, we favor the idea that apoptosis is triggered in response to defective actin filament formation or bundling, since most retinal cells with altered *Datx2* dosage exhibited filamentous actin anomalies while relatively few were positive for apoptosis. Furthermore, apoptosis was not observed in egg chambers prior to defects in actin morphology, nor was it observed in epithelial cells making bristles (data not shown). The increased levels of apoptosis in $Datx2^{X1}$ eye disc clones relative to eye clones from the hypomorphic *Datx2* alleles suggest that apoptosis is at least partly responsible for the severe eye phenotype in these mutants. These data suggest that *Datx2*-mediated perturbations in actin filament formation trigger apoptosis of retinal cells.

The finding that *Datx2* overexpression was toxic in all tissues tested suggests that the pathways regulated by *Datx2* are dosage sensitive. Alternatively, excessive

production of Datx2 protein could be toxic for reasons unrelated to the normal cellular function of this protein. Two observations suggest that the overexpression phenotypes stem from perturbation of pathways normally regulated by *Datx2*. First, the disorganized actin structures observed in the developing retinas of flies overexpressing *Datx2* closely resembles those seen in retinal clones of the *Datx2* loss-of-function alleles, suggesting that the *Datx2* overexpression phenotypes also derive from perturbation of the actin cytoskeleton. Second, as is seen in partially rescued *Datx2* mutants, ubiquitous overexpression of *Datx2* results in defective bristle morphology, again suggesting that overexpression of *Datx2* perturbs actin filament polymerization or bundling. Together, these results argue that the *Datx2* overexpression phenotypes result from perturbation of the actin cytoskeleton and, thus, that the normal cellular role played by *Datx2* is dosage sensitive.

A couple observations suggest that *Datx2* plays an indirect role in actin filament formation. First, our experiments show that Datx2 fails to physically interact with actin filaments. Second conserved sequence motifs in the ataxin-2 family suggest that ataxin-2 proteins function in RNA metabolism. Given these observations, we suggest that *Datx2* functions by regulating the expression of a subset of transcripts encoding mediators of actin polymerization or bundling. Alternatively, *Datx2* may function in a more general capacity to regulate expression of a broad class of transcripts, so that the phenotypes resulting from altered *Datx2* dosage represent those of the most dosage-sensitive genes. Although definitive evidence distinguishing these two models will require further work, two lines of evidence lead us to favor the former possibility. First, Drosophila mutants with compromised translational capacity exhibit short thin bristles with reduced ridging

(SAEBOE-LARSSEN *et al.* 1998; KOREY *et al.* 2001), whereas the bristles in *Datx2* mutants are bent and forked with disorganized ridging and thus more closely resemble those produced by mutations specifically affecting actin filament formation pathways (CANT *et al.* 1994; MAHAJAN-MIKLOS and COOLEY 1994; HOPMANN *et al.* 1996; CHEN *et al.* 2001; GRIESHABER *et al.* 2001). Second, altered *Datx2* dosage does not appear to significantly affect the overall abundance of actin, demonstrating that altered levels of this potentially limiting component do not account for the *Datx2* phenotypes. Thus, we favor a model whereby *Datx2* regulates a subset of RNAs, at least some of which encode mediators of actin filament formation. This regulation could be at the level of transcript stability, transcript localization, or translational regulation, and the molecular basis of this regulation is the focus of current experimentation.

Figure 2.1

Ataxin-2 homologs. Alignment of conserved amino acid sequences of human ataxin-2 (HATX2), human ataxin-2 related protein (HATX2RP), *Drosophila melanogaster* Datx2 (DATX2), *C. elegans* ATX-2 (CATX2), two ataxin-2 homologs from *A. thaliana* (AATX2a and AATX2b), and *S. cerevisiae* poly(A)-binding protein 1 (PBP1P). Amino acid similarities within the ATX2-N and ATX2-C domains shared by at least four ataxin-2 members are shaded. Amino acid identities within the ATX2-N and ATX2-C domains shared by at least six ataxin-2 family members are boxed. The Drosophila ataxin-2 polypeptide exhibits 43 and 62% amino acid identity to human ataxin-2 within the ATX2-N and ATX2-C domains respectively. The Sm motifs within the ATX2-N domain are highlighted by large rounded boxes. The ATX2-C consensus sequence, representing positions of identity shared by four or more ataxin-2 family members, is shown in alignment with a conserved sequence present in peptides known to bind to the carboxyl terminus of PABP (designated PAM2 consensus). The polyglutamine tracts in the human and Drosophila ataxin-2 sequences are represented by black boxes. The peptide sequence used to generate the Datx2 antiserum is represented by the crosshatched box.

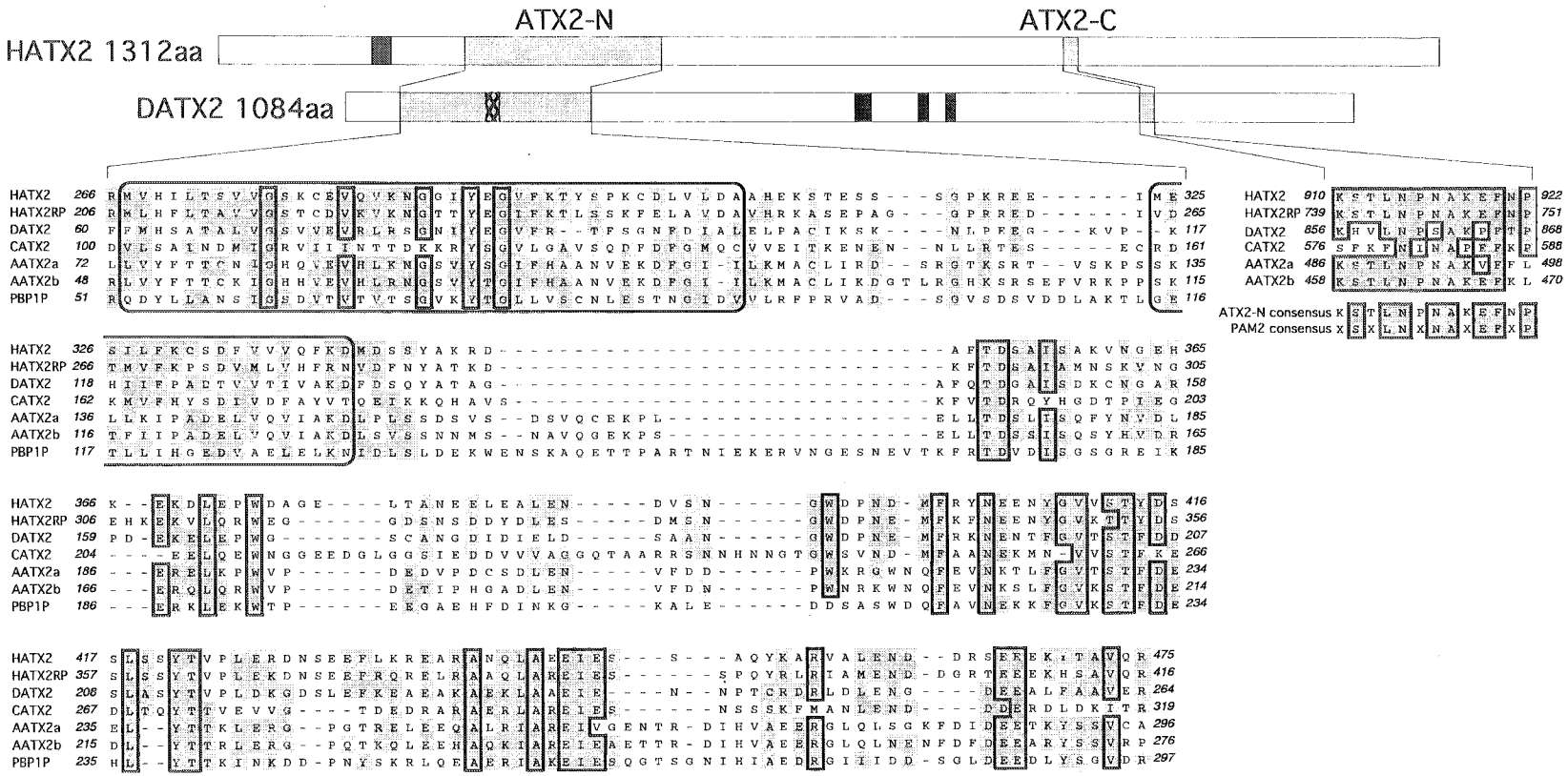
ATX2-N
ATX2-C
HATX2 1312aa
DATX2 1084aa
HATX2 266 RMVHILTSVVQSKCEVQVKNGGIYEGVFKTYSPKCDLVLDAAHEKSTESS---SGPKREE------IME 325
HATX2RP 206 RMLHFLTAVVQSTCDVKVKNGTTYEGIFKTLSSKFELAVDAVHRKASEPAG---GPRREDI------VD 265
DATX2 60 FFMHSATALVQSVVEVRLRSGNIYEGVFR--TFSGNFDIALELPACIKSK----NLPFEG---KVP--K 117
CATX2 100 DVLSAINDMIQRVIIINTTDKKRYSGVLGAVSQDFDPGMQCVVEITKENEN--NLLRTES------ECRD 161
AATX2a 72 LLVYFTTCNIQHQVEVHLKNGSVYSGIFHAANVEKDPGI-ILKMACLIRD--SRGTKSRT--VSKPSSK 135
AATX2b 48 RLVYFTTCKIQHHVEVHLRNGSVYTGIFHAANVEKDPGI-ILKMACLIKDGTLRGHKSRSEFVRKPPSK 115
PBP1P 51 RQDYLLANSIQSDVTVTVTSGVKVTGLLVSCNLESTNGIDVVLRFPRVAD---SGVSDSVDDLAKTLGE 116
HATX2 910 KSTLNPNAKEFNP 922
HATX2RP 739 KSTLNPNAKEFNP 751
DATX2 856 KHVLNPSAKPPTP 868
CATX2 576 SPKFNINAPEFKP 588
AATX2a 486 KSTLNPNAKVFFL 498
AATX2b 458 KSTLNPNAKEFKL 470
ATX2-N consensus KSTLNPNAKEFNP
PAM2 consensus XSXLNXNAXEFXP
HATX2 326 SILFKCSDFVVVQFKDMDSSYAKRD----------AFTDSAISAKVNGEH 365
HATX2RP 266 TMVFKPSDVMLVHFRNVDFNYATKD----------KFTDSAIAMNSKVNG 305
DATX2 118 HIIFPADTVVTIVAKDFDSQYATAG----------AFQTDGAISDKCNGAR 158
CATX2 162 KMVFHYSDIVDFAYVTQEIKKQHAVS----------KFVTDRQYHGDTPIEG 203
AATX2a 136 LLKIPADELVQVIAKDLPLSSDSVS--DSVQCEKPL----------ELLTDSLISQFYNVDL 185
AATX2b 116 TFIIPADELVQVIAKDLSVSSNNMS--NAVQGEKPS----------ELLTDSSISQSYHVDR 165
PBP1P 117 TLLIHGEDVAELELKNIDLSLDEKWENSKAQETTPARTNIEKERVNGESNEVTKFRTDVDIGSGSGREIK 185
HATX2 366 K--EKDLEPWDAGE----LTANEELEALEN-----DVSN------GWDPND-MFRYNEENYGVVSTYDS 416
HATX2RP 306 EHKEKVLQRWEG------GDSNSDDYDLES-----DMSN------GWDPNE-MFKFNEENYGVKTTYDS 356
DATX2 159 PD-EKELEPWG-------SCANGDIDIELD-----SAAN------GWDPNE-MFRKNENTFGVTSTFDD 207
CATX2 204 ----EELQEWNGGEEDGLGGSIEDDVVVAGGQTAARRSNNHNNGTGWSVND-MFAANEKMN-VVSTFKE 266
AATX2a 186 ---ERELKPWVP------DEDVPDCSDLEN-----VFDD------PWKRGWNQFEVNKTLFGVTSTFDE 234
AATX2b 166 ---ERQLQRWVP------DETIPHGADLEN-----VFDN------PWNRKWNQFEVNKSLFGVKSTFDE 214
PBP1P 186 ---ERKLEKWTP------EEGAEHFDINKG-----KALE------DDSASWDQFAVNEKKFGVKSTFDE 234
HATX2 417 SLSSYTVPLERDNSEEFLKREARANQLAEEIES---S---AQYKARVALENDD--DRSEEEKITAVQR 475
HATX2RP 357 SLSSYTVPLEKDNSEEFRQRELRAAQLAREIES------SPQYRLRIAMENDD-DGRTEEEKHSAVQR 416
DATX2 208 SLASYTVPLDKGDSLEFKEAEAKAEKLAAEIE----N--NPTCRDRLDLENG----DEEALFAAVER 264
CATX2 267 DLTQYTTVEVVG----TDEDRARAERLAREIES------NSSSKFMANLENDD----DEERDLDKITR 319
AATX2a 235 EL--YTTKLERG--PGTRELEEQALRIAREIVGENTR-DIHVAEERGLQLSGKFDIDEETKYSSVCA 296
AATX2b 215 DL--YTTRLERG--PQTKQLEEHAQKIAREIEAETTR-DIHVAEERGLQLNENFDFDEEARYSSVRP 276
PBP1P 235 HL--YTTKINKDD-PNYSKRLQEAERIAKEIESQGTSGNIHIAEDRGIIIDD-SGLDEEDLYSGVDR 297

Figure 2.2

***Datx2* expression pattern.** (A) RT-PCR analysis of *Datx2* transcript levels normalized to ribosomal protein 49 transcript abundance at multiple development stages. E, embryo; 1L-3L, first through third instar larvae; P, pupae; AH, adult head; AB adult body. (B) Protein extracts from wild-type flies (WT) and transgenic flies bearing a *UAS-Datx2* transgene and a heat-shock-inducible GAL4 transgene following a 1-hr heat shock at 38°C (HS-Datx2). Both extracts contain a 140-kD protein that is recognized by serum from a rabbit immunized with a Datx2 peptide, but not by preimmune serum. The total amount of extract loaded in lanes labeled HS-Datx2 corresponds to one-sixteenth the amount loaded in lanes containing protein extract from wild-type flies to reduce signal intensity. (C) Late-stage Drosophila embryo stained with Datx2 antiserum. Datx2 is ubiquitously expressed but enriched in the central nervous system (arrow). (D) Late-stage embryo stained with preimmune serum. (E) Cells of the third instar larval ventral ganglion stained with Datx2 antiserum reveal a cytoplasmic distribution of Datx2 protein. (F) Larval ventral ganglion cells stained with preimmune serum.

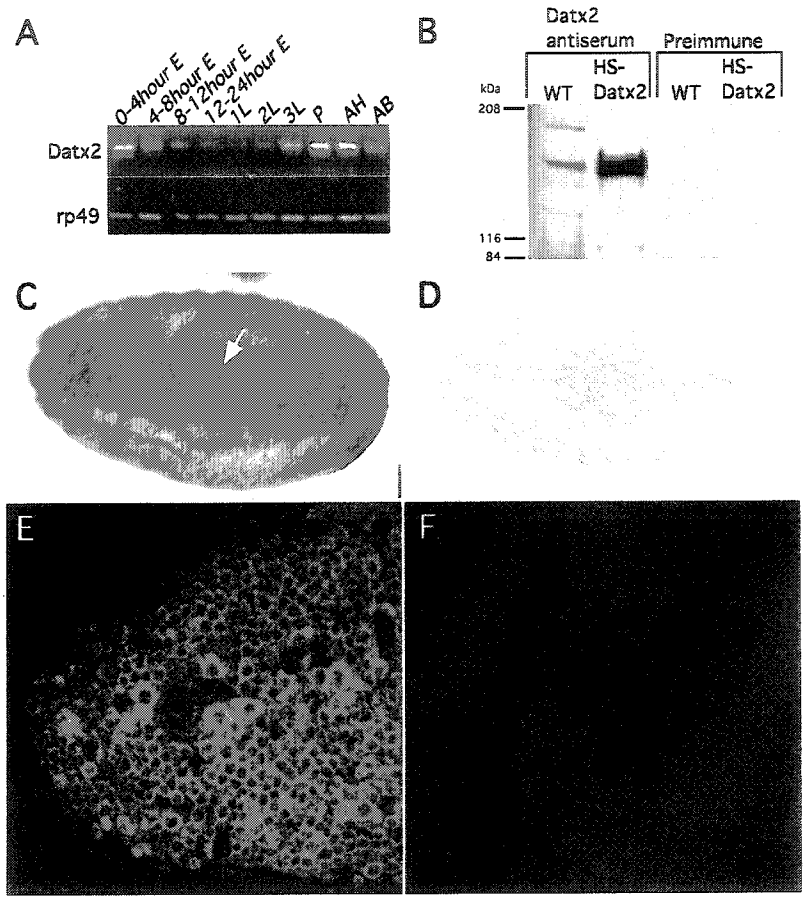
A
0-4hour E
4-8hour E
8-12hour E
12-24hour E
1L
2L
3L
P
AH
AB
Datx2
rp49
B
Datx2
antiserum
Preimmune
WT
HS-
Datx2
WT
HS-
Datx2
kDa
208
116
84
C
D
E
F

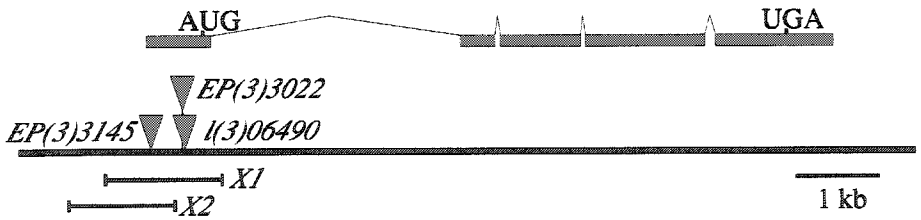

Figure 2.3 *Datx2* mutations. The *Datx2* transcript is shown relative to genomic DNA (designated by a heavy solid line). Solid boxes correspond to *Datx2* exon sequences and the AUG and UGA sequences correspond to the start and stop codons, respectively. The *EP(3)3145*, *EP(3)3022*, and *l(3)06490 P*-element insertions (triangles) all reside in the *Datx2* 5'-UTR and lie 667, 269, and 235 bp upstream of the putative *Datx2* start codon, respectively. The orientations of the EP insertions are indicated with arrows. The $Datx2^{X1}$ and $Datx2^{X2}$ deletions derived from imprecise excision of the *EP(3)3145* *P*-element are depicted as horizontal bars below the genomic DNA.

Figure 2.4

***Datx2* is required for normal eye development.** (A) Compound eye from wild-type fly. (B) Compound eye from a fly homozygous for the *Datx2l(3)06490* allele in the retina. Note the disorganized ommatidial structure and decreased size relative to the wild-type eye. Similar results were obtained with the $Datx2^{EP(3)3022}$ allele (data not shown). (C) Compound eye of a fly homozygous for the $Datx2^{X1}$ allele in the retina. Note the dramatic decrease in size of the compound eye and lack of ommatidial structure. Identical results were obtained with the $Datx2^{X2}$ allele (data not shown). (D-F) TUNEL assays for apoptosis in *Datx2* mutant eye discs. Third instar eye discs from w^{1118} control (D), $Datx2^{l(3)06490}$ homozygous eye clones (E), and $Datx2^{X1}$ homozygous eye clones (F) are shown. Apoptotic cells appear as bright spots indicated with arrows. The background was increased in D so that the eye disc could be seen in the absence of apoptotic cells. (G-I) Third instar larval eye discs stained with anti-Elav to compare eye disc size and ommatidial structure in the *Datx2* mutants with respect to wild type. (G) w^{1118} control. (H) $Datx2^{l(3)06490}$ eye clone. (I) $Datx2^{X1}$ eye clone.

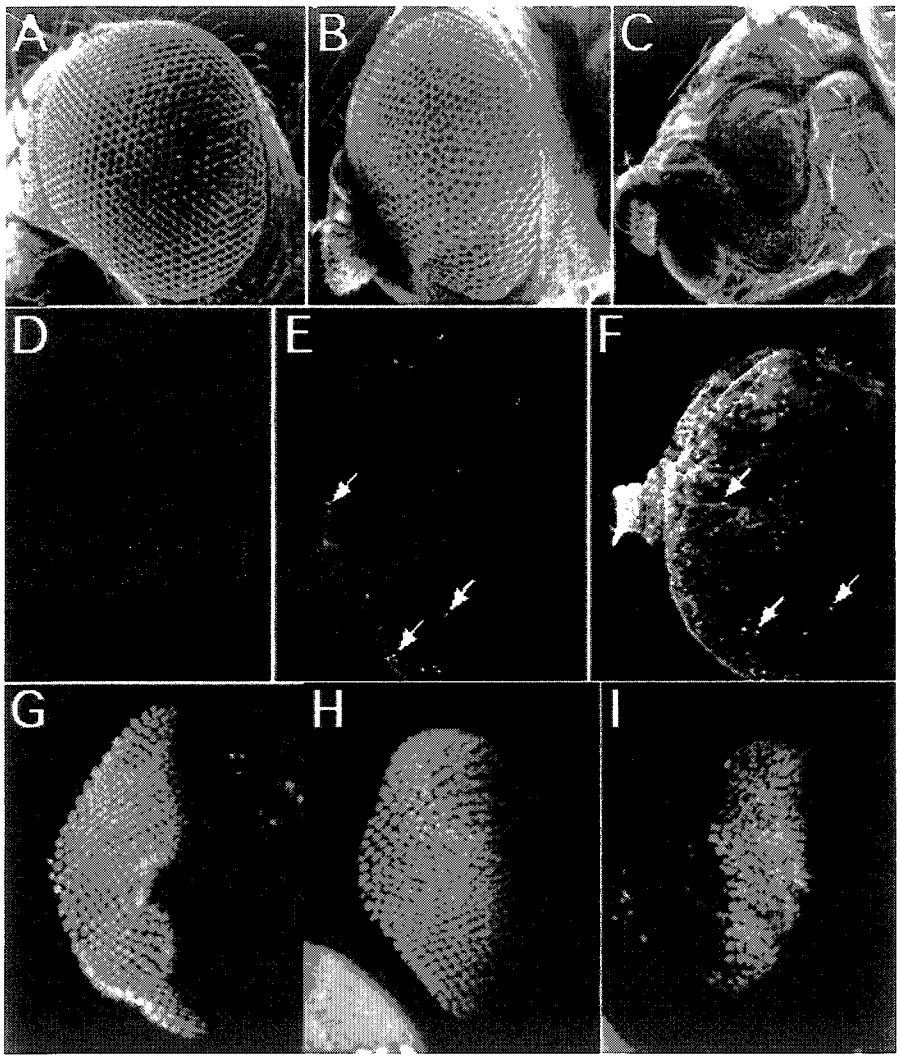
A
B
C
D
E
F
G
H
I

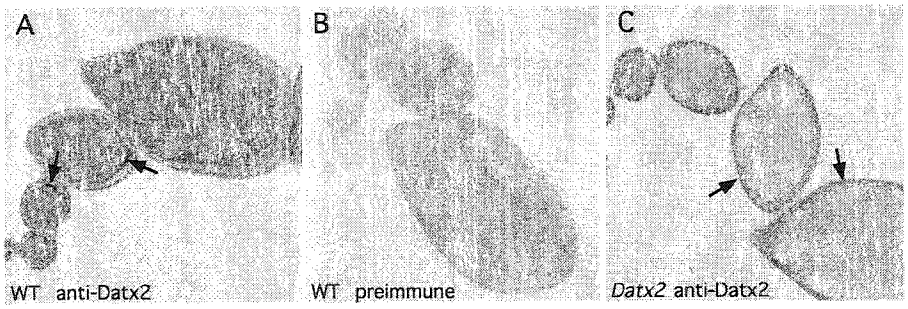

Figure 2.5 Datx2 is present in egg chambers and is enriched in the oocyte. (A) Wild-type egg chambers stained with Datx2 antiserum. Datx2 is distributed throughout the germline cytoplasm and is enriched in developing oocytes (arrows). (B) Wild-type egg chambers stained with preimmune serum. (C) Datx2 immunoreactivity is abolished in egg chambers derived from $Datx2^{l(3)06490}$ germline clones (GLC). Note that staining in somatic follicle cells, which are heterozygous for the $Datx2^{l(3)06490}$ mutation, is retained (arrows).

Figure 2.6

***Datx2* is required for actin filament formation, oocyte specification, and oocyte positioning in the female germline.** (A-D) Egg chambers stained with DAPI (blue) and fluorescently labeled phalloidin (red) to highlight cell nuclei and filamentous actin, respectively. (A) Wild-type egg chamber immediately prior to cytoplasmic transport. (B) Arrested $Datx2^{l(3)06490}$ mutant egg chamber. Note irregular arrangement of nurse cell nuclei (arrows) compared to the wild type. (C) Wild-type egg chamber after cytoplasmic transport has occurred. Not increase in oocyte volume (denoted by dashed line) and concomitant decrease in nurse cell volume. (D) $Datx2^{l(3)06490}$ mutant egg chamber after the cytoplasmic transport stage. Note large volume of nurse cells and small volume of oocyte (denote by dashed line) relative to wild type. (E) Confocal image of phalloidin-stained wild-type egg chamber immediately prior to cytoplasmic transport. Note prominent array of cytoplasmic actin filaments. (F) Confocal image of phalloidin-stained $Datx2^{l(3)06490}$ mutant egg chamber just prior to cytoplasmic transport. Note the decreased density of actin filaments compared to wild type. (G and H) Magnified views of two different $Datx2^{l(3)06490}$ mutant egg chambers showing nurse cell nuclei stretching toward and through cytoplasmic bridges (ring canals) connecting nurse cells to the oocyte (arrows). (I and J) Confocal images of early stage egg chambers stained with DAPI to highlight nuclei. (I) Wild-type egg chamber with 15 nurse cells (numbered) and an oocyte (oc). (J) $Datx2^{X1}$ mutant egg chamber with 16 nurse cells (numbered). (K and L) Confocal images of early stage egg chambers stained with phalloidin. (K) In wild-type egg chambers, columnar follicle cells surround the oocyte at the posterior end (denoted by dashed line) and border cells (bc) can be seen delaminating from the follicular epithelium and migrating toward the oocyte. (L) In the $Datx2^{X1}$ mutant egg chamber the oocyte (oc) is located near the middle of the egg chamber. Note the presence of columnar follicle cells (dashed lines) in the vicinity of the misplaced oocyte and migration of border (bc) toward the misplace oocyte.

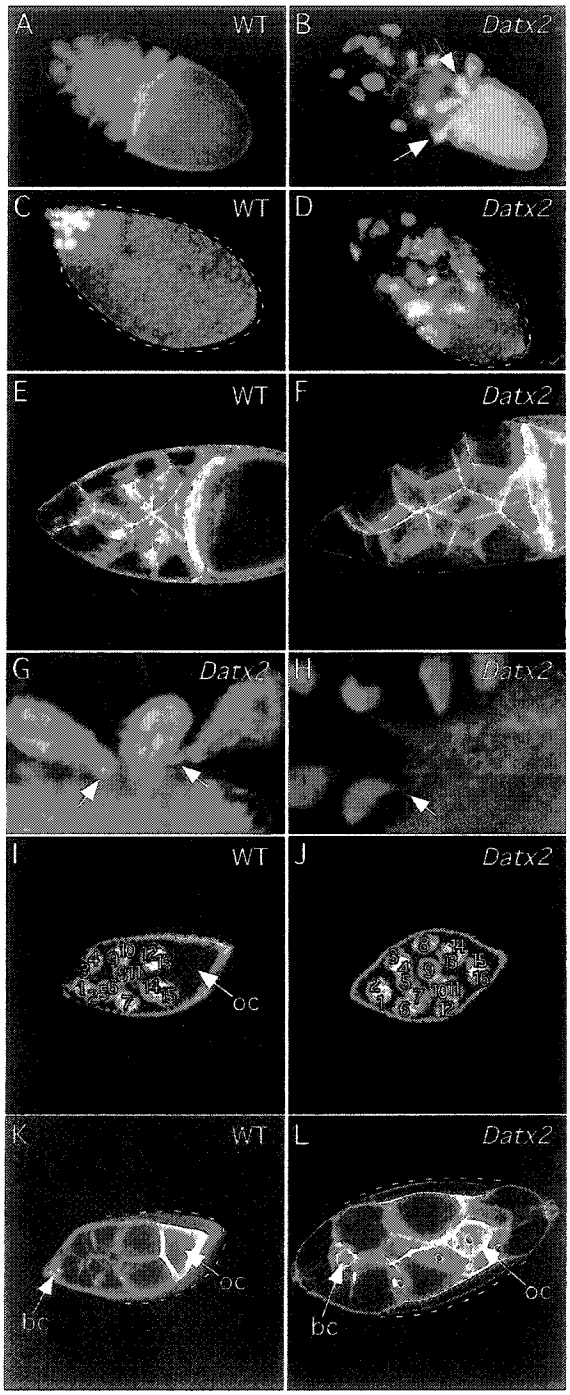
A
WT
B
Datx2
C
WT
D
Datx2
E
WT
F
Datx2
G
Datx2
H
Datx2
I
WT
J
Datx2
oc
K
WT
L
Datx2
oc
bc
oc
bc

Figure 2.7

***Datx2* is required for normal bristle morphology.** Scanning electron micrographs of thoracic bristles from wild-type flies (A and C) and from $Datx2^{X1}$ mutants rescued with the *UAS-Datx2.4* transgene (B and D) are shown. Wild-type bristles exhibit a regular alignment of cuticular ridges (C) and taper to a tip (A). Thoracic bristles from partially rescued *Datx2* mutants are often split (B) and exhibit twisted and irregular cuticular ridges (D). (E-H) Confocal micrographs of phalloidin-stained bristles from 48-hr-old pupae. Actin bundles in wild-type flies are homogeneous in size and exhibit regular transverse breaks (E), whereas actin bundles from $Datx2^{X1}$ mutants rescued with the *UAS-Datx2.4* transgene (F) or from $Datx2^{X1}$ clones (G and H) were shorter and thinner than those from wild type. Note the irregular spacing of transverse gaps in bundled filaments relative to wild type. (I and J) Scanning electron micrographs of bristles from wild-type fly (I) and from a fly ubiquitously overexpressing *Datx2* (J). Note the increased bending and ribbon-like appearance in the fly overexpressing *Datx2* (J). Bars: A-H, 5 μm; I and J, 50 μm.

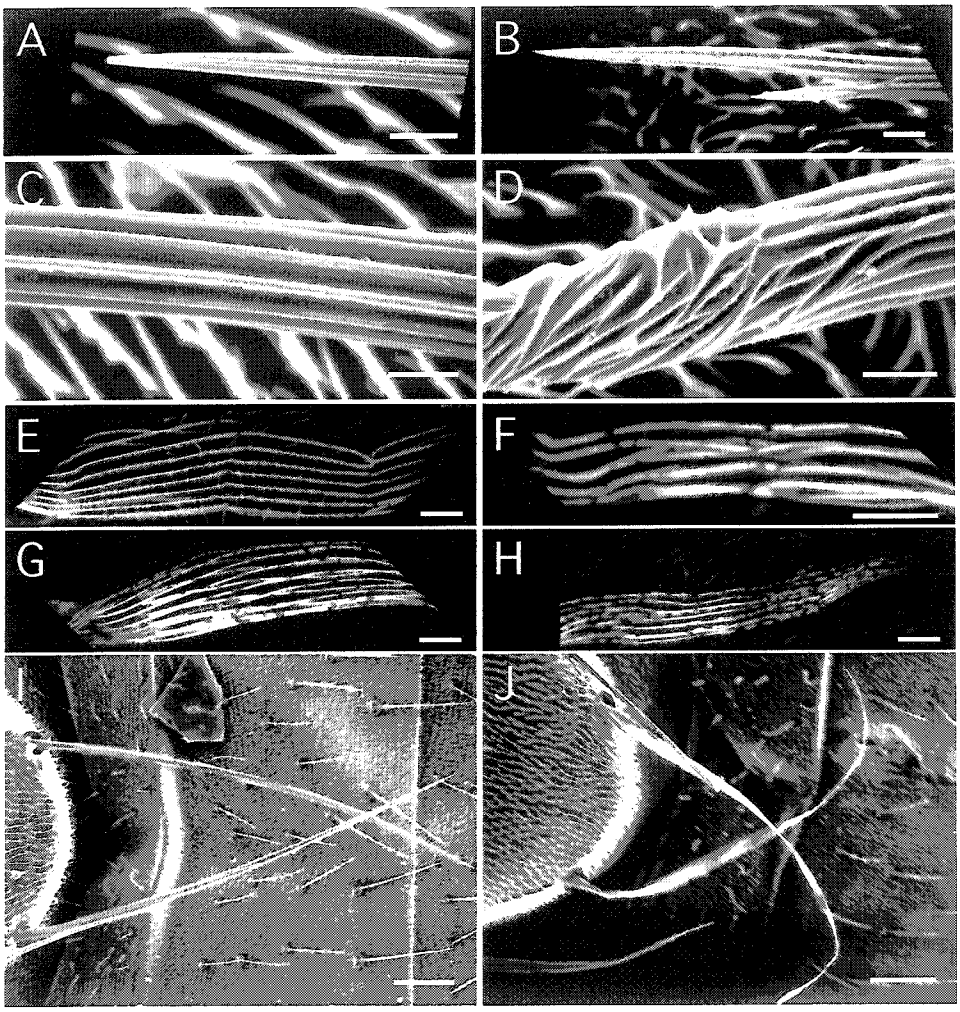
A
B
C
D
E
F
G
H
I
J

Figure 2.8

Overexpression of *Datx2* during eye development is toxic. Wild-type flies expressing *Datx2* in the retina under control of the *GMR-GAL4* driver (C-F) exhibit rough eyes, disorganized ommatidia, and loss of pigment cells relative to control flies bearing only the *GMR-GAL4* driver (A and B) or flies bearing only a *UAS-Datx2* transgene (data not shown). The degree of retinal disruption depends on the *Datx2* transgenic line used and the age of the fly. Flies expressing *Datx2* in the retina from a weakly expressing *Datx2* transgene (*UAS-Datx2.1B*) display a mild rough eye phenotype at 1 day (C), progressing to loss of eye pigmentation by 4 weeks of age (D). Control flies bearing only the *GMR-GAL4* driver at 1 day and 4 weeks (A and B, respectively) or the *UAS-Datx2.1B* transgene alone (data not shown) at the same time points exhibit normal eyes. Stronger *Datx2* transgenic lines (*UAS-Datx2.4* and *UAS-Datx2.3*) result in severe disruption of eye structure (E and F, respectively).

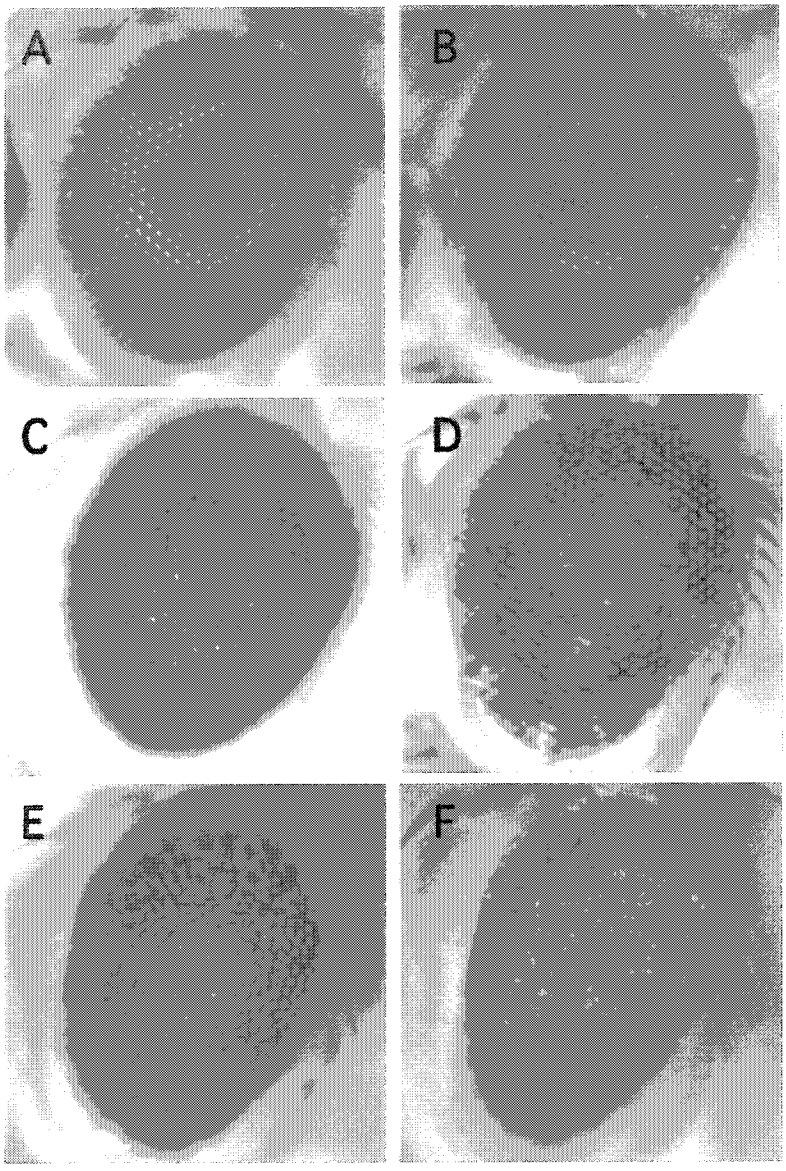
A
B
C
D
E
F

Figure 2.9

Altered *Datx2* gene dosage triggers the formation of aberrant filamentous actin structures in eye discs. The field shown is posterior to the morphogenetic furrow and is at a similar developmental stage. (A) Confocal projection of wild-type third instar eye disc stained with fluorescently labeled phalloidin to highlight filamentous actin. Rosettes are indicated with arrows. (B) Eye disc fully homozygous for the *Datx2l(3)06490* mutation stained with phalloidin. Note the bright, punctate actin-staining structures in the cells of the rosette (arrows). (C) Eye disc from a fly ectopically expressing *Datx2* from the *UAS-Datx2.3* transgene under the direction of *GMR-GAL4*. Like the *Datx2* loss-of-function discs, actin staining was punctate and disorganized in these discs as a result of *Datx2* overexpression (arrows). Bars, 5 μm.

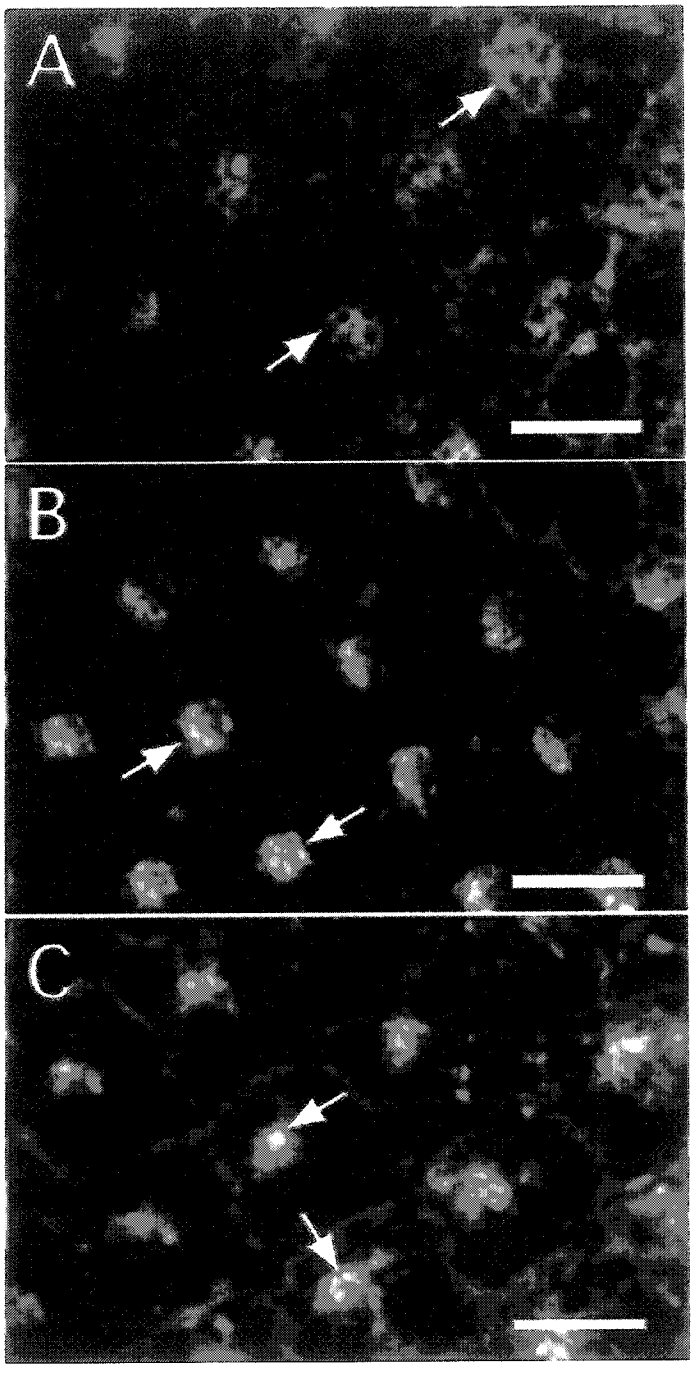
A
B
C

Figure 2.10

***Datx2* does not regulate actin abundance or physically associate with filamentous actin.** (A) Identical amounts of total ovarian protein extract (10 μg) obtained from the indicated genotypes were subjected to Western blot analysis using antisera to Datx2, actin, and alcohol dehydrogenase (ADH). The residual Datx2 and increased abundance of actin and ADH immunoreactivity present in extracts from the *Datx2X1* germline clones likely derive from increased contributions of somatic tissues owing to the early oogenesis arrest in these mutants. (B) Ovarian extracts were incubated with biotinylated phalloidin and precipitated with streptavidin beads. The resulting supernatant and pellet fractions were subjected to Western blot analysis using antisera to Datx2 and actin. Note that although a large fraction of actin is precipitated by phalloidin, no Datx2 precipitation is detected in these fractions.

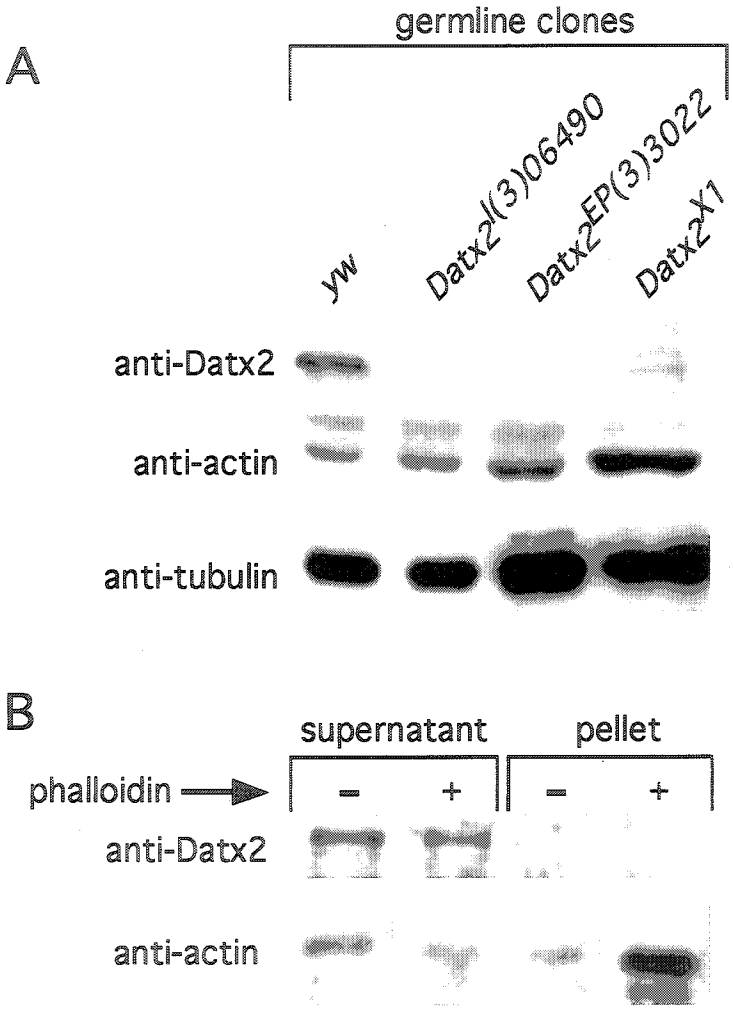
A
germline clones
yw
Datx2l(3)06490
Datx2EP(3)3022
Datx2X1
anti-Datx2
anti-actin
anti-tubulin
B
supernatant
pellet
phalloidin
-
+
-
+
anti-Datx2
anti-actin

Table 2.1
Rescue efficiency of UAS-Datx2 transgenes

UAS-Datx2 transgenic line	Rescue efficiency[a] (%)
UAS-Datx2.1B	0.3%
UAS-Datx2.3	7.9%
UAS-Datx2.4	16%

a. Rescue efficiency is defined as the percentage of homozygous $Datx2^{l(3)06490}$ mutants recovered from a cross of $Datx2^{l(3)06490}$ heterozygotes to *UAS-Datx2;*$Datx2^{l(3)06490}$ heterozygotes, relative to Mendelian expectations for full rescue. A minimum of 600 progeny were scored for each cross.

Table 2.2
Summary of Datx2 female germline clone phenotypes

	normal pre-cytoplasmic dumping egg chambers[a]	normal post-cytoplasmic dumping egg chambers[b]	mis-positioned oocyte	oocyte specification failure	degenerating egg chambers[c]	extra germline cells	fewer germline cells	cytoplasmic dumping failure	
$Datx2^{l(3)06490PE}$[d] (Control)	72%	27%	0%	0%	1%	0%	0%	0%	N=373
$Datx2^{l(3)06490}$	56%	0%	4%	0%	8%	0%	0%	29%	N=467[e]
$Datx2^{X1}$	4%	0%	22%	42%	19%	10%	4%	N/A[f]	N=189[e]

Tallies are the distribution percentage of all egg chambers produced by these females. NA, not applicable.

[a]Includes all egg chambers prior to the cytoplasmic dumping stage.

[b]Includes all egg chambers beyond the cytoplasmic dumping stage.

[c]Includes degenerating egg chambers from all stages.

[d]$Datx2^{l(3)06490PE}$ represents a precise excision derivative of the *l(3)06490 Datx2* insertion. This precise excision allele was used to generate germline clones using the same procedure used for the $Datx2^{l(3)06490}$ and *Datx2* alleles.

[e]Percentages do not total 100% due to rounding.

[f]No egg chambers from $Datx2^{X1}$ clones progress to the cytoplasmic dumping stage.

Table 2.3
***Datx2* overexpression phenotypes**

GAL4 line (expression pattern)	*Datx2* transgenic lines[a]		
	UAS-Datx2.1B	*UAS-Datx2.4*	*UAS-Datx2.3*
HSP-GAL4 (25C) (ubiquitous)	no detectable phenotype	semi-lethal[b]	semi-lethal[b]
elav-GAL4 (all neurons)	no detectable phenotype	semi-lethal[b]	semi-lethal[b];survivors are uncoordinated
ey-GAL4 (adult head)	no detectable phenotype	lethal[c]; head structures absent	lethal[c]; head structures absent
24B-GAL4 (mesoderm)	lethal[c]	lethal[c]	lethal[c]
GMR-GAL4 (retina)	mild rough eye; pigment cell degeneration	rough eye	severe rough eye

[a]All results shown are derived from ectopic expression of *Datx2* in a wild-type background.

[b]"semi-lethal" indicates that fewer than 50% of the expected Mendelian proportions of this genotype were recovered from crosses designed to generate these flies.

[c]"lethal" indicates that no progeny of this genotype were recovered from crosses designed to generate these flies.
A minimum of 400 flies were scored in each cross.

CHAPTER 3:

Human and Drosophila ataxin-2 assemble with mRNA as components of messenger ribonucleoproteins and polyribosomes

INTRODUCTION

In this study we show that Datx2 and human ataxin-2 proteins assemble with translating mRNAs (polyribosomes) as a component of messenger ribonucleoprotein particles (mRNPs). Both conserved Datx2 domains, the N-terminal ATX2N domain and the ATX2C/PAM2 domain, can each independently assemble with RNA. Like its yeast and worm counterparts, Datx2 physically interacts with PABP. We find that the ATX2C/PAM2 domain is necessary for this interaction and for the *in vivo* activity of Datx2. Taken with previous results, our results support a model whereby ataxin-2 proteins play a direct role in RNA metabolism through their assembly with mRNA. These results raise the possibility that polyglutamine expansions in ataxin-2 cause harmful alterations in mRNA metabolism that may underlie or contribute to the pathogenesis of SCA2.

MATERIALS AND METHODS

Extract preparations:

50 ovaries were dissected into cold PBS (with 100 μg/ml cycloheximide). Ovaries were placed in 0.7 ml cold mDXB (125 mM sucrose, 25 mM HEPES, pH 6.9, 100 mM KCl, 5 mM MgCl2, 1 mM DTT) supplemented with Complete protease inhibitor cocktail (Roche) and then subjected to 30 strokes in a pre-chilled 2 ml dounce homogenizer. Post-mitochondrial supernatants were obtained by centrifuging extracts at 10,000*g* for 10

min at 4°C. Kc cells and S2 cells were grown into log phase, and 2 X 10^7 Cells were incubated with 100 μg/ml cycloheximide (Sigma) for 10 min. Cells were washed with cold PBS (with 100 μg/ml cycloheximide) and resuspended in 1ml polyribosome lysis buffer (PLB: 25mM HEPES, pH 6.9, 100 mM KCl, 5 mM $MgCl_2$, 1 mM DTT, 0.5% NP-40) supplemented with Complete protease inhibitor cocktail (Roche) and incubated on ice for 10 min. We obtained post-mitochondrial supernatants were prepared as described above.

Sucrose gradient analysis:

For ovaries and cultured cells, extracts (15-20 O.D. A_{260} units) were layered onto 10 mL 10-50% (w/v) linear sucrose gradients made in polysome buffer (PB: 25 mM HEPES, pH 6.9, 100 mM KCl, 5mM $MgCl_2$, 1 mM DTT) supplemented with Complete protease inhibitor cocktail (Roche) and 100 μg/mL cycloheximide. For EDTA disruption of polyribosomes, 25 mM EDTA was used in place of $MgCl_2$ in the lysis and gradient buffers. For RNase disruption of polyribosomes, 100 μg/mL RNase A (Sigma) was added to the extract and incubated for 10 min at room temperature before loading onto gradients. Gradients were centrifuged in a Beckman SW41-Ti rotor at 36,000 rpm for 1 h 50 min at 4°C followed collection of 12-1 ml fractions. Proteins in each fraction were precipitated with 10% trichloroacetic acid (TCA), and following two washes with cold 95% ethanol, proteins pellets were resuspended by incubation at 37°C for 10 min in 20 μl 100 mM Tris, pH 8.0 containing 1% sodium dodecyl sulfate (SDS). 20 μl 2X SDS sample buffer was added, and proteins were denatured by boiling for 10 min. 20 μl of each sample was used for analysis by SDS-PAGE.

Cell electroporation:

S2 cells were maintained at 25°C in Schneider's media (Invitrogen) supplemented with 10% fetal calf serum and 1X penicillin-streptomycin-glutamine (Invitrogen). For transfections, log-phase cells were washed twice with serum-free Schneider's media (Sigma) and each 6 mL of cells was pelleted and resuspended in 780 μl of serum-free media and placed into 0.4 cm-gap electroporation cuvettes (BioRad). 20 μg (1 μg/μl) was added and cells were electroporated (400 V, 960 μF) using a Gene Pulser II (BioRad). Each sample was resuspended in 6 mL of complete Schneider's media. For each construct, 12 mL of cells were transected and plated into a 75 cm2 tissue culture flask. 24 hours post-transfection, protein expression was induced by adding $CuSO_4$ to 500 μM. Cells were harvested for gradient analysis 48 hours post-induction.

SDS-PAGE analysis:

Proteins were separated by SDS-PAGE on 8% acrylamide gels and electrophoretically transferred onto nitrocellulose membranes (Amersham). Immunodetection of FLAG-modified proteins, Datx2, dPABP, ribosomal P0, and ataxin-2 was performed using anti-FLAG M2 monoclonal antibody (1:10,000; Sigma), rabbit anti-Datx2 (1:15,000; SATTERFIELD *et al.* 2002). rabbit anti-dPABP (1:5000; ROY *et al.* 2004), human anti-P0 (1:3000; Immunovision), and mouse anti-ataxin-2 (1:250; BD Transduction Labs) respectively.

Drosophila strains:

Flies were reared on standard molasses corn meal agar, and all crosses were performed at 25 °C. To generate transgenic flies, modified *Datx2* constructs were all cloned as BglII-Xho fragments into the transformation vector pUAST (BRAND and PERRIMON 1993). Germline transformation was performed using standard procedures (ASHBURNER 1989).

Rescue experiments:

The Df(3R)Po4 stock, which removes the *Datx2* locus, was used in complementation and lethal phase analysis with the *Datx2* mutants. At least 100 progeny were scored from each cross. Flies of the genotype pUAST::5'UTR-DATX2/Cyo;Datx2^{X1}/TM6B were crossed to Df(3R)Po4/TM6B flies. All offspring from the cross were scored and percent rescue was calculated based on Mendelian expectation.

RESULTS

Datx2 and ataxin-2 associate with polyribosomes:

Our previous work demonstrated that the Drosophila *SCA2* ortholog, *Datx2*, encodes a widely expressed cytoplasmic protein. Taken with the presence of Sm and PAM2 motifs in Datx2 (SATTERFIELD *et al.* 2002), the cytoplasmic localization of the protein prompted us to speculate that Datx2 may be a component of cytoplasmic messenger ribonucleoprotein complexes (mRNPs). To address whether Datx2 is a component of mRNPs, we analyzed the sedimentation properties of Datx2. Because our

previous work indicates that Datx2 is essential for normal ovary development, we chose to initially analyze extracts prepared from ovaries (SATTERFIELD *et al.* 2002). We prepared post-mitochondrial extracts from Drosophila ovaries and subjected the extracts to sedimentation through 10-50% (w/v) continuous sucrose gradients. We collected 12 fractions from the gradient and used Western analysis to determine which fractions contained Datx2 protein. We observed Datx2 in all gradient fractions (Figure 3.1). In the upper regions of the gradient, Datx2 cofractionated with free protein, ribosomal subunits, and monosomes. In the lower, more dense regions, Datx2 cofractionated with polyribosomes, as indicated by cofractionation with poly(A)-binding protein (PABP) and the 60S ribosomal protein P0 (TCHORZEWSKI *et al.* 2003).

If Datx2 migrates into dense regions of the gradient because it physically associates with polyribosomes, then destruction of polyribosomes ought shift Datx2 to the upper, less dense, region of the gradient. RNase (100 μg/mL) destroys the mRNA linking translating ribosomes to one another while keeping the ribosomes intact. When ovary extract was treated with RNase A (100 μg/mL; Sigma) prior to sedimentation, Datx2 remained in the upper-most region of the gradient (Figure 3.1). While Datx2 is enriched at the top of the gradient, the ribosomal P0 protein remains enriched in the 80S region of the gradient, indicating that monosomes remain intact under these conditions.

EDTA treatment is another way to disrupt polyribosomes (GANDER *et al.* 1975). While leaving the mRNA intact, EDTA removes ribosomes from mRNAs by forcing ribosomes to dissociate into their 40S and 60S subunits. Because ribosomes are very large and dense complexes, their disruption prevents polyribosomal mRNAs and their associated proteins from migrating into dense regions of the gradient. When treated with

EDTA (25 mM), the distribution of Datx2 shifted upward, though not as much as when treated with RNase A (Figure 3.1). With EDTA treatment, while P0 is enriched in the 60S region, Datx2 continues to sediment as a component of complexes ranging from free protein to greater than 80S. This result indicates that Datx2 exists as a component of polyribosomes and as a component of non-polyribosomal complexes. These EDTA-resistant complexes likely represent mRNPs since they mostly disappear in the presence of RNase. Taken together, these results indicate that that Datx2 is a component of polyribosomes and mRNP complexes.

We next addressed whether mammalian ataxin-2 also assembles with polyribosomes and mRNPs. To do this we analyzed extracts from a mouse neuronal cell line (MN1; SALAZAR-GRUESO *et al.* 1991). We prepared extracts from MN1 cells and subjected them to sedimentation on 10-50% (w/v) sucrose gradients. These analyses revealed that, like Datx2, ataxin-2 was present in fractions containing free protein, ribosomal subunits, monosomes, and polyribosomes (Figure 3.2). A significant amount of ataxin-2 cofractionated with polyribosomes. RNase treatment caused the majority of ataxin-2 to remain in the upper one third of the gradient, a region containing free protein, ribosomal subunits, and monosomes (Figure 3.2). Though significant, the RNase induced shift of ataxin-2 was not as dramatic as that of Datx2, and might reflect inefficient hydrolysis of some RNA species. EDTA treatment also caused ataxin-2 to shift upward in the gradient. Similar to what we observed for Datx2, with EDTA, ataxin-2 had a slightly broader distribution than with RNase treatment (Figure 3.2). Under either condition ataxin-2 did not strictly comigrate with the ribosomal marker P0, suggesting

that, like Datx2, ataxin-2 does not physically bind ribosomes. These results indicate that ataxin-2 is component of polyribosomes and mRNPs.

The ATX2N and ATX2C domains mediate Datx2 assembly with RNA:

To determine which Datx2 domains mediate interactions between Datx2 and RNA, we used sucrose gradients to analyze the sedimentation properties of Datx2 derivatives bearing targeted deletions. The conserved ATX2N domain (residues 60-270) contains RNA-binding Sm motifs, and thus alone may be sufficient to associate with RNA. The conserved ATX2C/PAM2 domain (residues 856-868), in other proteins, directly interacts with the RNA-binding protein PABP, making it possible that ATX2C/PAM2 indirectly links Datx2 with RNA through PABP. We engineered several *Datx2* expression constructs, all encoding proteins bearing an N-terminal FLAG epitope and deletions of ATX2N, ATX2C, or both (Figure 3.3A). Each construct was transfected into Drosophila S2 cells for expression and subsequent analysis.

To confirm that the FLAG epitope does not prevent Datx2 from assembling with mRNA, we analyzed the sedimentation of a Datx2 protein appended with the FLAG epitope. We found that, like endogenous Datx2, FLAG-Datx2 sediments throughout the gradient, shifting upwards when first treated with RNase (Figure 3.3B). The conserved ATX2N domain of Datx2 (residues 60-264) contains Sm motifs, and is predicted to bind RNA directly (ALBRECHT *et al.* 2004). Based on this we reasoned that the ATX2N domain would be alone sufficient to assemble with mRNA. To test this we generated a construct (FLAG-DATX2-ΔC1) that carries a deletion of the entire C-terminus (residues 280-1084), starting immediately past the ATX2N domain (Figure 3.3A). Like

endogenous Datx2, FLAG-Datx2-ΔC1 was present in all fractions of the gradient, demonstrating that the ATX2N domain alone can assemble with RNA (Figure 3.3B).

Having demonstrated that the ATX2N domain is sufficient to mediate Datx2 assembly with RNA, we sought to determine whether ATX2N is necessary for this interaction. To address this we generated a construct (FLAG-Datx2-ΔN) that carries an amino-terminal deletion (residues 1-280) spanning ATX2N (Figure 3.3A). Though missing the entire ATX2N domain, FLAG-Datx2-ΔN was present in all gradient fractions, demonstrating that the ATX2N domain is not necessary for Datx2 assembly with RNA (Figure 3.3B).

The only conserved region outside of ATX2N is the carboxyl-terminal ATX2C/PAM2. In other proteins, PAM2 is known to mediate physical interactions with poly(A)-binding protein (ROY *et al.* 2002; KOZLOV *et al.* 2004). Based on this, we reasoned that the ATX2C/PAM2 domain might allow Datx2 to associate with RNA. To address this, we generated a construct (FLAG-Datx2-ΔNC) that carries the ATX2N deletion (residues 1-280) and a small deletion (residues 856-868) that precisely removes the ATX2C/PAM2 domain (Figure 3.3A). This 12-residue deletion of ATX2C/PAM2 is the only feature distinguishing FLAG-Datx2-ΔNC from FLAG-Datx2-ΔN. When analyzed by sucrose gradient, we found that FLAG-Datx2-ΔNC remains at the top of the gradient (Figure 3.3B). The failure of this protein to migrate into the gradient indicates that, in contrast to proteins bearing single deletions of either ATX2N or ATX2C, FLAG-Datx2-ΔNC cannot assemble with RNA. Taken together, these results indicate that the ATX2N and ATX2C domains can independently mediate interactions between Datx2 and RNA.

The ATX2C/PAM2 domain is required for *Datx2* function *in vivo*:

Given that the ATX2N and ATX2C domains both mediate Datx2 assembly with RNA, we sought to investigate whether these domains are required for the *in vivo* activity of Datx2. Transgenic rescue of *Datx2* mutants apparently requires that *Datx2* rescue constructs have an intact 5' UTR (SATTERFIELD *et al.* 2002 and unpublished observations). Limited restriction sites precluded us from generating a deletion of ATX2N without disrupting the 5' UTR of the *Datx2* cDNA. Nevertheless, we tested whether the ATX2C/PAM2 domain is required to rescue the lethal phenotypes of flies homozygous for *Datx2* null mutations. To address this, we generated a *Datx2* construct (*Datx2-ΔC1*) bearing the same precise ΔC/PAM2 deletion used in gradient analyses. *Datx2-ΔC1* has a fully intact 5' UTR, and apart from the ΔC/PAM2 deletion, it is identical to the functional *Datx2* rescue construct we described previously (SATTERFIELD *et al.* 2002). We generated several independent transgenic lines, and used three for analysis. Western analysis revealed that the degree of transgene expression in these lines is similar to that seen in lines that can successfully rescue *Datx2* lethality (data not shown).

Flies homozygous for *Datx2* null mutations normally die in the 2nd instar larval stage. When crossed into a *Datx2* mutant background, an unmodified *Datx2* transgene rescued *Datx2* mutants to adulthood at 56% of Mendelian expectation (Table 3.1). In contrast, none of the three *Datx2-ΔC1* transgenes rescued *Datx2* mutants to adulthood. Notably, although the *Datx2-ΔC1* crosses did not yield any adults, two of the three *Datx2-ΔC1* transgenes did extend the viability of *Datx2* mutants beyond the larval stage

and into the late pupal stage. We dissected several mutant pupae from their cases and observed that several of these pupae had bent and forked bristles that appeared similar to the defective bristles we reported previously for transgenically rescued *Datx2* adults (data not shown). These results indicate that although the ATX2C/PAM2 domain of Datx2 appears dispensable for some Datx2 activity, ATX2C/PAM2 is strictly required for the full *in vivo* activity of *Datx2*.

DISCUSSION

In this study we demonstrated that Datx2 and ataxin-2 proteins assemble with polyribosomes and mRNPs. When subjected to sucrose gradient sedimentation, Datx2 and ataxin-2 both cosediment with polyribosomes and mRNPs. RNase treatment destroys polyribosomes and mRNPs, and shifts the distributions of both proteins. Similarly, EDTA-mediated disruption of polyribosomes also shifts the distributions of these proteins. Using constructs carrying various targeted deletions within *Datx2*, we demonstrated that the conserved amino-terminal ATX2N domain and the conserved carboxyl-terminal ATX2C/PAM2 domain are each able to assemble with polyribosomes and mRNPs. Consistent with an important functional role the ATX2C/PAM2 domain, we also discovered that this domain is required to rescue the lethality caused by *Datx2* null mutations.

How do Datx2 and ataxin-2 assemble with polyribosomes?:

Polyribosomal proteins can assemble with polyribosomes in a few ways. 1) Proteins can assemble directly with the ribosome (TCHORZEWSKI *et al.* 2004). 2)

Proteins can bind directly to the mRNA being translated (BROWN *et al.* 2001). 3) Proteins can associate with the mRNA indirectly by attaching to RNA-binding proteins (CRAIG *et al.* 1998). How then do Datx2 and ataxin-2 assemble with RNA? Three observations suggest that these proteins do not directly bind ribosomes. First, when polyribosomes are disrupted with RNase treatment, monosomes accumulate in the 80S region of the gradient. This is confirmed by enrichment of the P0 protein in this region. If Datx2 binds ribosomes, then under these conditions, it too ought to be enriched in the 80S region. This is not observed. Whereas P0 is enriched in the 80S region, Datx2 is enriched mostly in the less dense regions that contain free protein. Second, upon EDTA treatment, ribosomes dissociate into their 40S and 60S subunits. Under these conditions, whereas P0 is enriched in the 60S region of the gradient, Datx2 has a substantially broader distribution that extends beyond 80S. The observation that substantial amounts of Datx2 can sediment far beyond 60S indicates that substantial amounts of Datx2 exist as part of non-ribosomal complexes. Although the overlap of Datx2 and P0 distributions makes it formally possible that small amounts of Datx2 may bind ribosomes, it seems more likely that this overlap reflects coincidental similarities between the sizes of ribosomal complexes and Datx2 mRNPs. Third, whereas the distribution of Datx2 does not closely correlate with the distribution of ribosomes, it is almost identical to the distribution of poly(A)-binding protein, a protein that directly binds mRNAs. The similar sedimentation properties of Datx2 and ataxin-2 suggest that like, Datx2, it is unlikely that ataxin-2 directly binds ribosomes.

Instead of binding ribosomes, it is more likely that Datx2 assembles with polyribosomes by directly binding mRNAs. This interpretation is supported by structural

predictions that indicate that the Sm motifs of the ATX2N domain are functional RNA-binding motifs (ALBRECHT *et al.* 2004). Furthermore, the prediction that the ATX2N domain can directly bind RNA, is supported by our observation that the ATX2N domain is alone sufficient to mediate Datx2 assembly with RNA. Direct assembly with RNA via the ATX2N domain is not the only way that Datx2 can assemble with RNA. In other proteins, the PAM2 motif is known to mediate physical interactions with poly(A)-binding protein (ROY *et al.* 2002; KOZLOV *et al.* 2004). Taken with this, our observation that the ATX2C/PAM domain alone can mediate RNA assembly suggests that Datx2 might assemble with RNA indirectly, possibly through interactions with poly(A)-binding protein and/or related proteins.

Ataxin-2 proteins and translation:

Our observation that Datx2 and ataxin2 proteins assemble with translating mRNAs provides a direct link between ataxin-2 proteins and translational regulation. A role for these proteins in translation is also supported by other studies. The study of several ataxin-2 orthologs indicates that these proteins might function as translational repressors. In *C. elegans* reduced activity of ATX2 causes ectopic translation of several repressed germline mRNAs (CIOSK *et al.* 2004). This translational defect causes abnormal accumulation of specific proteins and leads to aberrant masculinization of the germline.

Mutation of the yeast *SCA2* ortholog (*PBP1*) suppresses the lethal phenotype of yeast *PABP* (*PAB1*) mutants (MANGUS *et al.* 1998). Because *PAB1* is a positive regulator of translation, loss of *PBP1* likely compensates for loss of *PAB1* by causing an

increase in protein synthesis. Consistent with this interpretation, several other mutations that suppress *PAB1* are known to act by increasing protein synthesis (DUNN and JENSEN 2003).

The mutant phenotype of *PBP1* also suggests that *PBP1* might inhibit translation. *PBP1* mutants cannot live without mitochondrial DNA, a phenotype called "petite-negative" (DUNN and JENSEN 2003). The *PBP1* phenotype is thought to stem from excessive accumulation of cellular proteins. Consistent with this interpretation, the *PBP1* phenotype can be suppressed by inhibiting translation. Additionally, overexpression of *PBP1* suppresses the phenotype of *TIM18* mutants, a phenotype also thought to stem from excessive protein accumulation (DUNN and JENSEN 2003). This interaction further suggests that *PBP1* inhibits translation.

Models of ataxin-2 activity:

Taken with our results, the available data on ataxin-2 proteins suggest a model in which these proteins inhibit translation by direct physical interactions with mRNAs and their associated proteins. The observation that Datx2 uses two separate domains to assemble with mRNA suggests that ataxin-2 proteins might use several approaches to influence translation. Specifically how might these domains influence translation?

Studies of other Sm motif proteins indicate that, like these proteins, ataxin-2 proteins might mediate RNA-RNA interactions. Most eukaryotic Sm proteins function in pre-mRNA splicing as components of the spliceosome (reviewed in KRAMER 1996). Within the spliceosome, Sm proteins form hexameric structures that appear to facilitate splicing by stabilizing interactions between non-coding small nuclear RNAs (snRNAs)

and pre-mRNAs. Sm proteins in bacteria also regulate RNA-RNA interactions. Hfq, a well studied bacterial Sm protein, influences RNA stability and translation by stabilizing interactions between non-coding microRNAs (miRNAs) and their mRNA targets (reviewed in STORZ *et al.* 2004). Several Sm proteins in yeast appear to function in mRNA decay (THARUN *et al.* 2000). The roles of Sm proteins in this process are unclear. Nevertheless, recent experiments indicate that microRNAs can direct mRNA decay, raising the possibility that Sm proteins are linked to mRNA decay through microRNAs (SHEN and GOODMAN 2004).

Ataxin-2 proteins might also regulate translation by modulating the activity of PABP. PABP binds to the poly(A) tail of mature mRNAs and stimulates translation by physically bridging the 3' and 5' ends of mRNAs. By influencing the interactions of poly(A)-bound PABP with the 5' cap, proteins containing PAM2 motifs can either enhance or inhibit translation (CRAIG *et al.* 1998; KHALEGHPOUR *et al.* 2001). The presence of the ATX2/PAM2 motif in ataxin-2 thus suggests that ataxin-2 proteins might also influence the interaction of poly(A)-bound PABP with the 5' cap. This model predicts that some ataxin-2 would be found physically attached to poly(A)-bound PABP. Our observation that Datx2 can attach to polyribosomes using its ATX2/PAM2 domain provides strong support for such a model. Though PAM2 containing proteins can either enhance or inhibit the activity of PABP, the genetic evidence described above suggests that ataxin-2 proteins probably inhibit PABP activity.

Based the above arguments, we propose a speculative model in which ataxin-2 proteins repress translation using two distinct mechanisms (Figure 3.4). In the first, the Sm containing ATX2N domain stabilizes interactions between microRNAs and their

mRNA targets. Similar interactions mediated by Hfq, these RNA-RNA interactions might block either translational initiation or elongation (reviewd in STORZ *et al.* 2004). In the second mechanism, the ATX2C domain binds to poly(A)-bound PABP and blocks its activity by preventing it from interacting with the 5' cap. Though crude, this model fits the limited data on ataxin-2 and related proteins. Additionally, it provides a framework to test specific hypotheses about the molecular activities of ataxin-2 proteins.

Implications for SCA2 disease:

Although transcriptional repression appears to underlie the pathogenesis of several polyglutamine diseases, the observation that SCA2 derives from a cytoplasmic disturbance makes it unlikely that SCA2 is caused by aberrant transcription. To the contrary, the results presented here raise the possibility that polyglutamine expansions in ataxin-2 cause SCA2 by interfering with mRNA translation. Based on the fact that polyglutamine expansions in several transcriptional regulators induce pathogenic changes in transcription, an intriguing possibility is that expansions in ataxin-2 analogously induce pathogenic changes in translation. If true, this would indicate that polyglutamine diseases collectively arise from aberrations in gene expression that can occur at the level of DNA or RNA.

In this vein, it is noteworthy that overexpression of wild-type *Datx2* synergistically enhances polyglutamine-induced toxicity Drosophila (SHULMAN and FEANY 2003). This genetic interaction indicates that *Datx2* and expanded polyglutamine might impinge on related pathways. Based on our model, one possibility is that *Datx2* overexpression exacerbates the polyglutamine-induced transcriptional

repression by further reducing gene expression at the level of translation. Though intriguing, the specific mechanisms underlying this interaction await further analysis.

Though we speculate on how ataxin-2 might influence RNA metabolism, several questions remain. Does ataxin-2 function to regulate translation? Does ataxin-2 regulate global translation or just specific mRNA targets? How does polyglutamine expansion affect the activity of ataxin-2? Is there evidence for aberrant translation in the brains of SCA2 patients? We suspect these questions will be central to a complete understanding SCA2 pathogenesis. Answering them will likely help us better understand SCA2 and other polyglutamine diseases.

Figure 3.1

Datx2 associates with polyribosomes. Cytoplasmic extracts from Drosophila ovaries were analyzed by sedimentation through sucrose density gradients before or after treatment with RNase A (100 μg/mL) or EDTA (25 mM). Samples containing ~20 A_{260} units were loaded onto linear 10-50% (w/v) sucrose gradients and centrifuged for 1 h 50 min at 36,000 r.p.m. at 4°C. Each of 12 fractions was analyzed by immunoblotting for Datx2, poly(A)-binding protein (PABP), and the ribosomal protein P0.

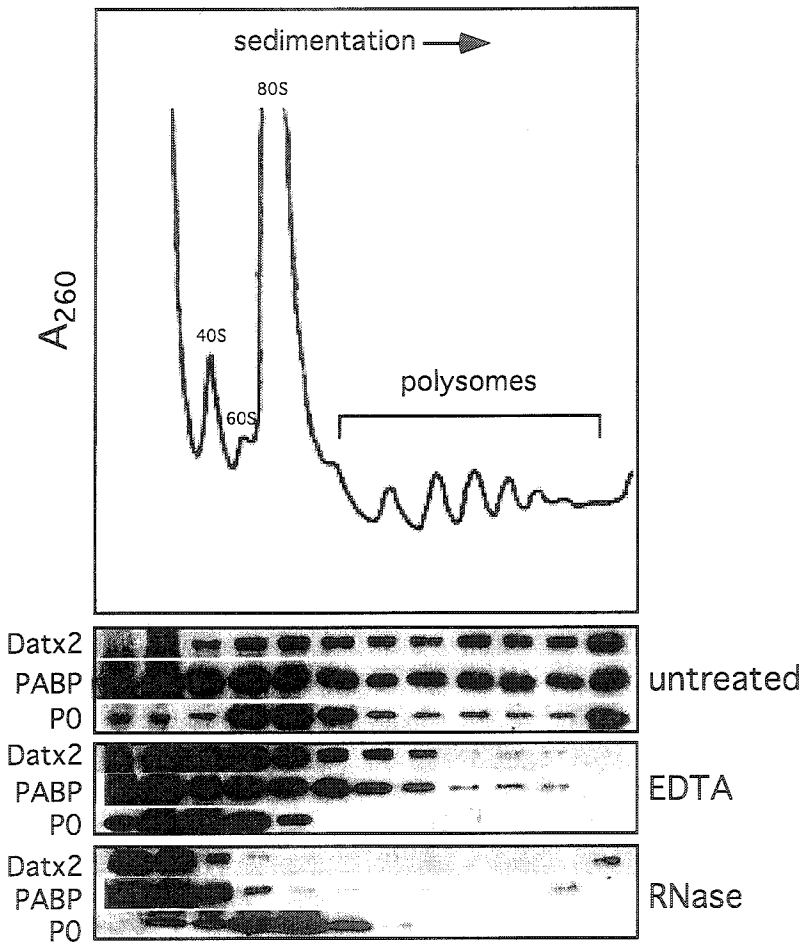
sedimentation
80S
40S
60S
polysomes
A_{260}
Datx2
PABP
P0
untreated
Datx2
PABP
P0
EDTA
Datx2
PABP
P0
RNase

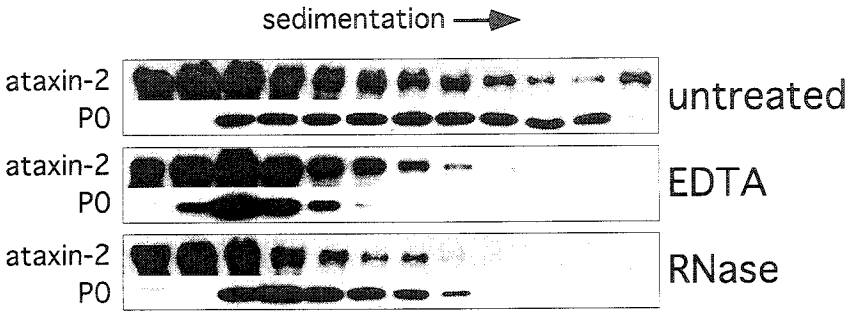

Figure 3.2 Ataxin-2 associates with polyribosomes. Cytoplasmic extracts from cultured MN1 motor neurons were analyzed by sedimentation through sucrose density gradients before or after treatment with RNase A (100 μg/mL) or EDTA (25 mM). Samples containing ~20 A_{260} units were loaded onto linear 10-50% (w/v) sucrose gradients and centrifuged for 1 h 50 min at 36,000 r.p.m. at 4°C. Each of 12 fractions was analyzed by immunoblotting for ataxin-2 and the ribosomal protein P0.

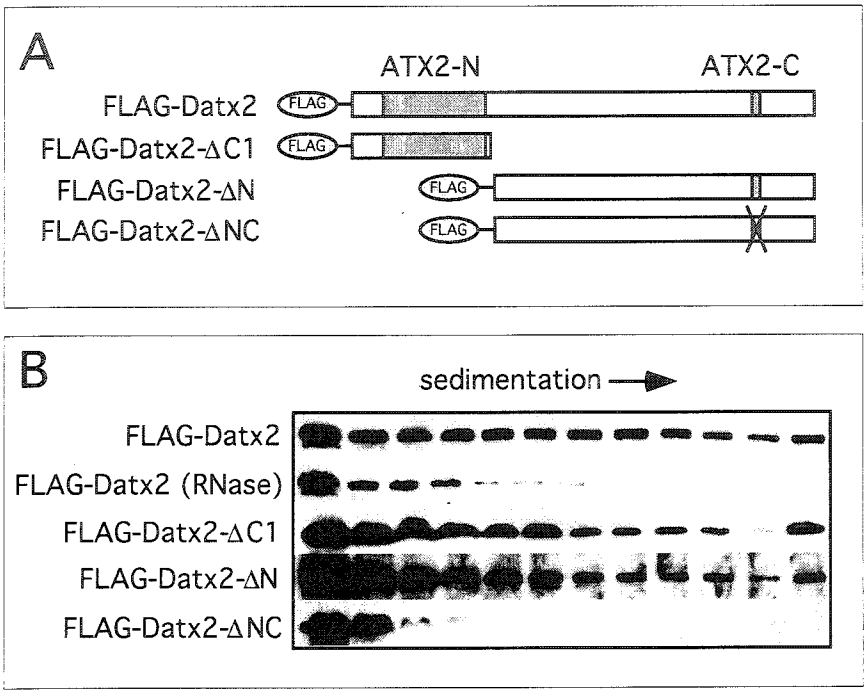

Figure 3.3. ATX2N and ATX2C domains mediate assembly with polyribosomes. (A) FLAG epitope tagged Datx2 and Datx2 deletion constructs. (B) Constructs were expressed in S2 cells. Cytoplasmic extracts were isolated and loaded onto 10-50% (w/v) sucrose gradients and centrifuged for 1 h 50 min at 36,000 r.p.m. at 4°C. Each of twelve fractions was analyzed by immunoblotting with a FLAG antibody.

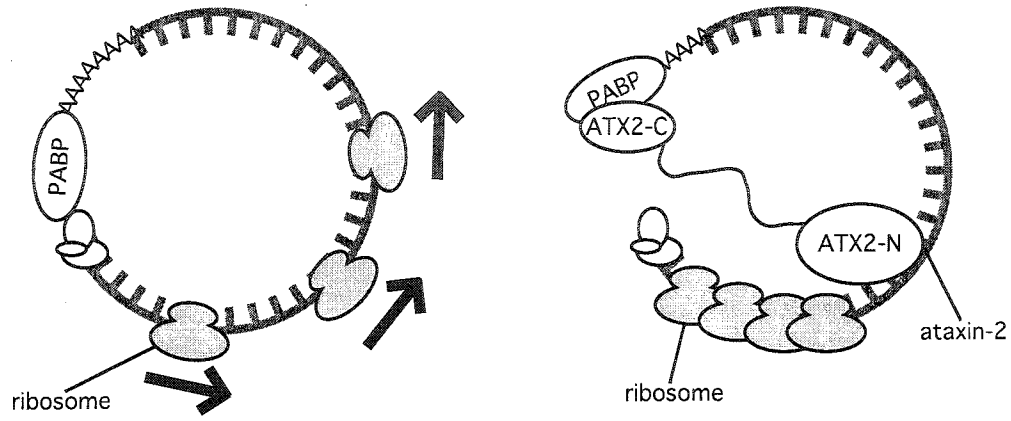

Figure 3.4. Model of ataxin-2 activity. (A) Schematic depicted mRNA translation. Ribosomes migrate along the mRNA, and poly(A)-binding protein (PABP) stimulates translation by promoting interactions between the 5' and 3' ends of the mRNA molecule. (B) The ATX2-N domain of ataxin-2 might use microRNAs to impede ribosomal translocation, while the ATX-2C domain might impede translation by blocking poly(A)-binding protein from interacting with the 5' end of the mRNA.

Table 3.1
Rescue efficiencies of *Datx2-ΔC* transgenes

Datx2 transgenic line	% rescue[a] efficiency
UAS-Datx2.4	56.3
UAS-Datx2-ΔC.1A++	0
UAS-Datx2-ΔC.1A(3)	0
UAS-Datx2-ΔC.2	0

[a]Rescue efficiency is defined as the percentage of homozygous $Datx2^{X1}$ mutants recovered from a cross of $Datx2^{X1}$ heterozygotes to *UAS-Datx2;* $Datx2^{X1}$ heterozygotes relative to Mendelian expectations for full rescue. A minimum of 500 flies were scored for each cross.

CHAPTER 4:

Modification Screen

To identify genomic regions that might contain genes that interact with *Datx2*, I performed a genetic screen to identify genomic regions that, when deleted, modify the effects of *Datx2* overexpression (Figure 4.1). As described above, overexpression of *Datx2* in the eye causes disorganization of the eye ommatidia and defective organization of eye bristles. To facilitate rapid screening, I generated flies carrying the eye-specific *GMR-GAL4* driver (ELLIS *et al.* 1993) and the UAS-Datx2 transgene on the same chromosome (chromosome 2). Flies carrying this "overexpression cassette" will have rough eyes because the *GMR-GAL4* driver promotes overexpression of *Datx2* from the UAS transgene.

To identify specific modifying deficiencies, I individually mated flies bearing the overexpression cassette with individual flies bearing deficiencies that remove various regions on chromosome 2 and chromosome 3 (Figure 4.2). In the offspring of these crosses, I then compared flies carrying the overexpression cassette to flies carrying the overexpression cassette and a deficiency. I tested 72 deficiency stocks from chromosome 2 and 40 deletions from chromosome 3 (Tables 4.1 and 4.2). Of the 72 deficiencies from chromosome 2, four suppressed the rough eye phenotype caused by *Datx2* overexpression and three enhanced it (Figure 4.3 and Table 4.1). Of the 40 deficiency stocks from chromosome 3, three suppressed the rough eye phenotype and one enhanced it (Figure 4.4 and Table 4.2).

The finding that the most deletions had no effect on the rough eye phenotype caused by *Datx2* overexpression indicates that this phenotype is not readily modified. This suggests that the effects of *Datx2* overexpression are only influenced by a limited subset of genes. Presumably, the *Datx2* overexpression phenotype is modified by the

reduced expression of genes that are removed by the modifying deletions, though other possibilities exist. One possibility is that other mutations on the deletion chromosomes are responsible for the phenotypic modification. Because some of the modifying deletions also carry duplications and other aberrations, it is possible that the modification activity stems from these other aberrations. To identify the specific genes responsible for the modifying effects of the modifying deletions, future studies should focus on using smaller deletions that overlap the modifying deletions to narrow the region containing the modifying activity. Once a small modifying region identified, then mutations in individual genes can be tested to identify the gene responsible for modifying the *Datx2* overexpression phenotype.

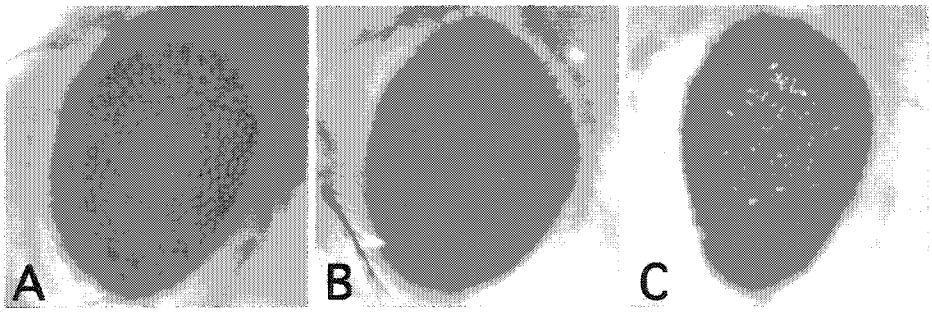

Figure 4.1. Chromosomal deficiencies can modify the effects of *Datx2* overexpression. (A) Wild-type flies expressing *Datx2* in the retina under control of the *GMR-GAL4* driver exhibit rough eyes and disorganized ommatidia. (B) Example of a chromosomal deficiency [Df(2L)C144] that suppresses the phenotypes caused *Datx2* overxpression. (C) Example of a chromosomal deficiency [Df(3R)e-N19] that enhances the phenotypes caused by *Datx2* overexpression.

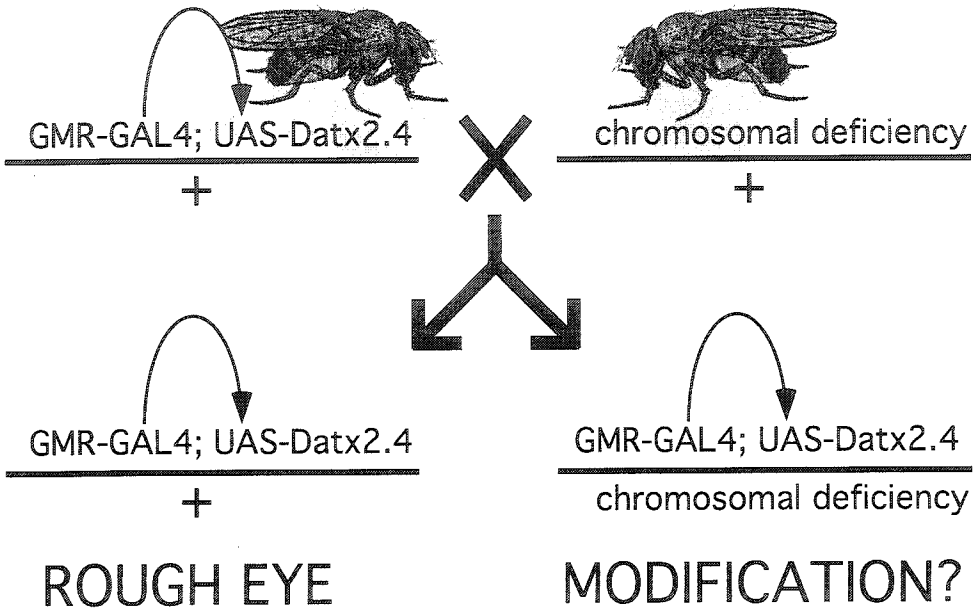

Figure 4.2. *Datx2* modifier screen strategy. Flies carrying the *GMR-GAL4* driver and a *Datx2* transgene (*UAS-Datx2.4*) on chromosome 2 were systematically crossed to flies bearing individual chromosomal deficiencies. Offspring bearing the *GMR-GAL4*; *UAS-Datx2.4* chromosome were compared to offspring bearing the *GMR-GAL4*; *UAS-Datx2.4* chromosome and a chromosomal deficiency.

Figure 4.3

Chromosome two deficiency modifiers of *Datx2* overexpression. Deficiencies that do not modify the *Datx2* eye overexpression phenotype are shown in black. Deficiencies that suppress the phenotype are shown in green. Deficiencies that enhance the phenotype are shown in red.

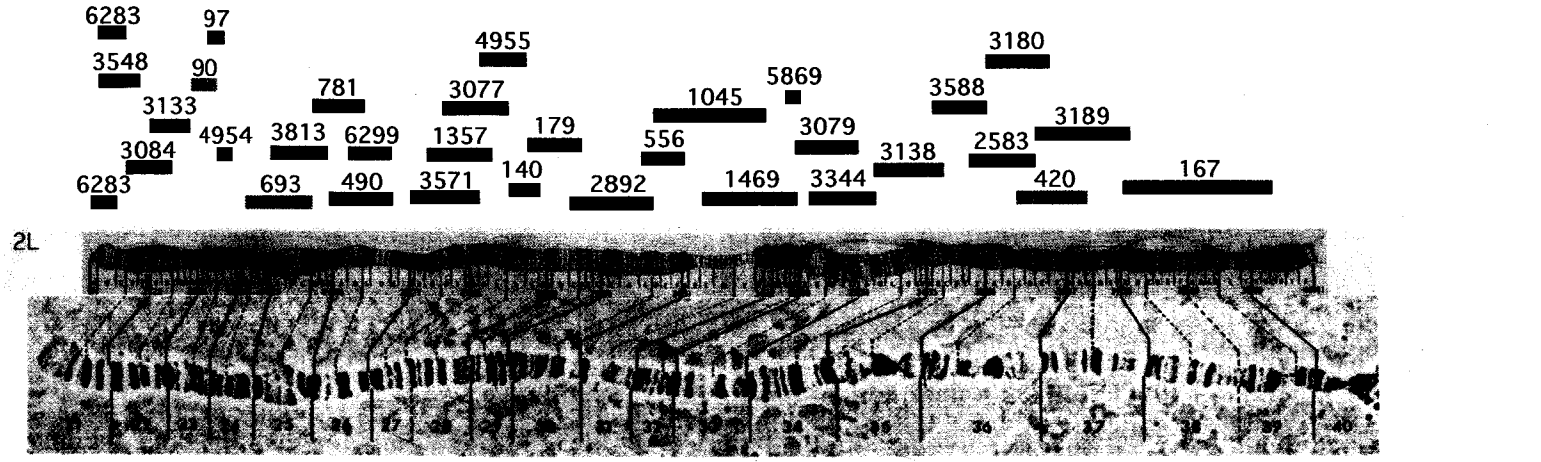
6283
97
3548
90
4955
3180
3133
781
3077
5869
1045
3588
3189
4954
3813
6299
1357
179
556
3079
2583
3084
3138
6283
693
490
3571
140
2892
1469
3344
420
167
2L

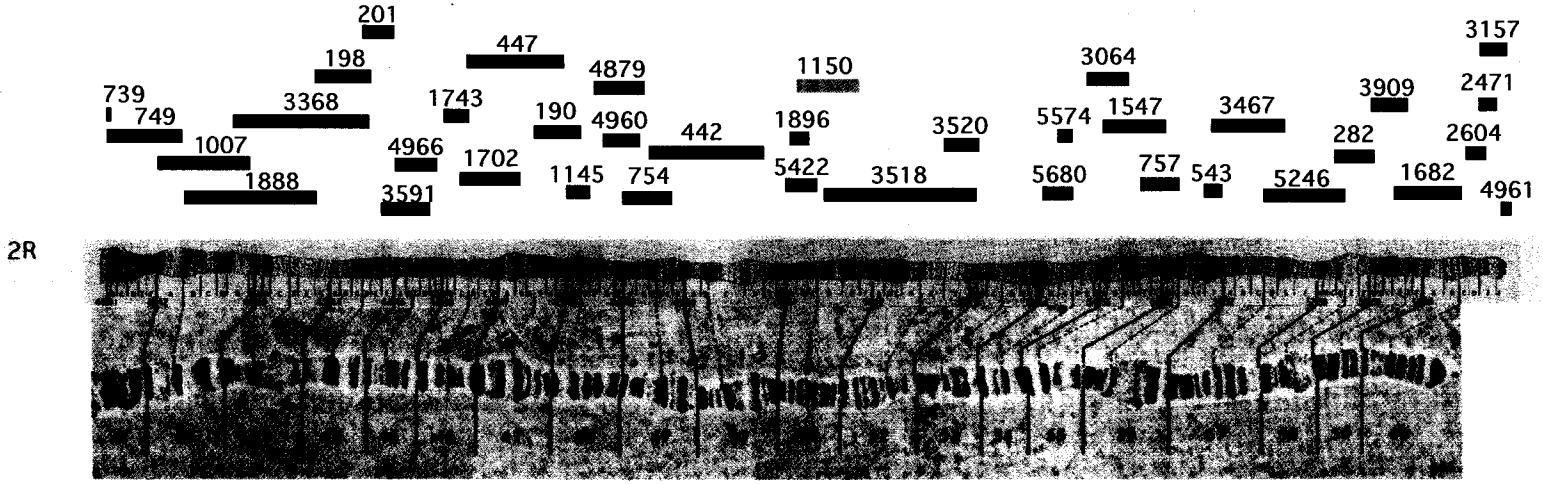
201
3157
198
447
3064
739
4879
1150
3909
2471
749
3368
1743
190
4960
1896
5574
1547
3467
3520
282
2604
1007
4966
1702
442
1145
754
5422
3518
5680
757
543
5246
1682
1888
3591
4961
2R

Figure 4.4

Chromosome three deficiency modifiers of *Datx2* overexpression. Deficiencies that do not modify the *Datx2* eye overexpression phenotype are shown in black. Deficiencies that suppress the phenotype are shown in green. Deficiencies that enhance the phenotype are shown in red.

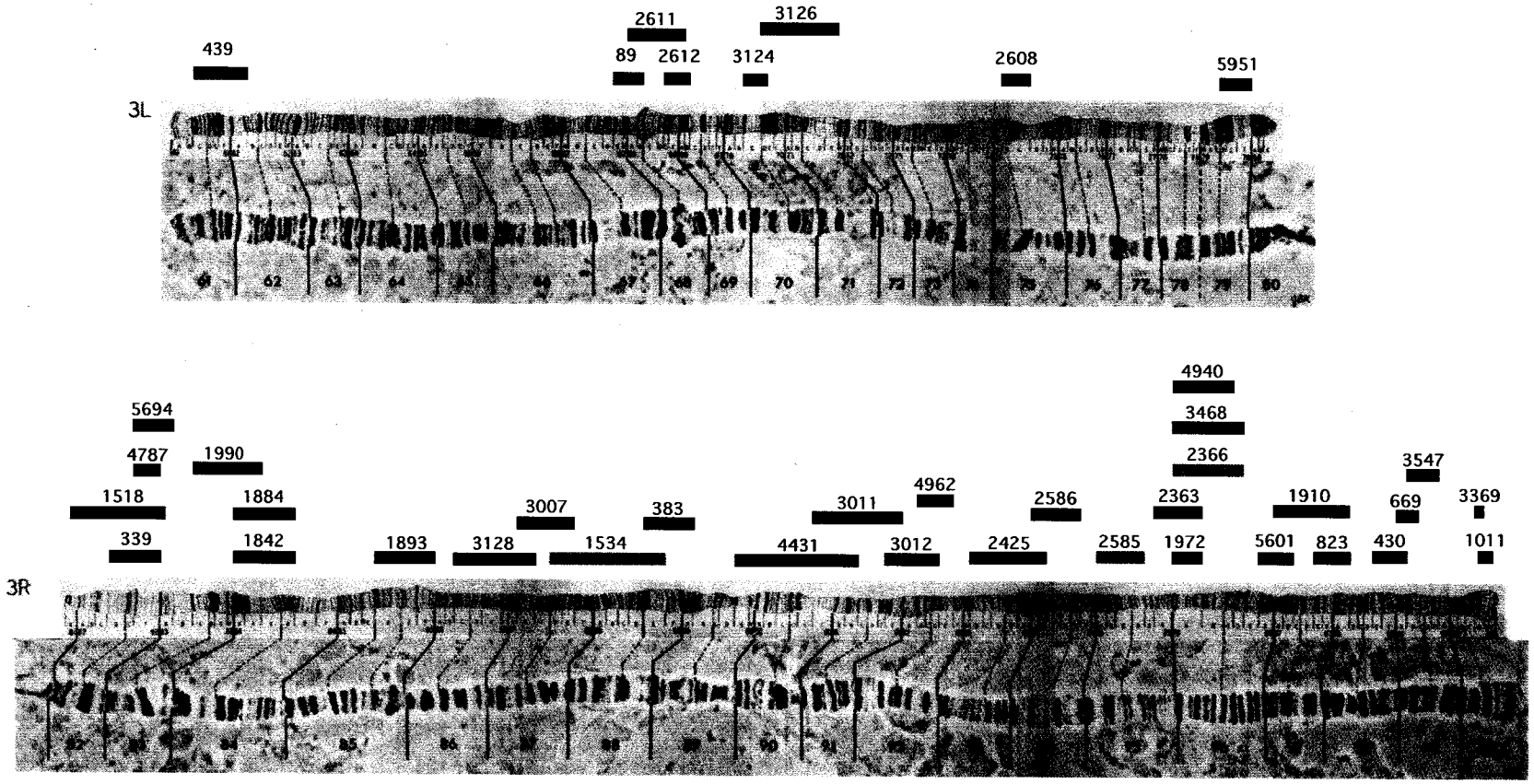
439
2611
89
2612
3126
3124
2608
5951
3L
62
63
64
69
70
71
72
4940
5694
3468
4787
1990
2366
3547
1518
1884
3007
383
3011
4962
2586
2363
1910
669
3369
339
1842
1893
3128
1534
4431
3012
2425
2585
1972
5601
823
430
1011
3R

Table 4.1. Chromosome 2 deficiencies tested in modification screen.

Bloomington Stock	Deficiency	breakpoints	modification	other abberations
90	Df(2L)C144	22F3-4; 23C3-5	suppressor	
97	Df(2L)JS32	23C3-5; 23D1-2	none	
140	Df(2L)Trf-C6R31	28D; 28-E	none	
167	Df(2LTW161	36A6; 40A4-B1	none	
179	Df(2L)TE29Aa-11	28E4-7; 29B2-C1	none	
190	Df(2R)en-A	47D3; 48A5	none	
198	Df(2R)H3C1	43F; 44D3-8	none	
201	Df(2R)H3E1	44D1-4; 44F12	none	
282	Df(2R)X58-12	58D1-2; 59A1	none	
420	Df(2L)TW137	36C2-4; 37B9-10	suppressor	
447	Df(2R)stan1	46D7-9; 47F15-16	none	
490	Df(2L)E110	25F3-26A1; 26D3-11	none	
543	Df(2R)017	56F5; 56F15	none	
556	Df(2L)S1402	30C1-2; 30F	none	
693	Df(2L)sc19-8	24C2-3; 25C8	suppressor	
739	Df(2R)M41A4	h44-h46; 42A1-2	none	
749	In(2R)bw^{VDE2L}Cy^{R}	42A-3; 58A4 and h42-h43; 59E1	none	
754	Df(2R)vg-C	49B2-3; 49E2	none	
757	Df(2R)P34	55E6-F3; 56C1	none	
781	Df(2L)cl-h3	25D2-3; 26B2-5	none	
1007	Df(2R)nap9	42A1-2; 42E6-F1	none	
1145	Df(2R)en30	48A3; 48C6-8	none	
1150	Df(2R)knSA3	51B5-11; 51C1-D1	suppressor	
1357	Df(2L)J-H	27C5-9; 28B3-4	none	
1469	Df(2L)J39	31C; 32D1-E5	none	Dp(1;Y)B[s]Yy[+]
			none	Dp(2;Y)cb50
1547	Df(2R)PC4	55A1; 55F1-2	none	
1682	Df(2R)or-BR6	59D5-10; 60B3-8	none	In(2LR)lt^{G16L}bw^{V32gR}
1702	Df(2R)X1	46C2; 47A1	none	
1743	Df(2R)B5	46A1-4; 46C3-12	none	
1888	Df(2R)ST1	42B3-4; 43E18	none	
1896	Df(2R)trix	51A2; 51B6	none	
2471	Df(2R)M60E	60e6-9; 60E11	none	In(2LR)bw^{V32g}
2583	Df(2L)cact-255rv64	35F6-12; 36D	none	
2604	Df(2R)Px2	60C6; 60D9-10	none	
2892	Df(2L)N22-14	29C1-2; 30C8-9; 30D1-2; 31A1-2	none	
3064	Df(2R)Pc17B	54E8-F1; 55B9-C1	none	
3077	Df(2L)spd	27E; 28C1-4	none	
3079	Df(2L)Prl	32F1-3; 33F1-2	none	
3084	Df(2L)ast2	21D1-2; 22B2-3	none	

Table 4.1. Continued.

3138	Df(2L)b87e25	34C1; 35C1	none	
3157	Df(2R)ES1	60e6; 60F1-2	none	
3180	Df(2L)H20	36A8-9; 36F1	none	
3189	Df(2L)TW50	36E4-F1; 38A6-7	none	Dp(2;2)M(2)m^{+}
3344	Df(2L)prd1.7	33B3; 34A1-2	none	
3467	Df(2R)AA21	56F9-11; 57D12; <57D12	none	
3518	Df(2R)Jp1	51C3; 52F8-9	none	
3520	Df(2R)Jp8	52F5-9; 53A1	none	
3548	Df(2L)al	21C1; 21C7	none	In(2L)Cy
3571	Df(2L)Dwee-d5	27A; 28A	none	Dp(?;2)bw^{D}
3588	Df(2L)TE35BC-24	35B4-6; 35E1-2	none	
3591	Df(2R)Np5	44F11;45D9-E1	none	In(2LR)w45-32n
3638	Df(2L)net-PMF	21A1; 21B7-8	none	
3909	Df(2R)59AD	59A1-3; 59D1-4	none	
4954	Df(2L)S2590	23D2; 23E3	none	
4955	Df(2L)XE-2750	28A5-B1; 28C1-9	none	
4960	Df(2R)CB21	48E; 49A	none	
4961	DF(2R)Kr10	60E10; 60F5	none	
4966	Df(2R)w45-30n	45A6-7; 45E2-3	none	
5246	Df(2R)Egfr5	57D2-8; 58D1	none	
5422	Df(2R)03072	51A5; 51C1	none	
5574	Df(2R)k10408	54C1-4; 54C1-4 (?)	none	
5680	Df(2R)robl-c	54B17-C4; 54C1-4	none	
5879	Df(2R)BSC3	48E12-F4; 49A11-B6	none	
6283	Df(2L)BSC4	21B7-C1; 21C2-3	none	

Table 4.2. Chromosome 3 deficiencies tested in modification screen.

Bloomington Stock	Deficiency	breakpoints	modification	other abberations
339	Df(3R)6-7	82D5; 82F3-6	none	
383	Df(3R)ea	88E7-13; 89A1	none	
430	Df(3R)3450	98E3; 99A6	none	
669	Df(3R)Dr-rv1	99A1-2; 99B6-11	none	
823	Df(3R)D605	97E3; 98A5	none	
1011	Df(3R)faf-BP	100D1-2; 100E-F	none	
1518	Df(3R)ME15	81F3-6; 82F5-7	none	
1534	Tp(3;Y)ry506-85C	87D1; 88E5-6; h1-h25	suppressor	
1842	Df(3R)Antp17	84A5; 84D14	none	
1884	Df(3R)Scr	84A1; 84B1-2	none	
1893	Df(3R)by62	85D10-11; 85F8-11	none	
1910	Df(eR)Tl-P	97A; 98A1-2	none	
1990	Df(3R)Tpl10	83C1-2; 84B2	none	
1972	Df(3R)XS	96A1-7; 96A21-25	none	
2363	Df(3R)crb87-5	95F7; 96A18	none	
2366	Df(eR)XTA1	96A17-21; 96D1	suppressor	Dp(3;3)M95A[+]13
[redacted]				
2585	Df(3R)mbc-R1	95A5-7; 95D6-11	suppressor	
2586	Df(3R)23D1	94A3-4; 94D1-4	none	
3007	Df(3R)ry615	87B12; 87E8	none	
3011	Df(3R)Cha7	90F1-2; 91F5	none	
3012	Df(3R)Dl-BX12	91F1-2; 92D3-6	none	
3128	Df(3R)M-Kx1	86C1; 87B5	none	
3369	Df(3R)awd-KRB	100D1; 100D3-4	none	
3468	Df(3R)slo8	96A2-7; 96D2-4	none	Dp(3;3)Su8
4787	Df(3R)3-4	82F3-4; 82F10-11	none	
4940	Df(3R)mbc-30	95A5-7; 95C10-11	none	
4962	Df(3R)H-B79	92B3; 92F13	none	
5601	Df(3R)Espl3	96F1; 97B1	none	
5694	Df(3R)e1025-14	82F8-10; 83A1-3	none	
3547	Df(3R)L127	99B5-6; 99E4-F1	none	Dp(3;1)B152
4431	Df(3R)DG2	89E-F; 91B1-2	none	
89	Df(3L)lxd6	67E5-7; 68B2-4	none	
2608	Df(3L)W10	75A6-7; 75C2	none	
3124	Df(3L)fz-GF3b	70C2; 70D5	none	
5951	Df(3L)HD1	79D3-E1; 79F2-6	none	
3126	Df(3L)fz-M21	70D2; 71E4-5	none	
2611	Df(3L)vin5	68A2; 69A1	none	
439	Df(3L)Ar14-8	61C4; 62A8	none	
2612	Df(3L)vin7	68C8; 69B4-5	none	

CHAPTER 5:

Summary and Future Directions

The data presented in this dissertation indicate that *Datx2* is an essential gene that is required for in several Drosophila tissues. Mosaic analyses indicate that *Datx2* is essential for eye development, oocyte specification and organization of the actin cytoskeleton. Consistent with the presence of Sm and PAM2 motifs in ataxin-2 proteins, biochemical studies demonstrate that Datx2 and ataxin-2 assemble with polyribosomes and mRNPs. Structure and function analyses indicate that the regions containing the conserved Sm motifs and PAM2 domain can each independently assemble with mRNA.

Ataxin-2 proteins repress translation

What do ataxin-2 proteins do when bound to polyribosomes and mRNPs? Several observations indicate that these proteins function as translational repressors. In yeast, mutations in the yeast *PBP1* gene can suppress the lethality caused by mutations in the *PAB1* gene, a positive regulator of translation (MANGUS *et al.* 1998). This result indicates that these genes have opposing activities. The finding that Pbp1p and Pab1 physically interact suggests that Pbp1p may counteract the activity of Pab1 by physically blocking the translation promoting activities of Pab1 (MANGUS *et al.* 1998). Because *PAB1* promotes translation, it is likely that *PBP1* represses translation. In *C. elegans* reducing the activity of *ATX-2* causes ectopic translation of repressed mRNAs (CIOSK *et al.* 2004). Taken with my data demonstrating that Datx2 and ataxin-2 assemble with polyribosomes and mRNPs, these observations suggest that ataxin-2 proteins repress translation, in part, by directly assembling with polyribosomes and poly(A)-binding protein.

The presence of Sm motifs in ataxin-2 proteins suggest a potential molecular mechanism of ataxin-2 activity. Sm motifs are found in proteins that regulate various aspects of RNA metabolism, including mRNA translation and pre-mRNA splicing (THARUN *et al.* 1999; MAYES *et al.* 2000; STORZ *et al.* 2004). Whether they regulate translation or splicing, however, Sm proteins appear to function by mediating RNA-RNA interactions. For example, the bacterial protein Hfq is a well-studied Sm protein that regulates the translation of many mRNAs in bacteria (STORZ *et al.* 2004). Hfq does this by facilitating the interaction of small non-coding RNAs, known as microRNAs, with their mRNA targets. By altering the secondary structures of their targets, most microRNAs in bacteria function to repress the translation of their targets. In eukaryotes, Sm proteins are best known as components of the splicing machinery (MAYES *et al.* 1999; PANNONE *et al.* 2000). Within the spliceosome Sm proteins stabilize the interactions between the small non-coding snRNAs and their target pre-mRNAs. In this manner these Sm proteins facilitate splicing.

Taken with my observation that Datx2 and ataxin-2 assemble directly with polyribosomes and cytoplasmic mRNPs, the observation that Sm proteins regulate RNA-RNA interactions, raises the intriguing possibility that ataxin-2 proteins might regulate the mRNA translation through the use of microRNAs. Though many eukaryotic Sm proteins regulate RNA splicing, ataxin-2 proteins are unlikely to function in this process because they are not present in the nucleus. It is much more likely that, if ataxin-2 proteins mediate RNA-RNA interactions, they do so as a means to regulate translation.

***Datx2* phenotypes reflect aberrant mRNA regulation**

Considering the substantial evidence linking ataxin-2 proteins to mRNA translation, it is likely that the various phenotypes observed in *Datx2* mutant tissues derive from primary defects in the translational regulation of mRNAs. Comparing the *Datx2* phenotypes with the phenotypes of other Drosophila mutants supports this interpretation. In the Drosophila egg chambers, many translationally repressed mRNAs are transported to the oocyte (MACDONALD 2004; TADROS AND LIPSHITZ 2005). Similar to loss of *Datx2* activity, failure in the transport or translational regulation of these mRNAs can defective oocyte specification. *BicD* and *egl* encode proteins that regulate the transport of mRNAs (MACH AND LEHMANN 1997). Mutations in either of these two genes cause oocyte specification failure. *Vasa* encodes an RNA-helicase, and mutations in this gene also cause oocyte specification failure (STYHLER *et al.* 1998).

Though many Drosophila mutants that show cytoplasmic dumping defects carry mutations in genes encoding cytoskeletal components (reviewed by ROBINSON AND COOLEY 1997), at least one mutant with this phenotype carries a mutation in an RNA-binding protein. *Lark* encodes an RNA-binding protein, and mutations in *lark* causes mislocalization of hu-li-tai-shao protein. Hu-li-tai-shao is a component of the actin cytoskeleton that is required to anchor the cytoskeleton to the plasma membrane. Given the RNA-binding properties of lark, it is likely that *lark* mutations cause cytoskeleton defects by causing misregulation of mRNAs, possibly *hu-li-tai-shao*. The observations that *lark* and *Datx2* both encode RNA-binding proteins and that mutations in either gene cause failure in cytoplasmic dumping failure suggest that these genes may be required in

the same genetic pathway. The observed misregulation of *hu-li-tai-shao* expression in *lark* mutants might underlie the cytoplasmic dumping defect and raises the possibility that misregulation of *hu-li-tai-shao* might also underlie the defects observed in *Datx2* mutants.

What are the mRNA targets of Datx2?:

Identification of the mRNA targets of Datx2 will be useful for developing a more detailed understanding of how this protein regulates mRNA metabolism. Based on the phenotypic analysis, it appears possible that *hu-li-tai-shao* mRNA might be a target of Datx2 regulation. This hypothesis can be readily tested by performing immunoprecipitation of Datx2 from ovary extracts followed by using RT-PCR or northern analysis to test for the presence of the *hu-li-tai-shao* transcript in the pull-down material. This approach could be used to test for any mRNA that is a candidate target of Datx2 activity.

Although this candidate approach can prove useful, the success of this approach relies heavily on proper interpretation of *Datx2* mutant phenotypes. Thus the candidate approach is necessarily limited. Because of this, future studies should also be aimed at a comprehensive analysis of Datx2 and ataxin-2 mRNA targets. An important question is whether ataxin-2 proteins regulate large numbers of mRNAs or whether they regulate smaller numbers of specific mRNAs. The data on yeast *PBP1* suggests that it has a global influence on translation because *PBP1* mutations can suppress mutations in *PAB1*, a global regulator of translation. In contrast, reduced activity of *C. elegans ATX2* causes

germline defects that can be traced to misregulation of specific mRNAs. It is thus probable that the number and types of mRNA targets of ataxin-2 proteins differ among organisms.

To identify the mRNA targets of ataxin-2, one could affinity purify the protein followed by microarray analysis to identify mRNAs that physically associate with ataxin-2. This approach has been used successfully to identify targets of the translational repressor FMRP (BROWN *et al.* 2001; ZHANG *et al.* 2001). After putative mRNA targets are identified, specific mRNAs could be validated by different assays, like affinity purification followed by RT-PCR for specific transcripts. Upon target validation, one could perform *in vivo* tests to determine if the rates of turnover or translation of mRNA targets are altered by manipulating ataxin-2 activity. This approach could also be used to identify targets of Datx2.

Do ataxin-2 proteins physically associate with microRNAs?:

Future studies should determine if ataxin-2 proteins utilize miRNAs to regulate translation. As with the microarray experiment described above, epitope tags could be employed to purify ataxin-2 or Datx2. Instead of microarrays, however, one would need to perform Northern blots to test for the presence of specific miRNAs that may copurify with ataxin-2 or Datx2. Several miRNAs have been identified in humans and Drosophila (GESELLCHEN AND BOUTROS 2004; WEBER 2005). Many of these miRNAs have known or predicted mRNA targets. Thus, in addition to clarifying the molecular activities of ataxin-2 proteins, this approach could also implicate or validate specific mRNA targets of these proteins.

Is ataxin-2 a translational repressor?:

To understand SCA2 pathology better, it will be important to clarify the specific activity of ataxin-2. Though many observations indicate that ataxin-2 homologs function as translational repressors, this has not yet been demonstrated for ataxin-2. As an initial but crude approach, *in vitro* translation experiments could be performed with purified ataxin-2. A potential limitation with this approach is that ataxin-2 may regulate a subset of transcripts possessing certain sequences and/or secondary structures. If so, a generic *in vitro* translation transcript that lacks the necessary features may not be subject to regulation by ataxin-2. Another potential approach would be to generate *SCA2* knockout mice and look for phenotypes that may reflect altered RNA regulation. A similar genetic approach in *C. elegans* linked the worm ortholog to translational repression (CIOSK *et al.* 2004). Though potentially informative, however, this approach could be complicated by the presence of a redundant ataxin-2 related protein in mice.

A better approach to analyzing ataxin-2 activity will likely involve the identification of mRNA and/or microRNA targets of ataxin-2. Knowing what RNAs are targeted by ataxin-2 would allow a more refined analysis of ataxin-2 activity. For example, one could focus on a few ataxin-2 targets, analyzing how altered ataxin-2 activity may influence their turnover or translation. This approach would also be capable of identifying opposing ataxin-2 activities. As is the case for *E. coli* Hfq, ataxin-2 might act as to promote or inhibit translation, depending on the mRNA target.

Does polyglutamine expansion influence ataxin-2 activity?:

Long polyglutamine tracts repress gene expression at the level of transcription by interfering with the activities of transcriptional coactivators (Figure 5.1). Given that ataxin-2 likely regulates mRNA translation, expanded ataxin-2 may promote cellular dysfunction by excessively repressing translation (Figure 5.1). One could test this idea by manipulating rates of translation in mice expressing expanded ataxin-2. For example, if boosting translation in SCA2 mice improved their condition, taken with other data, this would suggest that expanded ataxin-2 promotes dysfunction by inducing excessive translational repression.

Future aims should also be directed at identifying proteins contained within the inclusion bodies (IB) observed in SCA2 patient brains. Previously, similar approaches successfully identified many transcription factors, including CREB-binding protein, in the aggregates of other polyglutamine diseases (MCCAMPBELL *et al.* 2000). These studies were important because some of them identified proteins, that when inactivated, contributed significantly to polyglutamine pathology. It is likely that analyses of SCA2 inclusion bodies will identify components with significant relevance to SCA2 pathology. Given that ataxin-2 functions in RNA metabolism and SCA2 inclusion bodies are mostly cytoplasmic, it is reasonable to suspect that SCA2 inclusion bodies contain RNAs and proteins involved in their regulation.

Polyglutamine diseases: diseases of aberrant gene expression?:

By directly linking ataxin-2 and Datx2 to mRNA metabolism, our data extend previous findings implicating the *S. cerevisae* and *C. elegans* ataxin-2 orthologs to RNA

metabolism. Further, by directly implicating ataxin-2 in mRNA metabolism, our data raise the possibility that defects in ataxin-2-mediated RNA metabolism contribute to or directly underlie the pathology of SCA2. If defects in RNA metabolism contribute to SCA2, this could be akin to the transcriptional dysregulation thought to underlie several other polyglutamine diseases. This would suggest that, collectively, polyglutamine diseases are diseases of aberrant gene expression.

Therapeutic Options:

Studies of other polyglutamine diseases have yielded promising ideas about potential therapies. Because several of these diseases appear to stem from transcriptional repression, current therapeutic efforts are primarily directed toward restoring normal levels of transcription with drugs called histone deacetylase (HDAC) inhibitors. These drugs promote transcription by helping maintain relaxed chromatin structure. Studies in cell culture, Drosophila, and mouse models suggest that HDAC inhibitors may be promising therapeutics (STEFFAN *et al.* 2001; HOCKLY *et al.* 2003; MINAMIYAMA *et al.* 2004). One interesting prospect is that HDAC inhibitors may also be therapeutic for SCA2. If SCA2 pathology stems from translational repression, and thereby reduced gene expression, these drugs could conceivably help overcome this by boosting gene expression at the level of transcription.

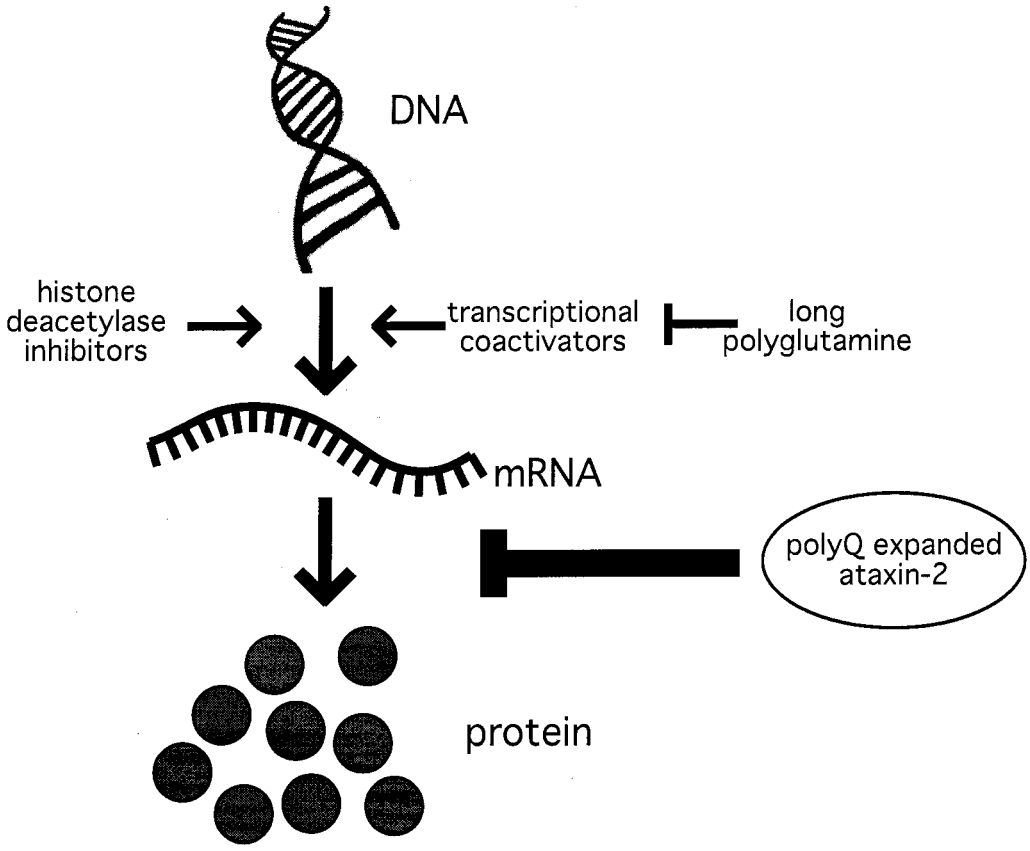

Figure 5.1. Polyglutamine diseases possibly stem from reduced gene expression. Long polyglutamine tracts repress gene expression at the level of transcription. Polyglutamine expanded ataxin-2 might similarly repress gene expression, but at the level of translation.

Bibliography

ADACHI, H., M. KATSUNO, M. MINAMIYAMA, C. SANG, G. PAGOULATOS et al., 2003 Heat shock protein 70 chaperone overexpression ameliorates phenotypes of the spinal and bulbar muscular atrophy transgenic mouse model by reducing nuclear-localized mutant androgen receptor protein. J Neurosci **23:** 2203-2211.

ADAMS, M. D., S. E. CELNIKER, R. A. HOLT, C. A. EVANS, J. D. GOCAYNE et al., 2000 The genome sequence of Drosophila melanogaster. Science **287:** 2185-2195.

ALBRECHT, M., M. GOLATTA, U. WULLNER and T. LENGAUER, 2004 Structural and functional analysis of ataxin-2 and ataxin-3. Eur J Biochem **271:** 3155-3170.

BABOVIC-VUKSANOVIC, D., K. SNOW, M. C. PATTERSON and V. V. MICHELS, 1998 Spinocerebellar ataxia type 2 (SCA 2) in an infant with extreme CAG repeat expansion. Am J Med Genet **79:** 383-387.

BANFI, S., A. SERVADIO, M. Y. CHUNG, T. J. KWIATKOWSKI, JR., A. E. MCCALL et al., 1994 Identification and characterization of the gene causing type 1 spinocerebellar ataxia. Nat Genet **7:** 513-520.

BARTH, A. I., I. S. NATHKE and W. J. NELSON, 1997 Cadherins, catenins and APC protein: interplay between cytoskeletal complexes and signaling pathways. Curr Opin Cell Biol **9:** 683-690.

BAULIEU, E. E., M. ATGER, M. BEST-BELPOMME, P. CORVOL, J. C. COURVALIN et al., 1975 Steroid hormone receptors. Vitam Horm **33:** 649-736.

BEERE, H. M., B. B. WOLF, K. CAIN, D. D. MOSSER, A. MAHBOUBI et al., 2000 Heat-shock protein 70 inhibits apoptosis by preventing recruitment of procaspase-9 to the Apaf-1 apoptosome. Nat Cell Biol **2:** 469-475.

BELAL, S., G. CANCEL, G. STEVANIN, F. HENTATI, C. KHATI et al., 1994 Clinical and genetic analysis of a Tunisian family with autosomal dominant cerebellar ataxia type 1 linked to the SCA2 locus. Neurology **44:** 1423-1426.

BOK, K. S., H. RHIM, Y. D. YOO, E. CHOI, K. AHN et al., 1999 Expanded polyglutamine tract itself induces cell death in cultured cells. Mol Cells **9:** 398-402.

BOUTELL, J. M., P. THOMAS, J. W. NEAL, V. J. WESTON, J. DUCE et al., 1999 Aberrant interactions of transcriptional repressor proteins with the Huntington's disease gene product, huntingtin. Hum Mol Genet **8:** 1647-1655.

BRAND, A. H., and N. PERRIMON, 1993 Targeted gene expression as a means of altering cell fates and generating dominant phenotypes. Development **118:** 401-415.

BROWN, L. Y., and S. A. BROWN, 2004 Alanine tracts: the expanding story of human illness and trinucleotide repeats. Trends Genet **20:** 51-58.

BROWN, V., P. JIN, S. CEMAN, J. C. DARNELL, W. T. O'DONNELL et al., 2001 Microarray identification of FMRP-associated brain mRNAs and altered mRNA translational profiles in fragile X syndrome. Cell **107:** 477-487.

CALLAERTS, P., S. LENG, J. CLEMENTS, C. BENASSAYAG, D. CRIBBS et al., 2001 Drosophila Pax-6/eyeless is essential for normal adult brain structure and function. J Neurobiol **46:** 73-88.

CANT, K., B. A. KNOWLES, M. S. MOOSEKER and L. COOLEY, 1994 Drosophila singed, a fascin homolog, is required for actin bundle formation during oogenesis and bristle extension. J Cell Biol **125:** 369-380.

CHAI, Y., S. L. KOPPENHAFER, N. M. BONINI and H. L. PAULSON, 1999 Analysis of the role of heat shock protein (Hsp) molecular chaperones in polyglutamine disease. J Neurosci **19:** 10338-10347.

CHAN, H. Y., J. M. WARRICK, G. L. GRAY-BOARD, H. L. PAULSON and N. M. BONINI, 2000 Mechanisms of chaperone suppression of polyglutamine disease: selectivity, synergy and modulation of protein solubility in Drosophila. Hum Mol Genet **9:** 2811-2820.

CHEN, B. S., and M. HAMPSEY, 2002 Transcription activation: unveiling the essential nature of TFIID. Curr Biol **12:** R620-622.

CHEN, Y. W., M. D. ALLEN, D. B. VEPRINTSEV, J. LOWE and M. BYCROFT, 2004 The structure of the AXH domain of spinocerebellar ataxin-1. J Biol Chem **279:** 3758-3765.

CHOU, T. B., E. NOLL and N. PERRIMON, 1993 Autosomal P[ovoD1] dominant female-sterile insertions in Drosophila and their use in generating germ-line chimeras. Development **119:** 1359-1369.

CIOSK, R., M. DEPALMA and J. R. PRIESS, 2004 ATX-2, the C. elegans ortholog of ataxin 2, functions in translational regulation in the germline. Development **131:** 4831-4841.

CRAIG, A. W., A. HAGHIGHAT, A. T. YU and N. SONENBERG, 1998 Interaction of polyadenylate-binding protein with the eIF4G homologue PAIP enhances

translation. Nature **392:** 520-523.

CREAGH, E. M., D. SHEEHAN and T. G. COTTER, 2000 Heat shock proteins--modulators of apoptosis in tumour cells. Leukemia **14:** 1161-1173.

CUMMINGS, C. J., M. A. MANCINI, B. ANTALFFY, D. B. DEFRANCO, H. T. ORR et al., 1998 Chaperone suppression of aggregation and altered subcellular proteasome localization imply protein misfolding in SCA1. Nat Genet **19:** 148-154.

CUMMINGS, C. J., Y. SUN, P. OPAL, B. ANTALFFY, R. MESTRIL et al., 2001 Over-expression of inducible HSP70 chaperone suppresses neuropathology and improves motor function in SCA1 mice. Hum Mol Genet **10:** 1511-1518.

CUMMINGS, C. J., and H. Y. ZOGHBI, 2000 Trinucleotide repeats: mechanisms and pathophysiology. Annu Rev Genomics Hum Genet **1:** 281-328.

DUNN, C. D., and R. E. JENSEN, 2003 Suppression of a defect in mitochondrial protein import identifies cytosolic proteins required for viability of yeast cells lacking mitochondrial DNA. Genetics **165:** 35-45.

ELLIS, M. C., E. M. O'NEILL and G. M. RUBIN, 1993 Expression of Drosophila glass protein and evidence for negative regulation of its activity in non-neuronal cells by another DNA-binding protein. Development **119:** 855-865.

ESTRADA, R., J. GALARRAGA, G. OROZCO, A. NODARSE and G. AUBURGER, 1999 Spinocerebellar ataxia 2 (SCA2): morphometric analyses in 11 autopsies. Acta Neuropathol (Berl) **97:** 306-310.

EVERETT, C. M., and N. W. WOOD, 2004 Trinucleotide repeats and neurodegenerative disease. Brain **127:** 2385-2405.

FURTADO, S., M. FARRER, Y. TSUBOI, M. L. KLIMEK, R. DE LA FUENTE-FERNANDEZ et al., 2002 SCA-2 presenting as parkinsonism in an Alberta family: clinical, genetic, and PET findings. Neurology **59:** 1625-1627.

GANDER, E. S., R. U. MUELLER, S. GOLDENBERG and C. MOREL, 1975 EDTA- and puromycin-derived duck- and rabbit globin-messenger ribonucleoprotein complexes isolated by oligo (dT)-cellulose chromatography. Mol Biol Rep **2:** 343-349.

GESCHWIND, D. H., S. PERLMAN, C. P. FIGUEROA, L. J. TREIMAN and S. M. PULST, 1997 The prevalence and wide clinical spectrum of the spinocerebellar ataxia type 2 trinucleotide repeat in patients with autosomal dominant cerebellar ataxia. Am J Hum Genet **60:** 842-850.

GESELLCHEN, V., and M. BOUTROS, 2004 Managing the genome: microRNAs in Drosophila. Differentiation **72:** 74-80.

GIUFFRIDA, S., S. LANZA, D. A. RESTIVO, R. SAPONARA, S. C. VALVO et al., 1999 Clinical and molecular analysis of 11 Sicilian SCA2 families: influence of gender on age at onset. Eur J Neurol **6:** 301-307.

GODT, D., and U. TEPASS, 1998 Drosophila oocyte localization is mediated by differential cadherin-based adhesion. Nature **395:** 387-391.

GRANT, P. A., D. SCHIELTZ, M. G. PRAY-GRANT, D. J. STEGER, J. C. REESE et al., 1998 A subset of TAF(II)s are integral components of the SAGA complex required for nucleosome acetylation and transcriptional stimulation. Cell **94:** 45-53.

GREENBERG, D. A., 1987 Calcium channels and calcium channel antagonists. Ann Neurol **21:** 317-330.

GRIESHABER, S. S., D. H. LANKENAU, T. TALBOT, S. HOLLAND and N. S. PETERSEN, 2001 Expression of the 53 kD forked protein rescues F-actin bundle formation and mutant bristle phenotypes in Drosophila. Cell Motil Cytoskeleton **50:** 198-206.

GROUP, T. H. S. D. C. R., 1993 A novel gene containing a trinucleotide repeat that is expanded and unstable on Huntington's disease chromosomes. The Huntington's Disease Collaborative Research Group. Cell **72:** 971-983.

GWINN-HARDY, K., J. Y. CHEN, H. C. LIU, T. Y. LIU, M. BOSS et al., 2000 Spinocerebellar ataxia type 2 with parkinsonism in ethnic Chinese. Neurology **55:** 800-805.

HACKAM, A. S., J. G. HODGSON, R. SINGARAJA, T. ZHANG, L. GAN et al., 1999 Evidence for both the nucleus and cytoplasm as subcellular sites of pathogenesis in Huntington's disease in cell culture and in transgenic mice expressing mutant huntingtin. Philos Trans R Soc Lond B Biol Sci **354:** 1047-1055.

HAHN, S., S. BURATOWSKI, P. A. SHARP and L. GUARENTE, 1989 Yeast TATA-binding protein TFIID binds to TATA elements with both consensus and nonconsensus DNA sequences. Proc Natl Acad Sci U S A **86:** 5718-5722.

HANSSON, O., J. NYLANDSTED, R. F. CASTILHO, M. LEIST, M. JAATTELA et al., 2003 Overexpression of heat shock protein 70 in R6/2 Huntington's disease mice has only modest effects on disease progression. Brain Res **970:** 47-57.

HE, W., and R. PARKER, 2000 Functions of Lsm proteins in mRNA degradation and splicing. Curr Opin Cell Biol **12:** 346-350.

HELMLINGER, D., J. BONNET, J. L. MANDEL, Y. TROTTIER and D. DEVYS, 2004 Hsp70 and Hsp40 chaperones do not modulate retinal phenotype in SCA7 mice. J Biol Chem **279:** 55969-55977.

HOCKLY, E., V. M. RICHON, B. WOODMAN, D. L. SMITH, X. ZHOU et al., 2003 Suberoylanilide hydroxamic acid, a histone deacetylase inhibitor, ameliorates motor deficits in a mouse model of Huntington's disease. Proc Natl Acad Sci U S A **100:** 2041-2046.

HOPMANN, R., J. A. COOPER and K. G. MILLER, 1996 Actin organization, bristle morphology, and viability are affected by actin capping protein mutations in Drosophila. J Cell Biol **133:** 1293-1305.

HUGHES, R. E., R. S. LO, C. DAVIS, A. D. STRAND, C. L. NEAL et al., 2001 Altered transcription in yeast expressing expanded polyglutamine. Proc Natl Acad Sci U S A **98:** 13201-13206.

HUYNH, D. P., M. R. DEL BIGIO, D. H. HO and S. M. PULST, 1999 Expression of ataxin-2 in brains from normal individuals and patients with Alzheimer's disease and spinocerebellar ataxia 2. Ann Neurol **45:** 232-241.

HUYNH, D. P., K. FIGUEROA, N. HOANG and S. M. PULST, 2000 Nuclear localization or inclusion body formation of ataxin-2 are not necessary for SCA2 pathogenesis in mouse or human. Nat Genet **26:** 44-50.

IHARA, T., H. SASAKI, A. WAKISAKA, A. TAKADA, T. YOSHIKI et al., 1994 Genetic heterogeneity of dominantly inherited olivopontocerebellar atrophy (OPCA) in the Japanese: linkage study of two pedigrees and evidence for the disease locus on chromosome 12q (SCA2). Jpn J Hum Genet **39:** 305-313.

IMBERT, G., F. SAUDOU, G. YVERT, D. DEVYS, Y. TROTTIER et al., 1996 Cloning of the gene for spinocerebellar ataxia 2 reveals a locus with high sensitivity to expanded CAG/glutamine repeats. Nat Genet **14:** 285-291.

INFANTE, J., J. BERCIANO, V. VOLPINI, J. CORRAL, J. M. POLO et al., 2004 Spinocerebellar ataxia type 2 with Levodopa-responsive parkinsonism culminating in motor neuron disease. Mov Disord **19:** 848-852.

IRWIN, S., M. VANDELFT, D. PINCHEV, J. L. HOWELL, J. GRACZYK et al., 2005 RNA association and nucleocytoplasmic shuttling by ataxin-1. J Cell Sci **118:** 233-242.

JACKSON, S. M., and C. A. BERG, 1999 Soma-to-germline interactions during Drosophila oogenesis are influenced by dose-sensitive interactions between cut and the genes cappuccino, ovarian tumor and agnostic. Genetics **153:** 289-303.

KAHVEJIAN, A., G. ROY and N. SONENBERG, 2001 The mRNA closed-loop model: the function of PABP and PABP-interacting proteins in mRNA translation. Cold Spring Harb Symp Quant Biol **66:** 293-300.

KALCHMAN, M. A., H. B. KOIDE, K. MCCUTCHEON, R. K. GRAHAM, K. NICHOL et al., 1997 HIP1, a human homologue of S. cerevisiae Sla2p, interacts with membrane-associated huntingtin in the brain. Nat Genet **16:** 44-53.

KATSUNO, M., H. ADACHI, F. TANAKA and G. SOBUE, 2004 Spinal and bulbar muscular atrophy: ligand-dependent pathogenesis and therapeutic perspectives. J Mol Med **82:** 298-307.

KAZEMI-ESFARJANI, P., and S. BENZER, 2000 Genetic suppression of polyglutamine toxicity in Drosophila. Science **287:** 1837-1840.

KEGEL, K. B., A. R. MELONI, Y. YI, Y. J. KIM, E. DOYLE et al., 2002 Huntingtin is present in the nucleus, interacts with the transcriptional corepressor C-terminal binding protein, and represses transcription. J Biol Chem **277:** 7466-7476.

KHALEGHPOUR, K., Y. V. SVITKIN, A. W. CRAIG, C. T. DEMARIA, R. C. DEO et al., 2001 Translational repression by a novel partner of human poly(A) binding protein, Paip2. Mol Cell **7:** 205-216.

KLEMENT, I. A., P. J. SKINNER, M. D. KAYTOR, H. YI, S. M. HERSCH et al., 1998 Ataxin-1 nuclear localization and aggregation: role in polyglutamine-induced disease in SCA1 transgenic mice. Cell **95:** 41-53.

KOIDE, R., T. IKEUCHI, O. ONODERA, H. TANAKA, S. IGARASHI et al., 1994 Unstable expansion of CAG repeat in hereditary dentatorubral-pallidoluysian atrophy (DRPLA). Nat Genet **6:** 9-13.

KOIDE, R., S. KOBAYASHI, T. SHIMOHATA, T. IKEUCHI, M. MARUYAMA et al., 1999 A neurological disease caused by an expanded CAG trinucleotide repeat in the TATA-binding protein gene: a new polyglutamine disease? Hum Mol Genet **8:** 2047-2053.

KOREY, C. A., G. WILKIE, I. DAVIS and D. VAN VACTOR, 2001 small bristles is required for the morphogenesis of multiple tissues during Drosophila development. Genetics **159:** 1659-1670.

KOZLOV, G., G. DE CRESCENZO, N. S. LIM, N. SIDDIQUI, D. FANTUS et al., 2004

Structural basis of ligand recognition by PABC, a highly specific peptide-binding domain found in poly(A)-binding protein and a HECT ubiquitin ligase. Embo J **23:** 272-281.

KOZLOV, G., J. F. TREMPE, K. KHALEGHPOUR, A. KAHVEJIAN, I. EKIEL et al., 2001 Structure and function of the C-terminal PABC domain of human poly(A)-binding protein. Proc Natl Acad Sci U S A **98:** 4409-4413.

KRAMER, A., 1996 The structure and function of proteins involved in mammalian pre-mRNA splicing. Annu Rev Biochem **65:** 367-409.

KUBIS, N., A. DURR, M. GUGENHEIM, H. CHNEIWEISS, P. MAZZETTI et al., 1999 Polyneuropathy in autosomal dominant cerebellar ataxias: phenotype-genotype correlation. Muscle Nerve **22:** 712-717.

LA SPADA, A. R., Y. H. FU, B. L. SOPHER, R. T. LIBBY, X. WANG et al., 2001 Polyglutamine-expanded ataxin-7 antagonizes CRX function and induces cone-rod dystrophy in a mouse model of SCA7. Neuron **31:** 913-927.

LA SPADA, A. R., E. M. WILSON, D. B. LUBAHN, A. E. HARDING and K. H. FISCHBECK, 1991 Androgen receptor gene mutations in X-linked spinal and bulbar muscular atrophy. Nature **352:** 77-79.

LAHUE, R. S., and D. L. SLATER, 2003 DNA repair and trinucleotide repeat instability. Front Biosci **8:** s653-665.

LI, F., T. MACFARLAN, R. N. PITTMAN and D. CHAKRAVARTI, 2002 Ataxin-3 is a histone-binding protein with two independent transcriptional corepressor activities. J Biol Chem **277:** 45004-45012.

LIVESEY, F. J., T. FURUKAWA, M. A. STEFFEN, G. M. CHURCH and C. L. CEPKO, 2000 Microarray analysis of the transcriptional network controlled by the photoreceptor homeobox gene Crx. Curr Biol **10:** 301-310.

LU, C. S., Y. H. WU CHOU, P. C. KUO, H. C. CHANG and Y. H. WENG, 2004 The parkinsonian phenotype of spinocerebellar ataxia type 2. Arch Neurol **61:** 35-38.

MACDONALD, P. M., 2004 Translational control: a cup half full. Curr Biol **14:** R282-283.

MACH, J. M., and R. LEHMANN, 1997 An Egalitarian-BicaudalD complex is essential for oocyte specification and axis determination in Drosophila. Genes Dev **11:** 423-435.

MAHAJAN-MIKLOS, S., and L. COOLEY, 1994 The villin-like protein encoded by the

Drosophila quail gene is required for actin bundle assembly during oogenesis. Cell **78:** 291-301.

MALANDRINI, A., L. GALLI, M. VILLANOVA, S. PALMERI, E. PARROTTA et al., 1998 CAG repeat expansion in an italian family with spinocerebellar ataxia type 2 (SCA2): a clinical and genetic study. Eur Neurol **40:** 164-168.

MANGUS, D. A., N. AMRANI and A. JACOBSON, 1998 Pbp1p, a factor interacting with Saccharomyces cerevisiae poly(A)-binding protein, regulates polyadenylation. Mol Cell Biol **18:** 7383-7396.

MARMORSTEIN, R., 2001 Structure and function of histone acetyltransferases. Cell Mol Life Sci **58:** 693-703.

MARSH, J. L., H. WALKER, H. THEISEN, Y. Z. ZHU, T. FIELDER et al., 2000 Expanded polyglutamine peptides alone are intrinsically cytotoxic and cause neurodegeneration in Drosophila. Hum Mol Genet **9:** 13-25.

MAYES, A. E., L. VERDONE, P. LEGRAIN and J. D. BEGGS, 1999 Characterization of Sm-like proteins in yeast and their association with U6 snRNA. Embo J **18:** 4321-4331.

MCCAMPBELL, A., A. A. TAYE, L. WHITTY, E. PENNEY, J. S. STEFFAN et al., 2001 Histone deacetylase inhibitors reduce polyglutamine toxicity. Proc Natl Acad Sci U S A **98:** 15179-15184.

MCEWAN, I. J., 2004 Molecular mechanisms of androgen receptor-mediated gene regulation: structure-function analysis of the AF-1 domain. Endocr Relat Cancer **11:** 281-293.

MCNEIL, G. P., F. SMITH and R. GALIOTO, 2004 The Drosophila RNA-binding protein Lark is required for the organization of the actin cytoskeleton and Hu-li tai shao localization during oogenesis. Genesis **40:** 90-100.

METZLER, M., V. LEGENDRE-GUILLEMIN, L. GAN, V. CHOPRA, A. KWOK et al., 2001 HIP1 functions in clathrin-mediated endocytosis through binding to clathrin and adaptor protein 2. J Biol Chem **276:** 39271-39276.

MEUNIER, C., D. BORDEREAUX, F. PORTEU, S. GISSELBRECHT, S. CHRETIEN et al., 2002 Cloning and characterization of a family of proteins associated with Mpl. J Biol Chem **277:** 9139-9147.

MINAMIYAMA, M., M. KATSUNO, H. ADACHI, M. WAZA, C. SANG et al., 2004 Sodium butyrate ameliorates phenotypic expression in a transgenic mouse model of spinal and bulbar muscular atrophy. Hum Mol Genet **13:** 1183-1192.

MORETTI, P., M. BLAZO, L. GARCIA, D. ARMSTRONG, R. A. LEWIS et al., 2004 Spinocerebellar ataxia type 2 (SCA2) presenting with ophthalmoplegia and developmental delay in infancy. Am J Med Genet A **124:** 392-396.

MUCHOWSKI, P. J., G. SCHAFFAR, A. SITTLER, E. E. WANKER, M. K. HAYER-HARTL et al., 2000 Hsp70 and hsp40 chaperones can inhibit self-assembly of polyglutamine proteins into amyloid-like fibrils. Proc Natl Acad Sci U S A **97:** 7841-7846.

NEUWALD, A. F., and E. V. KOONIN, 1998 Ataxin-2, global regulators of bacterial gene expression, and spliceosomal snRNP proteins share a conserved domain. J Mol Med **76:** 3-5.

NUCIFORA, F. C., JR., M. SASAKI, M. F. PETERS, H. HUANG, J. K. COOPER et al., 2001 Interference by huntingtin and atrophin-1 with cbp-mediated transcription leading to cellular toxicity. Science **291:** 2423-2428.

ORDWAY, J. M., S. TALLAKSEN-GREENE, C. A. GUTEKUNST, E. M. BERNSTEIN, J. A. CEARLEY et al., 1997 Ectopically expressed CAG repeats cause intranuclear inclusions and a progressive late onset neurological phenotype in the mouse. Cell **91:** 753-763.

OROZCO, G., R. ESTRADA, T. L. PERRY, J. ARANA, R. FERNANDEZ et al., 1989 Dominantly inherited olivopontocerebellar atrophy from eastern Cuba. Clinical, neuropathological, and biochemical findings. J Neurol Sci **93:** 37-50.

PANG, J. T., P. GIUNTI, S. CHAMBERLAIN, S. F. AN, R. VITALIANI et al., 2002 Neuronal intranuclear inclusions in SCA2: a genetic, morphological and immunohistochemical study of two cases. Brain **125:** 656-663.

PANNONE, B. K., and S. L. WOLIN, 2000 Sm-like proteins wRING the neck of mRNA. Curr Biol **10:** R478-481.

PAREYSON, D., C. GELLERA, B. CASTELLOTTI, A. ANTONELLI, M. C. RIGGIO et al., 1999 Clinical and molecular studies of 73 Italian families with autosomal dominant cerebellar ataxia type I: SCA1 and SCA2 are the most common genotypes. J Neurol **246:** 389-393.

PAULSON, H. L., 1999 Protein fate in neurodegenerative proteinopathies: polyglutamine diseases join the (mis)fold. Am J Hum Genet **64:** 339-345.

PEIFER, M., S. ORSULIC, D. SWEETON and E. WIESCHAUS, 1993 A role for the Drosophila segment polarity gene armadillo in cell adhesion and cytoskeletal integrity during oogenesis. Development **118:** 1191-1207.

PETERS, M. F., F. C. NUCIFORA, JR., J. KUSHI, H. C. SEAMAN, J. K. COOPER et al., 1999 Nuclear targeting of mutant Huntingtin increases toxicity. Mol Cell Neurosci **14:** 121-128.

PETRIJ, F., R. H. GILES, H. G. DAUWERSE, J. J. SARIS, R. C. HENNEKAM et al., 1995 Rubinstein-Taybi syndrome caused by mutations in the transcriptional co-activator CBP. Nature **376:** 348-351.

POGACAR, S., M. AMBLER, W. J. CONKLIN, W. A. O'NEIL and H. Y. LEE, 1978 Dominant spinopontine atrophy. Report of two additional members of family W. Arch Neurol **35:** 156-162.

PULST, S. M., A. NECHIPORUK, T. NECHIPORUK, S. GISPERT, X. N. CHEN et al., 1996 Moderate expansion of a normally biallelic trinucleotide repeat in spinocerebellar ataxia type 2. Nat Genet **14:** 269-276.

PULST, S. M., A. NECHIPORUK and S. STARKMAN, 1993 Anticipation in spinocerebellar ataxia type 2. Nat Genet **5:** 8-10.

RAGOTHAMAN, M., N. SARANGMATH, S. CHAUDHARY, V. KHARE, U. MITTAL et al., 2004 Complex phenotypes in an Indian family with homozygous SCA2 mutations. Ann Neurol **55:** 130-133.

RANUM, L. P., and J. W. DAY, 2004 Pathogenic RNA repeats: an expanding role in genetic disease. Trends Genet **20:** 506-512.

RIESS, O., F. A. LACCONE, S. GISPERT, L. SCHOLS, C. ZUHLKE et al., 1997 SCA2 trinucleotide expansion in German SCA patients. Neurogenetics **1:** 59-64.

ROBINOW, S., and K. WHITE, 1988 The locus elav of Drosophila melanogaster is expressed in neurons at all developmental stages. Dev Biol **126:** 294-303.

ROBINSON, D. N., and L. COOLEY, 1997 Genetic analysis of the actin cytoskeleton in the Drosophila ovary. Annu Rev Cell Dev Biol **13:** 147-170.

ROY, G., G. DE CRESCENZO, K. KHALEGHPOUR, A. KAHVEJIAN, M. O'CONNOR-MCCOURT et al., 2002 Paip1 interacts with poly(A) binding protein through two independent binding motifs. Mol Cell Biol **22:** 3769-3782.

ROY, G., M. MIRON, K. KHALEGHPOUR, P. LASKO and N. SONENBERG, 2004 The Drosophila poly(A) binding protein-interacting protein, dPaip2, is a novel effector of cell growth. Mol Cell Biol **24:** 1143-1154.

RUBIN, G. M., L. HONG, P. BROKSTEIN, M. EVANS-HOLM, E. FRISE et al., 2000

A Drosophila complementary DNA resource. Science **287:** 2222-2224.

SAEBOE-LARSSEN, S., M. LYAMOURI, J. MERRIAM, M. P. OKSVOLD and A. LAMBERTSSON, 1998 Ribosomal protein insufficiency and the minute syndrome in Drosophila: a dose-response relationship. Genetics **148:** 1215-1224.

SALAZAR-GRUESO, E. F., S. KIM and H. KIM, 1991 Embryonic mouse spinal cord motor neuron hybrid cells. Neuroreport **2:** 505-508.

SALEEM, Q., S. CHOUDHRY, M. MUKERJI, L. BASHYAM, M. V. PADMA et al., 2000 Molecular analysis of autosomal dominant hereditary ataxias in the Indian population: high frequency of SCA2 and evidence for a common founder mutation. Hum Genet **106:** 179-187.

SANCHEZ, I., C. MAHLKE and J. YUAN, 2003 Pivotal role of oligomerization in expanded polyglutamine neurodegenerative disorders. Nature **421:** 373-379.

SANPEI, K., H. TAKANO, S. IGARASHI, T. SATO, M. OYAKE et al., 1996 Identification of the spinocerebellar ataxia type 2 gene using a direct identification of repeat expansion and cloning technique, DIRECT. Nat Genet **14:** 277-284.

SASAKI, H., A. WAKISAKA, K. SANPEI, H. TAKANO, S. IGARASHI et al., 1998 Phenotype variation correlates with CAG repeat length in SCA2--a study of 28 Japanese patients. J Neurol Sci **159:** 202-208.

SATTERFIELD, T. F., S. M. JACKSON and L. J. PALLANCK, 2002 A Drosophila homolog of the polyglutamine disease gene SCA2 is a dosage-sensitive regulator of actin filament formation. Genetics **162:** 1687-1702.

SCHOLS, L., S. GISPERT, M. VORGERD, A. M. MENEZES VIEIRA-SAECKER, P. BLANKE et al., 1997 Spinocerebellar ataxia type 2. Genotype and phenotype in German kindreds. Arch Neurol **54:** 1073-1080.

SHAN, D. E., B. W. SOONG, C. M. SUN, S. J. LEE, K. K. LIAO et al., 2001 Spinocerebellar ataxia type 2 presenting as familial levodopa-responsive parkinsonism. Ann Neurol **50:** 812-815.

SHEN, B., and H. M. GOODMAN, 2004 Uridine addition after microRNA-directed cleavage. Science **306:** 997.

SHIBATA, H., D. P. HUYNH and S. M. PULST, 2000 A novel protein with RNA-binding motifs interacts with ataxin-2. Hum Mol Genet **9:** 1303-1313.

SHULMAN, J. M., and M. B. FEANY, 2003 Genetic modifiers of tauopathy in

Drosophila. Genetics **165:** 1233-1242.

SIMEONI, S., M. A. MANCINI, D. L. STENOIEN, M. MARCELLI, N. L. WEIGEL et al., 2000 Motoneuronal cell death is not correlated with aggregate formation of androgen receptors containing an elongated polyglutamine tract. Hum Mol Genet **9:** 133-144.

SOPHER, B. L., P. S. THOMAS, JR., M. A. LAFEVRE-BERNT, I. E. HOLM, S. A. WILKE et al., 2004 Androgen receptor YAC transgenic mice recapitulate SBMA motor neuronopathy and implicate VEGF164 in the motor neuron degeneration. Neuron **41:** 687-699.

SPRADLING, A. C., 1993 Germline cysts: communes that work. Cell **72:** 649-651.

STEFFAN, J. S., L. BODAI, J. PALLOS, M. POELMAN, A. MCCAMPBELL et al., 2001 Histone deacetylase inhibitors arrest polyglutamine-dependent neurodegeneration in Drosophila. Nature **413:** 739-743.

STENOIEN, D. L., C. J. CUMMINGS, H. P. ADAMS, M. G. MANCINI, K. PATEL et al., 1999 Polyglutamine-expanded androgen receptors form aggregates that sequester heat shock proteins, proteasome components and SRC-1, and are suppressed by the HDJ-2 chaperone. Hum Mol Genet **8:** 731-741.

STOREY, E., D. DU SART, J. H. SHAW, P. LORENTZOS, L. KELLY et al., 2000 Frequency of spinocerebellar ataxia types 1, 2, 3, 6, and 7 in Australian patients with spinocerebellar ataxia. Am J Med Genet **95:** 351-357.

STORZ, G., J. A. OPDYKE and A. ZHANG, 2004 Controlling mRNA stability and translation with small, noncoding RNAs. Curr Opin Microbiol **7:** 140-144.

STYHLER, S., A. NAKAMURA, A. SWAN, B. SUTER and P. LASKO, 1998 vasa is required for GURKEN accumulation in the oocyte, and is involved in oocyte differentiation and germline cyst development. Development **125:** 1569-1578.

TADROS, W., and H. D. LIPSHITZ, 2005 Setting the stage for development: mRNA translation and stability during oocyte maturation and egg activation in Drosophila. Dev Dyn **232:** 593-608.

TAKEYAMA, K., S. ITO, A. YAMAMOTO, H. TANIMOTO, T. FURUTANI et al., 2002 Androgen-dependent neurodegeneration by polyglutamine-expanded human androgen receptor in Drosophila. Neuron **35:** 855-864.

TCHORZEWSKI, M., D. KROKOWSKI, W. RZESKI, O. G. ISSINGER and N. GRANKOWSKI, 2003 The subcellular distribution of the human ribosomal "stalk" components: P1, P2 and P0 proteins. Int J Biochem Cell Biol **35:** 203-211.

THARUN, S., W. HE, A. E. MAYES, P. LENNERTZ, J. D. BEGGS et al., 2000 Yeast Sm-like proteins function in mRNA decapping and decay. Nature **404:** 515-518.

TOLAR, L. A., and L. PALLANCK, 1998 NSF function in neurotransmitter release involves rearrangement of the SNARE complex downstream of synaptic vesicle docking. J Neurosci **18:** 10250-10256.

VAN DE WARRENBURG, B. P., N. C. NOTERMANS, H. J. SCHELHAAS, N. VAN ALFEN, R. J. SINKE et al., 2004 Peripheral nerve involvement in spinocerebellar ataxias. Arch Neurol **61:** 257-261.

VAN DE WARRENBURG, B. P., R. J. SINKE, C. C. VERSCHUUREN-BEMELMANS, H. SCHEFFER, E. R. BRUNT et al., 2002 Spinocerebellar ataxias in the Netherlands: prevalence and age at onset variance analysis. Neurology **58:** 702-708.

VELIER, J., M. KIM, C. SCHWARZ, T. W. KIM, E. SAPP et al., 1998 Wild-type and mutant huntingtins function in vesicle trafficking in the secretory and endocytic pathways. Exp Neurol **152:** 34-40.

VERHEYEN, E. M., and L. COOLEY, 1994 Profilin mutations disrupt multiple actin-dependent processes during Drosophila development. Development **120:** 717-728.

VERKERK, A. J., M. PIERETTI, J. S. SUTCLIFFE, Y. H. W. FU, D. P. KUHL et al., 1991 Identification of a gene (FMR-1) containing a CGG repeat coincident with a breakpoint cluster region exhibiting length variation in fragile X syndrome. Cell **65:** 905-914.

WANKER, E. E., C. ROVIRA, E. SCHERZINGER, R. HASENBANK, S. WALTER et al., 1997 HIP-I: a huntingtin interacting protein isolated by the yeast two-hybrid system. Hum Mol Genet **6:** 487-495.

WARRICK, J. M., H. Y. CHAN, G. L. GRAY-BOARD, Y. CHAI, H. L. PAULSON et al., 1999 Suppression of polyglutamine-mediated neurodegeneration in Drosophila by the molecular chaperone HSP70. Nat Genet **23:** 425-428.

WATANABE, H., F. TANAKA, M. MATSUMOTO, M. DOYU, T. ANDO et al., 1998 Frequency analysis of autosomal dominant cerebellar ataxias in Japanese patients and clinical characterization of spinocerebellar ataxia type 6. Clin Genet **53:** 13-19.

WEBER, M. J., 2005 New human and mouse microRNA genes found by homology search. Febs J **272:** 59-73.

WIEDEMEYER, R., F. WESTERMANN, I. WITTKE, J. NOWOCK and M. SCHWAB, 2003 Ataxin-2 promotes apoptosis of human neuroblastoma cells. Oncogene **22:** 401-411.

WOOD, J. D., F. C. NUCIFORA, JR., K. DUAN, C. ZHANG, J. WANG et al., 2000 Atrophin-1, the dentato-rubral and pallido-luysian atrophy gene product, interacts with ETO/MTG8 in the nuclear matrix and represses transcription. J Cell Biol **150:** 939-948.

YUE, S., H. G. SERRA, H. Y. ZOGHBI and H. T. ORR, 2001 The spinocerebellar ataxia type 1 protein, ataxin-1, has RNA-binding activity that is inversely affected by the length of its polyglutamine tract. Hum Mol Genet **10:** 25-30.

ZHANG, S., L. XU, J. LEE and T. XU, 2002 Drosophila atrophin homolog functions as a transcriptional corepressor in multiple developmental processes. Cell **108:** 45-56.

ZHANG, Y. Q., A. M. BAILEY, H. J. MATTHIES, R. B. RENDEN, M. A. SMITH et al., 2001 Drosophila fragile X-related gene regulates the MAP1B homolog Futsch to control synaptic structure and function. Cell **107:** 591-603.

ZHAO, Y., E. K. TAN, H. Y. LAW, C. S. YOON, M. C. WONG et al., 2002 Prevalence and ethnic differences of autosomal-dominant cerebellar ataxia in Singapore. Clin Genet **62:** 478-481.

ZHOU, H., S. H. LI and X. J. LI, 2001 Chaperone suppression of cellular toxicity of huntingtin is independent of polyglutamine aggregation. J Biol Chem **276:** 48417-48424.

ZHUCHENKO, O., J. BAILEY, P. BONNEN, T. ASHIZAWA, D. W. STOCKTON et al., 1997 Autosomal dominant cerebellar ataxia (SCA6) associated with small polyglutamine expansions in the alpha 1A-voltage-dependent calcium channel. Nat Genet **15:** 62-69.

ZOGHBI, H. Y., and H. T. ORR, 2000 Glutamine repeats and neurodegeneration. Annu Rev Neurosci **23:** 217-247.

ZUCCATO, C., M. TARTARI, A. CROTTI, D. GOFFREDO, M. VALENZA et al., 2003 Huntingtin interacts with REST/NRSF to modulate the transcription of NRSE-controlled neuronal genes. Nat Genet **35:** 76-83.

VITA

Terrence Satterfield was born in San Francisco, California to Elmo and Celina Satterfield. He grew up in neighboring Oakland, California where he attended St. Augustine School and Bishop O' Dowd High School. Upon graduation from high school, Terrence attended Leland Stanford Junior University where he majored in human biology with an emphasis in neurobiology. In 1998 he joined the laboratory of Leo Pallanck in the Department of Genetics at University of Washington. In 2005 he earned his doctoral degree in genetics.